Institute for Reference Materials and Measurements

NEUTRON PHYSICS UNIT

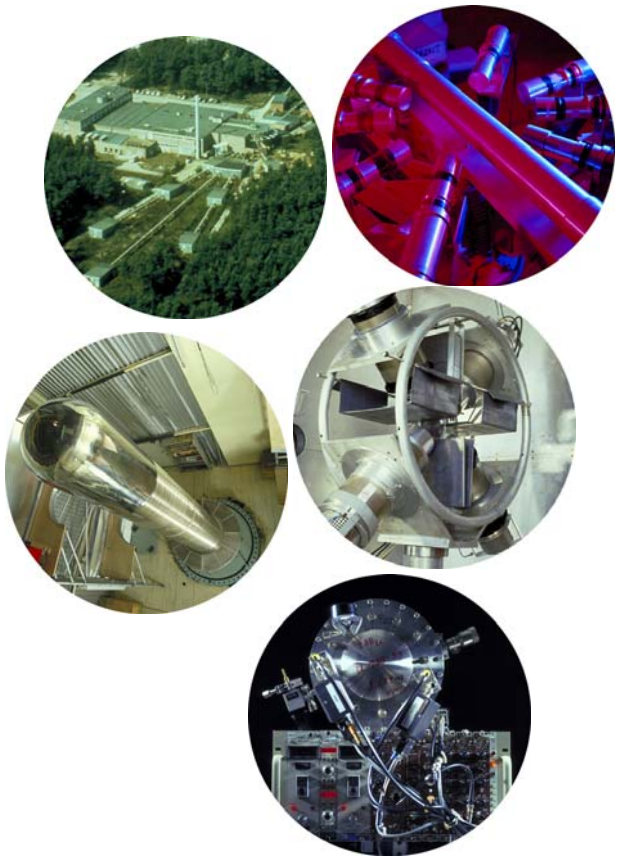

SCIENTIFIC REPORT

2002

EUROPEAN COMMISSION
JOINT RESEARCH CENTRE

Report EUR 20412 EN

The mission of IRMM is to promote a common European measurement system in support to EU policies, especially health and consumer protection, environment, agriculture, internal market and industrial standards

EUROPEAN COMMISSION
Directorate-General Joint Research Centre
Institute for Reference Materials and Measurements

EDITORS
This report was produced by Dr. S. Oberstedt (editor) and Prof. Dr. Peter Rullhusen
Inquiries should be addressed to:
The Neutron Physics Unit
Institute for Reference Materials and Measurements,
Retieseweg, B-2440 Geel

Phone +32 14 571 411
Fax +32 14 571 862
E-mail: peter.rullhusen@irmm.jrc.be

WEBSITE
Information on the institute may also be found on the Web page:
http://www.irmm.jrc.be

EUR Report 20684 EN
Luxembourg: Office for Official Publications of the European Communities

ISBN 92-894-5514-4

Printed in Belgium

SCIENTIFIC REPORT

2002

Preface

The year 2002 was the last year of the 5^{th} Framework Programme of the European Commission, and characterised by a transition phase towards the current 6^{th} Framework Programme. Main topics of our work programme addressed issues of nuclear waste transmutation and safety aspects of nuclear energy production, and these will remain the main topics of our research also in the following years. However, the need for maintaining the nuclear competence in Europe results in a widening of our research activities towards more basic physics problems, in order to enhance our contacts to universities and other research laboratories in support of a European Research Area. In the 6^{th} Framework Programme we will increase considerably our efforts to open our facilities to outside users for neutron research at Geel.

Of great advantage for us was the very efficient collaboration with highly qualified colleagues from Candidate Countries to an enlarged European Union. In total, nine colleagues from Bulgaria, Hungary and Romania were working during 2002 at our facilities and contributing to our work programme, as can be seen in the authors lists of the contributions to this report. In addition, five PhD fellows (cat. 20) and four post-docs (cat. 30) were working in our unit, of which four came from Candidate Countries.

On May 23-24, 2002 we had the pleasure to host the annual NEA-WPEC meeting at IRMM, together with the subgroup meeting on model codes, which is organised traditionally two days before the WPEC. The WPEC subgroup on activation cross-section measurements chaired by A. Plompen concluded its very successful activities with a final workshop at IRMM in January 2003.

The Van-de-Graaff accelerator operated very satisfactorily providing beam currents of up to 50 μA on target. New developments for improved cooling of solid TiT targets and for deuterium gas targets will help to increase further the produced neutron fluxes. The new klystrons for sections 2 and 3 of GELINA work very well but the old modulators had many failures, making the machine operation unreliable. In view of the envisaged increase of external groups making experiments at GELINA, this situation needs urgent improvement. We got additional support for upgrading the power supplies of these modulators, which will improve considerably the reliability of the machine. We also acknowledge the additional funding we received for ordering spare klystron units, thus ensuring the GELINA operation for the next Framework Programme.

The collaboration with CEA on neutron data measurements for nuclear waste transmutation continued with transmission and capture measurements on ^{129}I. The measurements were completed and the analysis of the data is progressing. These measurements in the resolved resonance region were complemented with activation cross-section measurements on (n, 2n), (n, p) and (n, α) reactions on ^{129}I in the 16-21 MeV energy range at the Van-de-Graaff accelerator. The previous transmission measurements on ^{237}Np were re-analysed by our colleagues from CEA and published in a CEA report. A final publication and submission of the data to the NEA databank is under preparation.

The measurement activities on ^{232}Th continued with transmission and capture mea-

surements in the resolved resonance region and in the unresolved resonance region up to 100 keV. In the 5-100 keV energy range the GELINA data are in close agreement with previous ORELA measurements indicating a slight underprediction in the ENDF/B-VI file of the order of 10 % in the 5-80 keV energy range and good agreements with this data file at higher energies.
The direct measurements of the ^{233}Pa(n, f) cross-section continued at the Van-de-Graaff accelerator in collaboration with the universities of Örebro and Uppsala. The measurements confirmed the previous findings of much smaller cross-sections as compared to the ENDF/B-VI and JENDL-3 datafiles and also compared to cross-sections deduced from the ^{232}Th(^{3}He, pf) reaction.
The measurement activities at GELINA investigating the (n, n'γ) reaction on structural materials continued with measurements on ^{58}Ni with high energy resolution. These activities will continue in Framework Programme 6 with measurements on Pb isotopes and on Bi.
In collaboration with V. Khriatchkov (IPPE Obninsk) the measurement technique with time-projection chambers was further elaborated at the Van-de-Graaff. It could be shown that in measurements of neutron induced light charged-particle production on light elements using ionisation chambers a kinematical effect (so-called particle-leaking) can lead to considerable underestimation of the cross-section, especially at high neutron energies. Advanced new data acquisition systems using fast signal digitisers improve considerably the accuracy of the experiments. The technique was applied successfully in measurements of the ^{10}B(n, α) cross-section in the 1.5-4.5 MeV energy range at the Van-de-Graaff accelerator.
In collaboration with the University of Delft a very interesting new application of neutron resonance-capture analysis (NRCA) was applied, profiting from the very good neutron energy resolution at the GELINA facility for non-destructive isotopic trace-element analysis of bronze artefacts from Roman/Etruscan origin. The possibility of relying on the high energy resolution of the neutron beam instead of using the spectral analysis of the emitted gamma rays in a conventional neutron activation method resulted in a much-increased sensitivity.

Prof. Dr. P. Rullhusen
Unit Head
Neutron Physics Unit

Neutron data for innovative nuclear applications

The ^{233}Pa fission cross-section.

F. Tovesson [1,2], V. Fritsch [2], F.-J. Hambsch [2], S. Oberstedt [2], A. Oberstedt [1], B. Fogelberg [3], E. Ramström [1,3]

[1] Örebro University, SE-70182 Örebro, [2] EC-JRC IRMM, B-2440 Geel, [3] Uppsala University, Dep. of Rad. Science,, SE-61182 Nyköping

The investigation of the fission cross section of ^{233}Pa has been continued at the IRMM 7 MV Van-de-Graaff accelerator. In contrast to the experimental run of 2001 [1], the region of incident neutron energies was this time situated around the second chance fission threshold. Mono-energetic neutrons are produced via the D(d, n)^{3}He reaction. Typical beam currents were between 20 and 30 μA, yielding neutron fluxes up to about 1.5x10^{7}cm^{-2}s^{-1}. The sample was again prepared at the Studsvik Neutron Research Laboratory, Sweden. The ^{233}Pa sample (0.43 $\pm$ 0.03 μg, having an activity of 0.33 Gbq) was mounted together with a ^{237}Np sample as reference back-to-back in a double Frisch-gridded ionisation chamber.

Based on MCNP calculations an improved shielding was constructed (see Fig. 1). Since this became now much bigger and hence, heavier, the whole setup had to be build up at another beam line, where the floor was stable enough to support the approximately 2.5 tons of weight. The distance of the shielding material to the ionisation chamber was now 1 m.

Cross section measurements with a ^{233}U sample were performed with the final measurement setup, too, in order to identify a possible influence of the shielding on the neutron-energy distribution and therefore, on the obtained effective cross-section measured. This was also done in view of the data reduction, where the contribution from the in-growth of the daughter nucleus ^{233}U with a larger fission cross-section needs to be corrected for. The measurements of the ^{233}Pa(n, f) were carried out in different runs of 10 to 24 hours, in total about 100 hours for each neutron-energy point. A further complication was the fact that with the use of a solid deuterium target additional background neutron sources became apparent at higher energies. Hence supplementary measurements of the neutron spectrum by time-of flight were performed.
For this purpose a NE-213 liquid scintillator was placed 2.3 m away from the neutron producing target to act as a neutron detector. Four neutron energies (6, 6.75, 7.5 and 8.5 MeV) were measured. The neutron detection efficiency was calculated using software codes developed at PTB, Germany [2]. A measured and calculated pulse-height

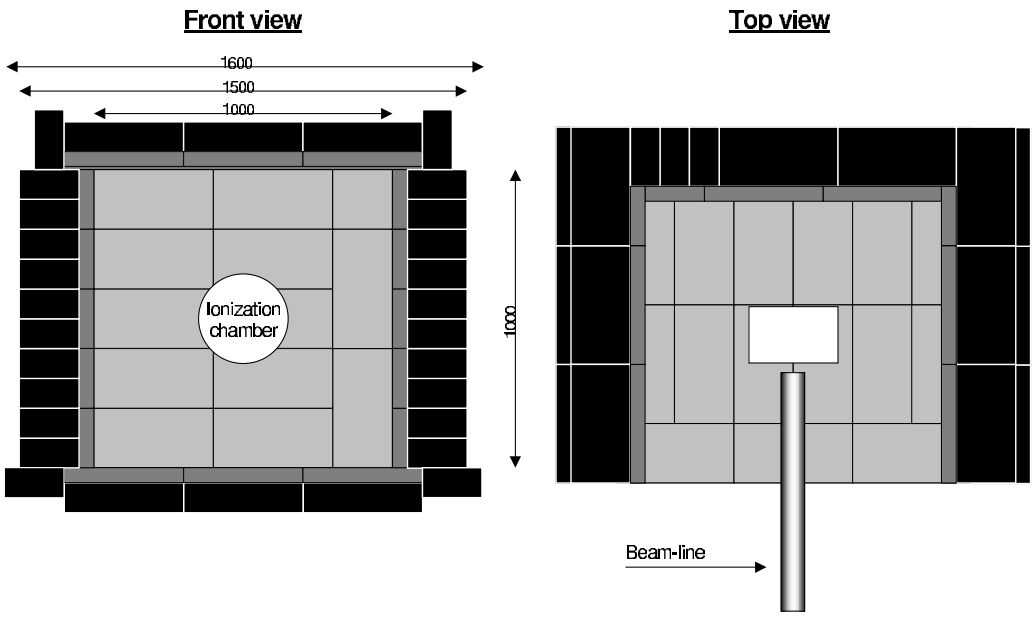

Fig. 1: The shielding design has been optimised on the bases of MCNP calculations. The paraffine and boron-carbide boxes are shown in black and grey, respectively.

distribution is shown in the left part of Fig. 2. In the right part of Fig. 2 the calculated detection efficiency is shown. The efficiency-corrected neutron energy spectra at the four incident neutron energies are finally shown in Fig. 4. It is obvious from this figure, that a low-energetic neutron peak is visible at about 2 MeV and 3 MeV in the spectrum for E_n = 7.5 MeV and 8.5 MeV, respectively. Its contribution has been corrected at those energies, since in the other cases no additional neutron peaks were visible above the detection threshold of the neutron detector.

The very preliminary results of this campaign together with those from 2001 are given in Fig. 5. Again, our results are significantly smaller than those from both evaluated datafiles (ENDF/B-VI and JENDL) and the indirect measurements of Barreau et al. [3]. It is planned to perform a third measurement campaign in the beginning of 2003 to add some additional data points at the first threshold and to verify the second threshold data utilising a deuterium-gas target. In this way no secondary reactions are expected, which might influence the neutron spectrum. Also, the neutron fluence will be significantly higher reducing the overall measurement time.

[1] F. Tovesson, F.-J. Hambsch, A. Oberstedt, B. Fogelberg, E. Ramström, S. Oberstedt, Phys. Rev. Lett. 2002 .

[2] G. Dietze and H. Klein, *NRESP4 and NEFF4 - Monte-Carlo codes for the calculation of neutron-response functions and detection effeciencies for NE213 scintillation detectors*, PTB, Braunschweig, Report PTB-ND-22 (1982)

[3] G. Barreau et al., private communication.

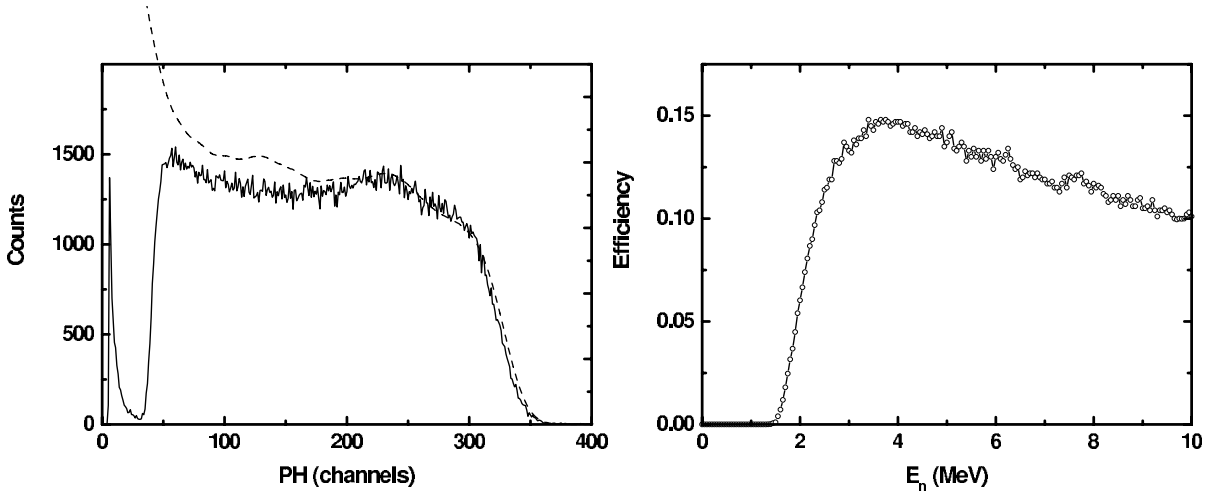

Fig. 2: Left: Measured (solid line) and NRESP-calculated (dashed line) pulse-height response of the NE-213 liquid scintillator up to 6 MeV neutrons [2]. Right: Calculated detection efficiency as a function of incident neutron energy calculated for the scintillator with NEFF [2].

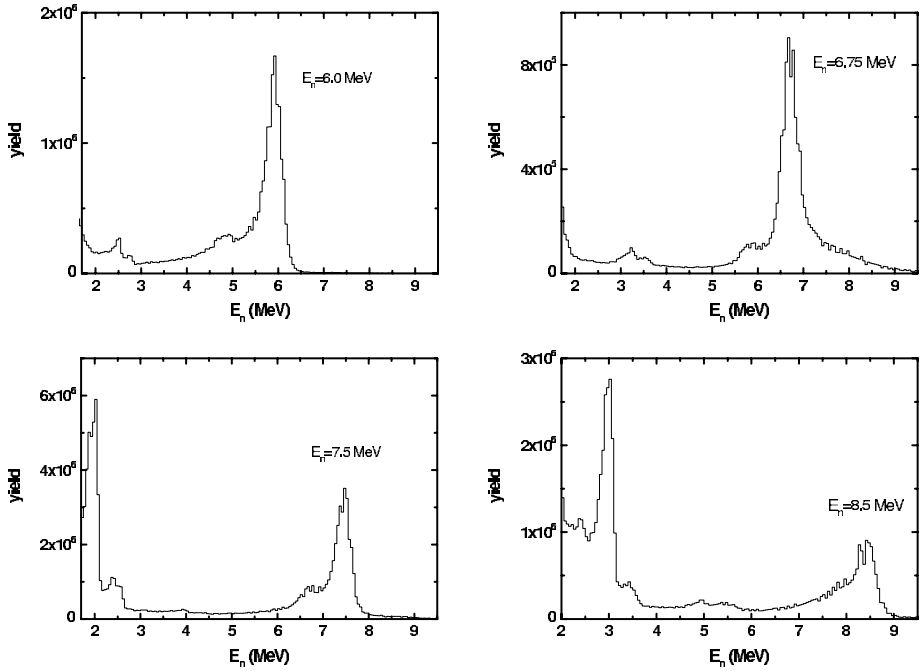

Fig. 3: The efficiency corrected neutron energy spectrum at the measured incident neutron energies given in each figure.

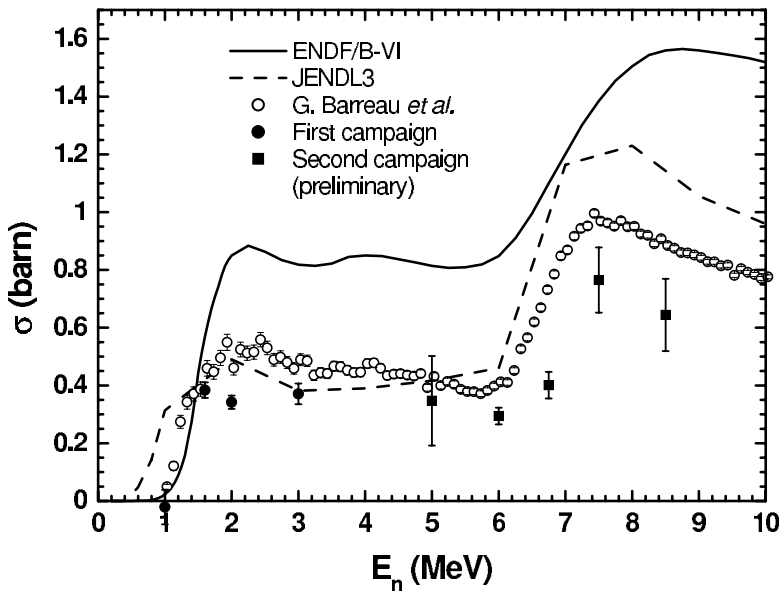

Fig. 4: Preliminary results of the ^{233}Pa(n, f) cross section, compared to evaluations as well as to the indirect measurement of G. Barreau et al. [3]

Determination of the resonance parameters for ^{232}Th from high resolution transmission and capture measurements at GELINA

A. Brusegan[1)], *G. Lobo*[1)], *P. Schillebeeckx*[1)], *A. Borella*[1)], *K. Volev*[2)], *N. Janeva*[2)]

[1] EC-JRC IRMM, B-2440 Geel, [2] INRNE, BG-1784 Sofia

To deduce the resonance parameters for ^{232}Th in the resolved resonance region, high resolution transmission and capture measurements are being performed. The measurements are performed at the Time-Of-Flight facility GELINA. A comparison of experimental data resulting from capture (top) and transmission (bottom) are shown in Fig. 1.

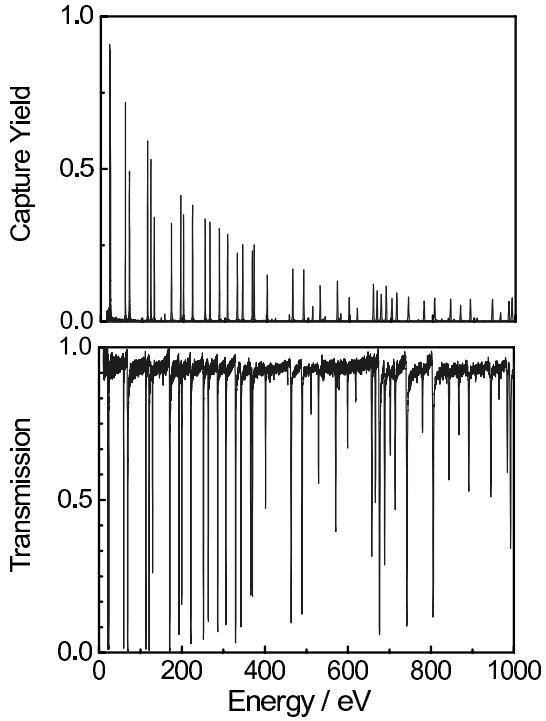

Fig. 1: A comparison of the capture yield (top) and the transmission (bottom) for ^{232}Th in the resolved resonance region up to 1000 eV

The transmission measurements are performed at a 50 m flight path. The neutrons are detected with a 0.25" thick lithium glass (NE912) placed in an Al sphere and viewed by a 5" EMI KQB photomultiplier orthogonal to the neutron beam axis. The injection of a stabilised light pulse in the detector during the measurements provided an efficient tool to control to better than 1 % the gain of the entire electronics. The experimental set-up includes a sample-changer, placed at 23 m from the neutron soruce, which is driven by

the acquisition system. The determination of the flight path length, was based on transmission of the 6.673 eV resonance of ^{238}U. In table 1 we summarise, for the different energy regions of interest, the measurement conditions: the operation frequency of the accelerator and the target thickness. A simultaneous analysis of the data using REFIT will result in the resonance parameters from 0 to 4 keV. In Fig. 2 we show the result of a resonance shape analysis for the resonances at 21.8 and 23.5 eV. The resulting resonance parameters are important for the energy calibration and normalisation of the capture measurements in both the resolved and unresolved resonance region [3].

Tab. 1: The conditions for transmission measurements at 50 m

Energy region	**Operation frequency**	**^{232}Th target thickness**
eV	Hz	at/b
0.14 - 10000	100	$8.51\ 10^{-4}$
11.00 - 10000	800	$34.04\ 10^{-4}$
11.00 - 10000	800	$68.08\ 10^{-4}$
11.00 - 10000	800	$85.10\ 10^{-4}$

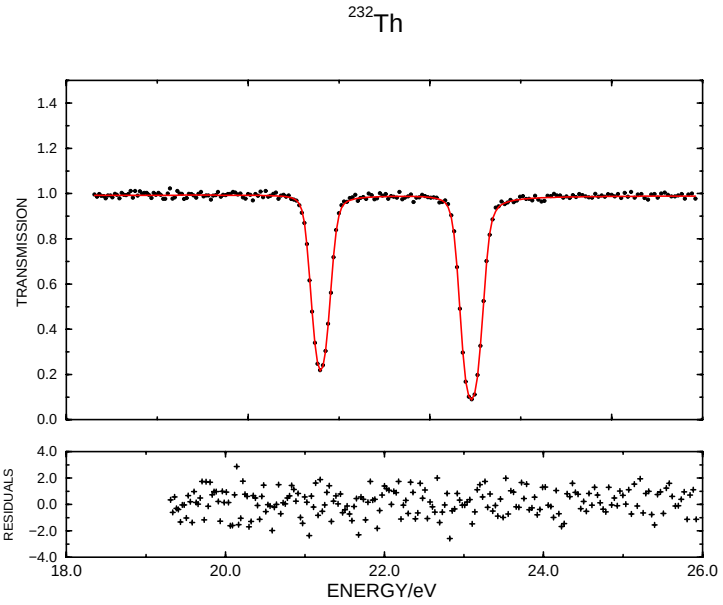

Fig. 2: The result of a resonance shape analysis with REFIT-IRMM for the 21.8 and 23.5 eV resonances of ^{232}Th. The full line is the calculated transmission and the points are the experimental data.

The capture measurements are completed and were performed at a 60 m flight path. The sample consisted of a metallic natural Thorium disc of 8 cm diameter and 1.0 mm thick, corresponding to a thickness of 3.176 10^{-3} at/b. The neutron flux was measured

with an ionisation chamber loaded with three back-to-back layers of about 40 μg/cm^2 ^{10}B. The gamma rays, originating from the ^{232}Th(n,γ) reaction, were detected by four C_6D_6-based liquid scintillators (NE230) placed perpendicular to the neutron beam. Each scintillator is coupled through a boron-free quartz window to an EMI9823-KQB photomultiplier. The pulse height weighting technique is used to derive the capture yield. The interpretation of the data in terms of resonance parameters is in progress, and will be based on a resonance shape analysis using REFIT_IRMM [3]. The energy calibration and normalisation of the capture data will be based on the parameters for the capture areas obtained from transmission measurements.

[1] G. Lobo, F. Corvi, P. Schillebeeckx, N. Janeva, A. Brusegan, P. Mutti, *Measurement of the Th neutron capture cross-section in the region 5 keV-150 keV*, J. of Nucl. Science and Techn., Supplement 2 ND2001 429

[2] A. Brusegan, G. Noguerre, F. Gunsing, *The Resolution Function in Neutron Time-of-Flight Experiments*, J. of Nucl. Science and Techn., Supplement 2 ND2001 685

Measurement of the ^{232}Th capture cross section in the energy region 5 keV - 150 keV

G. Lobo[1]*, P. Schillebeeckx*[1]*, A. Brusegan*[1]*, A. Borella*[1]*, F. Corvi*[1]*, N. Janeva*[2]*, K. Volev*[2]

[1] EC-JRC IRMM, B-2440 Geel, [2] INRNE, BG-1784 Sofia

The ^{232}Th(n,γ) neutron capture cross-section is of great importance for accelerator driven reactor (ADS) systems based on the Thorium-Uranium fuel cycle. An analysis of the required nuclear data [1], reveals that the status of the ^{232}Th capture data is far from the requested 2 % uncertainty level. Recently ^{232}Th average capture measurements, between 5-200 keV neutron energy, were performed at the FzK Karlsruhe (G) [4]. A comparison of the measured averaged capture cross section with the evaluated data files shows a reasonable agreement in the neutron energy range above 15 keV. However, discrepancies of up to 40 % at lower neutron energies are observed. The same order of discrepancies is observed when comparing their results with the results obtained by Macklin et al. [3, 4] at ORELA.

To clarify these discrepancies we measured at IRMM the average capture cross-section at the GELINA facility. The measurements were performed at a 14.37 m flight-path using the Time-Of-Flight (TOF) method. The gamma rays, originating from the ^{232}Th(n,γ) reaction, were detected by a pair of C_6D_6-based liquid scintillators applying the pulse-height weighting method. The neutron flux was measured with an ionisation chamber placed at 80 cm before the Thorium sample. This chamber has a cathode loaded with two back-to-back layers of about 40 μg/cm^2 ^{10}B. The sample consisted of a metallic natural Thorium disc of 8 cm diameter and 0.5 mm thick, corresponding to a thickness of 1.588 10^{-3} at/b.

The background for the capture measurements consists of a time independent and time dependent component. The former, mainly produced by the radioactive decay of the sample, was deduced from measurements with a closed beam. The latter was measured by replacing the Thorium sample with a 0.5 mm thick ^{208}Pb sample of the same size. Such a Pb sample has about the same scattering probability as the Thorium sample and has a negligible capture yield. Therefore, the ^{208}Pb run provides a good estimate of both the so-called ”open beam” background and of the contribution due to scattered neutrons.

The normalisation constant was determined from a resonance shape analysis of the well-isolated and nearly saturated resonances at 21.8 eV and 23.5 eV, with a peak transmission of respectively 4.7 % and 0.9 %. To estimate the systematic uncertainty related to the normalisation procedure, the experimental data were fitted in different energy regions, using resonance parameters from several evaluation data files. The

final normalisation and energy calibration will be obtained with resonance parameters resulting from recent transmission measurements. As discussed in [5] we used the SESH code [1] to correct for self-shielding and multiple scattering effects. The prelimanary capture cross-section values are plotted in Fig. 1, together with the ENDF-B VI values and the experimental data obtained by Wisshak et al. [4], Macklin et al. [3, 4] and Karamanis et al. [7]. Our data in the 5-100 keV region, agree within a 7 % systematic uncertainty with the data obtained by Macklin et al. [3, 4]. We do not confirm the large discrepancies at lower neutron energies reported by Wisshak et al. [4]. Our data between 5-80 keV are systematically 10 % higher compared to the evaluated data. In the 80-100 keV region the differences are much smaller. To confirm the present data an additional measurement campaign, including the measurement of the Au(n,γ) cross-section, was performed. The analysis of these data is in progress.

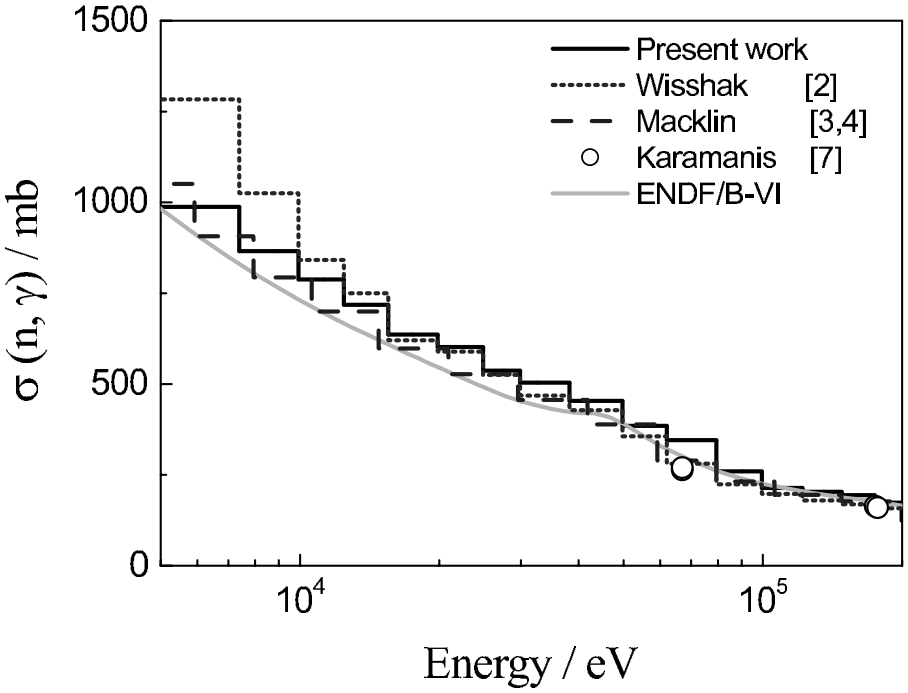

Fig. 1: A comparison of the average cross-section obtained at the IRMM with the ENDF/B-VI evaluation, the data from Wishak et al. [4], Macklin et al. [3, 4] and Karamanis et al. [7]

[1] B.D. Kuzminov, V.N. Manokhin, *Analysis of nuclear data for the Thorium fuel cycle*, Proc. Int. Conf. Nuclear Data for Science and Technology, Trieste, Italy, 19-24 May 1997, Part. II(1997) 1167

[2] K. Wisshak, F. Voss, and F. Käppeler, *Neutron capture cross section of ^{232}Th*, Nucl. Sci. Eng., 137 (2001) 183

[3] R.L. Macklin and J. Halperin, *^{232}Th(n,γ) cross sections from 2.6 to 800 keV*, Nucl. Sci. Eng., 64 (1977) 849

[4] R.L. Macklin and R.R. Winters, *Stable isotope capture cross sections from the Oak Ridge Electron Linear Accelerator*, Nucl. Sci. Eng., 78 (1981) 110

[5] A. Lukyanov, N. Koyumdjieva, N. Janeva, K. Volev, A. Brusegan, P. Schillebeeckx, G. Lobo and F. Corvi, *Neutron Capture of ^{232}Th in The Unresolved Resonance Region - Data Corrections and Analysis*, Nuclear Mathematical and Computational Sciences: A Century in Review, Anew, Gatlinburg, Tennesse, April 6-11, 2003

[6] F.H. Fröhner, Report GA-8380, Gulf General Atomic (1968)

[7] D. Karamanis et al. , Nucl. Sci. Eng., 139 (2001) 282

Determination of the resonance parameters for ^{206}Pb from high resolution transmission and capture measurements at GELINA

A. Borella[1)], *A. Brusegan*[1)], *P. Schillebeeckx*[1)], *G. Aerts*[2)], *F. Gunsing*[2)]

[1] *EC-JRC IRMM, B-2440 Geel,* [2] *CEA Saclay, F-91191 Gif sur Yvette*

The importance of the total and capture cross-section of ^{206}Pb is related to the choice of target, moderator and coolant material in Accelerator Driven Systems. This data can also be incorporated into stellar codes to investigate the details of the s-process models and for a quantitative assessment of the s-process abundance of Pb.
Since for ^{206}Pb the capture width is much smaller than the neutron width ($\Gamma_\gamma \ll \Gamma_n$), transmission and capture measurements are needed for an unambiguous determination of the resonance parameters. The transmission measurements will be performed at a 100 m flight path, with a neutron detector based on a 0.25" thick lithium glass (NE912) placed in an Al sphere and viewed by a 5" EMI KQB photomultiplier. The sample changer is placed at 23 m from the neutron source.
The capture measurements were already started, and are performed at a 60 m flight path. In Fig. 1 we compare the natural line width with the experimental resolution, the Doppler and total broadening. Since the average level spacings for p-wave resonances is about 5 keV, we can conclude that the resolution at 60 m is sufficient to resolve the resonances up to 500 keV. The gamma rays, originating from the ^{206}Pb(n,γ) reaction,

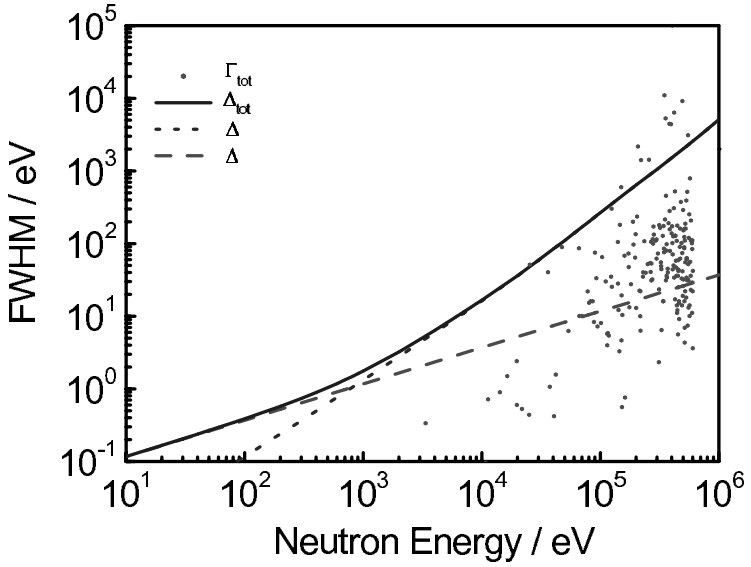

Fig. 1: For ^{206}Pb(n,γ) capture measurements at 60 m, we compare the natural line width with the experimental resolution, the Doppler and total broadening

are detected by four C_6D_6-based liquid scintillators. The pulse-height weighting tech-

nique is applied to make the detection efficiency proportional to the total gamma ray energy of the capture event. The weighting function will be deduced from Monte Carlo simulations [1], which will be verified by experiments. Measurements are performed with the capture detectors placed at 90° and 125° with respect to the neutron beam. Since the radiative decay for ^{206}Pb(n,γ) consists of one or very few gamma rays [2], angular correlation effects for resonances with l $\geq$ 1 may occur. The measurements at 125° eliminate this problem at least for p-wave resonances, which contribute by far the largest amount of capture in the region below 500 keV.

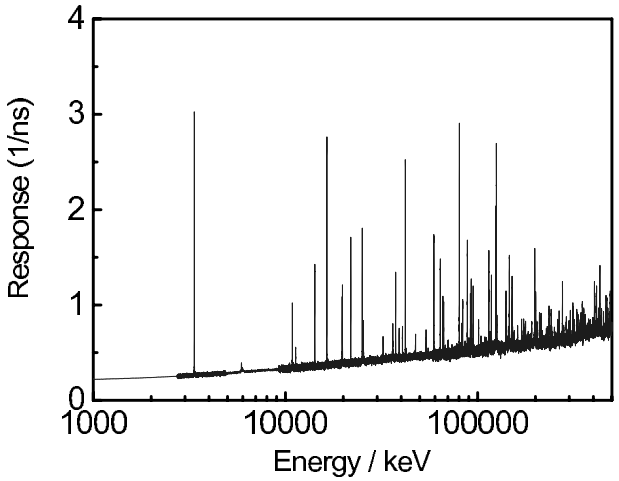

Fig. 2: The response of the capture detetection system for ^{206}Pb(n,γ) measurements at 60 m in the 125° geometry

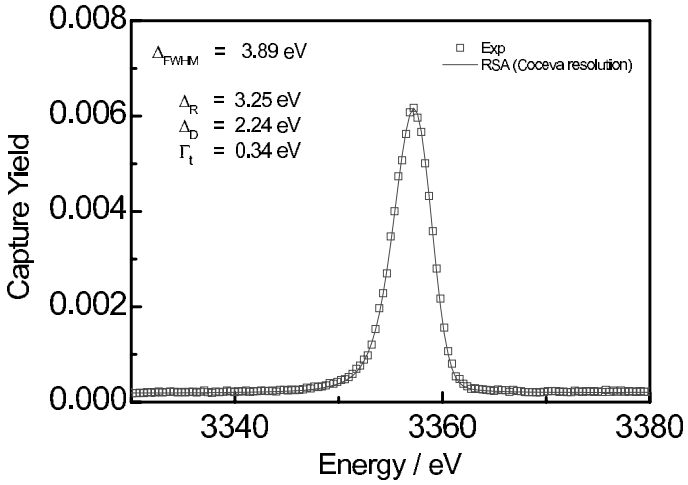

Fig. 3: A comparison of the capture yield for the 3.357 keV resonance of ^{206}Pb with the result of a resonance shape analysis

A typical response of the capture detection sytem for ^{206}Pb(n,γ) is shown in Fig. 2. The result of a resonance shape analysis on the 3.357 keV with the REFIT_IRMM code

[3] is shown in Fig. 3. Since the total broadening mainly originates from the experimental resolution (see Fig. 1), the results in Fig. 3 confirm the good description of the GELINA resolution function in this code [3]. For ^{206}Pb it is difficult to determine the capture area with an accuracy better than 5 % from transmission measurements. Therefore, the capture data will be normalised to the ^{56}Fe(n,γ) resonance at 1.15 keV, the ^{197}Au(n,γ) resonance at 4.9 eV and the ^{109}Ag(n,γ) resonance at 5.2 eV. To account for differences in gamma-ray attenuation between the reference samples and the ^{206}Pb sample, we perform additional measurements with mixed samples. In table 1 the result of normalisation measurements for the 90° geometry based on the ^{109}Ag(n,γ) saturated resonance at 5.2 eV is summarised. The data in table 1 show that about 15 % of the ^{109}Ag(n,γ) capture gamma rays are absorbed in the lead. The final normalisation of the ^{206}Pb data should also account for a difference in gamma ray spectra following the neuton capture in ^{206}Pb and ^{109}Ag. The influence of the gamma transport in the sample will be verified by Monte Carlo simulations.

Tab. 1: The normalisation constants for the different capture measurements performed at the 60 m measurement station. The detectors were placed perpendicular to the neutron beam

Sample	Ag thickness (at/b)	Pb thickness (at/b)	Normalisation
^{nat}Ag (thick)	10.69 10^{-4}		11.679 (0.019)
^{nat}Ag (thin)	4.90 10^{-4}		11.840 (0.025)
^{nat}Ag - ^{nat}Pb	4.96 10^{-4}	32.38 10^{-4}	13.609 (0.024)
^{nat}Ag - ^{206}Pb (sandwich)		35.46 10^{-4}	13.732 (0.024)

[1] G. Aerts, PhD thesis, in preparation

[2] M. Mizumoto et al., *Low-energy neutron resonances in ^{206}Pb*, Phys. Rev. 19 C (1979) 335

[3] A. Brusegan, G. Noguerre, F. Gunsing, *The Resolution Function in Neutron Time-of-Flight Experiments*, J. of Nucl. Science and Techn., Supplement 2 ND2001, 685

The neutron total and capture cross-section of ^{237}Np below 500 eV

A. Leprêtre [1], *A. Brusegan* [2], *N. Herault* [2], *G. Noguère* [2], *P. Siegler* [2], *E. Macavero* [2],

[1] CEA Saclay, F-91191 Gif-sur-Yvette, [2] EC-JRC IRMM, B-2440 Geel

The CEA-IRMM collaboration voices since years the general interest of large nuclear power contractors, like France, in the transmutation of long lived fission products and minor actinides. About 4000 kg of ^{237}Np are produced yearly in the reactors. Having a very long half-life (2.14*10^6 y), ^{237}Np is a noxious minor actinide and a candidate for transmutation a/o incineration due to its potential long- term radiotoxicity. An official request of France has been presented demanding neutron thermal and fast spectra measurements with emphasis on capture cross section data (NEA/NSC/DOC-97-4). For this isotope, the capture cross section is higher than the fission cross section. By the capture of a neutron, ^{237}Np transmutes in ^{238}Np, which undergoes β-decay with 2.1 y half-life to ^{238}Pu. The unsuitable increase of the amount of ^{238}Pu at the end of the process rises questions on the transmutation a/o incineration technique to be used, i.e. suggests resorting to fission ^{238}Np in high thermal flux reactors. The capture cross section of ^{237}Np is known with an accuracy of about 10 % for energies $<$ 100 eV and about 20 % above this energy.

Time-of-flight measurements (TOF) of the total and capture cross sections of ^{237}Np have been performed in the energy range from 0.14 eV up to 2 keV at the white neutron source GELINA of the Institute of Reference Materials and Measurements (IRMM) in Geel, Belgium. In 1999 the total cross section experiments carried out at the 50 m flight-path have been the object of a PHD thesis [1]. Several resonances of ^{237}Np have neutron capture widths greater than or of the order of the scattering widths. Being the fission cross section very small, high-resolution total cross section measurements may provide accurate values of the partial Γ_γ a/o Γ_n widths and at the same time accurate capture areas $g\Gamma_n\Gamma_\gamma/(\Gamma_n+\Gamma_\gamma)$. The present work is a re-analysis of the total cross section data and the results have been already published in a CEA report [2]). The part of the thesis related to the measurements and to the theoretical interpretation of the results is still valid. So are all the studies on the detectors, the samples, the different experimental techniques and the influence of the GELINA beam position. The target of the new analysis is a deeper investigation of the data reduction, of the background determination and of the R-Matrix analysis [3]. Systematic studies have been devoted to the influence of 'non-reproducibility of the measurements' on the final resonance parameters. Finally sensibility studies have been done producing a 'systematic covariance matrix' to be associated to the 'statistical covariance matrix'. The combination of all the sources of errors provides the overall precision of 3 % on Γ_n for the large resonances, and between 3 and 10 % on Γ_γ.

The parameters for more than 500 resonances have been determined in the energy range 0.3 eV - 500 eV. It is worth to say that Auchampaugh [4] could observe a larger number of resonances from his transmission experiment thanks to a thick cooled sam-

ple (77 K) and to a longer flight distance (78 m).

[1] Vincent Gressier, *Nouvelle determination experimentale des paramètres de resonances neutroniques de ^{237}Np en dessous de 500 eV*, PHD thesis, University of Paris XI Orsay, October 1999

[2] A. Lepretre, A. Brusegan, N. Herault, G. Noguere and P. Siegler, *Determination des paramètres de resonances neutroniques deu neptunium 237, en dessous de 500 eV, et otention des matrices de covariances statistiques et systematiques entre les paramètres des ces resonances*, CEA report DSM/DAPNIA-02-374

[3] M.C. Moxon, Refit, AEA-InTec-0470

[4] G.F. Auchampaugh, M.S. Moore, J.D. Moses, R.O. Nelson, C.E. Olsen, R.C. Extermann, N.W. Hill and J.A. Harvey, Los Alamos National Laboratory Report, LA-9756-MS(1983)

Measurements of the ^{127}I(n, γ), ^{127}I(n, tot), ^{129}I(n, γ) and ^{129}I(n, tot) reactions

A. Brusegan[1)], *G. Noguère*[1,2)], *N. Herault*[3)], *A. Leprêtre*[3)], *E. Macavero*[1], *O. Bouland*[1)], *G. Rudolf*[4)]

[1] EC-JRC IRMM, B-2440 Geel, [2] CEA Cadarache, F-13008 St Paul Lez Durance, [3] CEA Saclay F-91191 Gif sur Yvette, [4] IreS, F-67037 Strasbourg

For ^{129}I, a candidate for transmutation [1], neutron capture data have been requested from the thermal and up to the fast energy region (NEA/NSC/DOC-97-4). Measurements of the capture and total neutron cross sections were carried out at the 150 MeV pulsed neutron source GELINA of the Institute for Reference Materials and Measurements (IRMM) [2]. In the transmission measurements neutrons were detected by a Li-glass (NE912) placed at 49.3 m. The neutron capture set-up, located at 28.6 m from the neutron source, consisted of a ^{10}B ionisation-chamber flux detector and of two C_6D_6 liquid scintillators (NE230) placed at 90^o with respect to the neutron beam axis. The weighting method was applied to the capture events in order to obtain a response proportional to the total reaction energy.
Elemental iodine would have been the ideal target material, but after a few tests this was considered not to be practical in view of the radiological hazard, volatility and reactivity of elemental I_2. The compound PbI_2 was considered as a reasonable compromise. Starting from 210 l of waste solution from the french fuel reprocessing plant in la Hague, the separation involved three steps (acidification, oxidation and reduction) in order to obtain the final precipitation of PbI_2 [3]. In total about 140 g of ^{129}I were extracted and canned in four cylindrical Al-containers. The laboratory of the Paul Scherrer Institute (PSI) has determined the lead and iodine mass fraction and the iodine isotope ratio, by inductively coupled mass spectrometry (ICP-MS) and isotope dilution ID-ICP-MS. In addition to PSI complementary activation measurements were performed at the 7 MV van de Graff accelerator of IRMM in order to determine the ^{127}I and the lead mass fractions [4]. The final ^{129}I mass fraction was determined combining those results with iodine isotope ratio measurements done at Geel with the ICP-MS method. The detailed description of the procedure is given in Ref. [5]. The results from PSI are in a good agreement with those of IRMM being the resulting mass fractions of ^{129}I and of ^{127}I about 16.9 % and 3.4 % respectively.

The final capture and transmission spectra obtained from the measurements carried out on two thick PbI_2 samples are plotted in Fig. 1. The results of the simultaneous analysis of the capture and transmission data with the shape analysis programs REFIT and SAMMY are expected to contribute to the improvement of the European neutron data base JEF3.

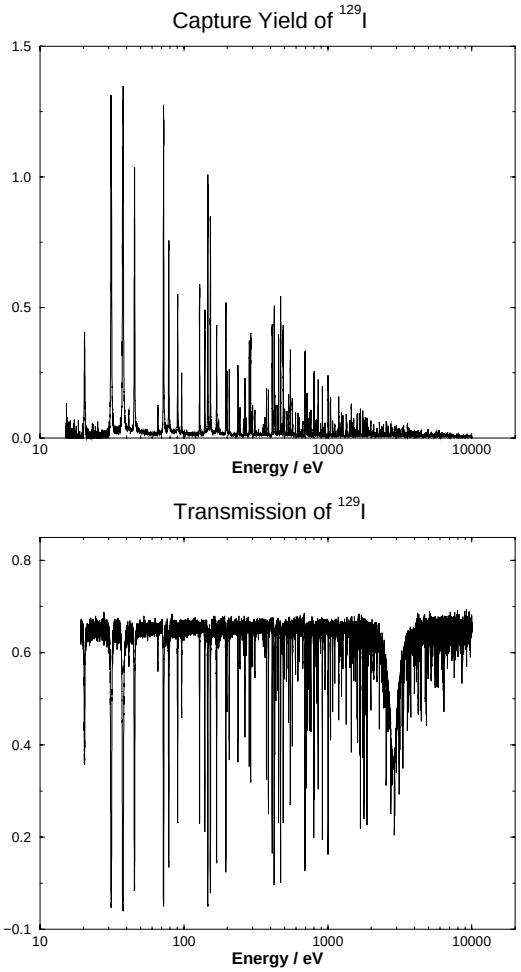

Fig. 1: Capture yield and transmission obtained from the measurement of two thick PbI_2 samples. The samples were a mixture of ^{129}I, ^{127}I, lead, sodium and sulfur.

[1] K. Nishihara, H.Takano, *Transmutation of ^{129}I using an accelerator-driven system*, Nucl.Tech. 135 (2002) 47

[2] G. Noguere, A. Brusegan, A. Lepretre, N. Herault, R. Galleano, E. Macavero, *The neutron total cross section of ^{129}I below 1 keV*, Int. Conf. on nuclear data for Science and Technology, Tsukuba, Japan (2001)

[3] C. Ingelbrecht, J. Lupo, K. Raptis, T. Altzizoglou, G. Noguére, *^{129}I targets for studies of nuclear waste transmutation*, Nucl. Inst. Meth. A 480 (2002)

[4] F. Cserpak, A. Plompen, private communication (2002)

[5] C. R. Quétel et al., *Examination of the performances exhibited by a high-resolution magnetic sector ICP-MS for uranium isotope abundance ratio measurements over almost three orders of magnitude and down to pg/g amount content level*, J.Anal. At. Spectrom 15 (2000) 353

R-matrix analysis of the total cross-section of ^{61}Ni below 100 keV

A. Brusegan, C. Van der Vorst

EC-JRC IRMM, B-2440 Geel

About 20 - 25 % of a large fast power reactor volume is allocated to stainless steel with typical composition: 60 - 70 % Fe; 18 - 20 % Cr; 10 - 13 % Ni; 2 % Mo and Mn. Core neutronics, neutron transport and shielding, gamma decay heating, activation and corrosion are strongly dependent from those materials. The demand [1] of more accurate data for the resonance structure of the neutron cross sections is due to the importance of resonance shielding and Doppler corrections. Since the capture cross measurement yields only values of g $\Gamma_n\Gamma_\gamma/\Gamma$, high resolution total cross section measurements are needed to correct for the multiple scattering in the sample and the neutron sensitivity of the capture γ-ray detectors. Time of flight transmission experiments with a ^{61}Ni sample, 1.902*10^{-2} at/b thick, were performed at the 48 m flight path of the 150 MeV pulsed neutron source GELINA of IRMM. The neutrons, produced by a 1 ns electron burst, were detected by a 5 mm thick sintered B_4C slab viewed by four 5"x2" C_6F_6 liquid scintillators. The metallic sample, on loan from ORNL, contained 91.78 % of ^{61}Ni, 2.06 % of ^{58}Ni, 5.21 % of ^{60}Ni, 0.94 % of ^{62}Ni and a minor contamination ($<$ 0.05 %) of ^{64}Ni. The transmission spectra, see Fig. 1, were analysed with the R-Matrix code REFIT [2, 3] modified to access Monte-Carlo estimates of the GELINA resolution function [4].

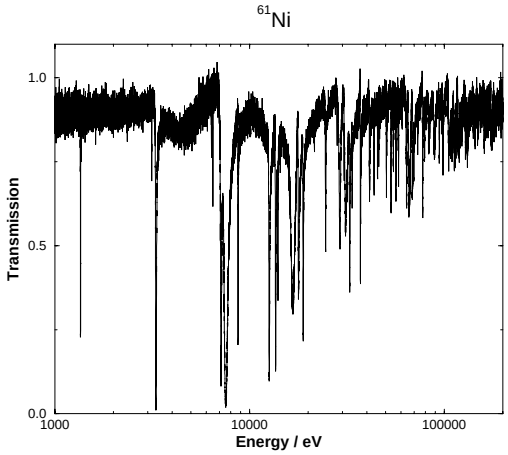

Fig. 1: ^{61}Ni transmission spectrum for a 1.902$\times$10^{-2} at/b sample.

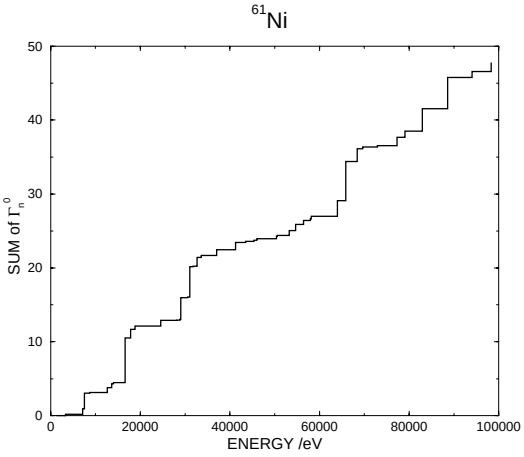

Fig. 2: Sum of the reduced neutron width Γ_n^0 of ^{61}Ni for the 44 s-wave resonances observed below 100 keV.

Neutron widths and, in few cases, Γ_γ-widths have been determined for about 100 resonances in the given energy range up to 100 keV, i.e. well above the 69 keV of previous experiments. Of the 44 s-wave resonances in the energy range up to 100 keV, 8 have

energies larger than 69 keV. The 36 s-wave levels below this energy include 6 new resonances, 4 spin re-assignments and 2 orbital momentum re-attribution. In the same energy interval, the calculated strength function, S_0 = (5.2$\pm$1.2)$\times 10^{-4}$ (see Fig. 2), is larger than the value of (3.2$\pm$0.8)$\times 10^{-4}$ given in Refs. [5, 6]. The observation and the assignment of new s-wave resonances seem to be the cause of the discrepancy. For the total number of levels up to 100 keV the strength function is S_0=(4.8$\pm$1.0)$\times 10^{-4}$. The quoted errors on S_0 are calculated as $(2/N)^{1/2} S_0$. For all the s-wave resonances Fig. 3 shows the cumulative distributions of the reduced neutron widths Γ_n^0. The comparison of the J = 1 with the J = 2 distributions suggests a lack of small J=1 levels having Γ_n^0 less than 0.05. Missing resonances may account for the difference between the calculated average s-wave spacing, D_0 = (2.25$\pm$0.18) keV, the result of the fit, D_0 = 2.03 keV, and the value of D_0 = (1.8$\pm$0.3) keV given in Ref. [5]. The quoted error on D_0 is calculated from the formula $((4 - \pi)/\pi N)^{1/2}$. The potential scattering length for s-waves resonances is (R'/fm=7.64$\pm$0.23) to be compared with the value (R'/fm=6.5$\pm$0.3) in Ref. [5].

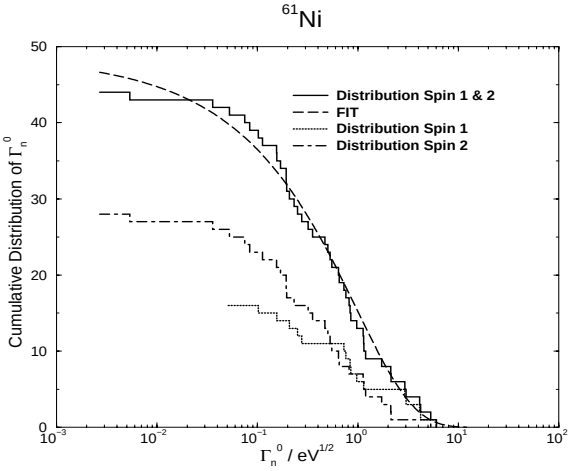

Fig. 3: Cumulative distributions of the s-wave reduced neutron widths of ^{61}Ni for spins J = 1 and J = 2. A fit is shown for the cumulative distribution of all the s-wave levels.

[1] J.L. Rowlands, *Nuclear Data for Reactor design, Operation and Safety*, Proc. Conf. On Neutron Physics and Nuclear Data, Harwell (1978)

[2] M.C. Moxon, AEA-InTec-0470M

[3] A. Brusegan, *REFIT-IRMM modified to access Monte-Carlo calculation*

[4] C. Coceva, A. Magnani, *Resolution of a Rotary Target*, EC-JRC IRMM Internal report, GE/R/ND/96 (1996)

[5] S. F. Mughabghab, M. Divadeenam, N. E. Holden, Neutron Cross Sections (1981) Vol 1

[6] S. F. Mughabghab, Neutron Cross Section and Technology, Knoxville, Tenn. (1971) 386

Neutron activation cross-sections on different isotopes of Ni and Co for 14 to 21 MeV incident energy.

V. Semkova[1,2]*, V. Avrigeanu*[1,3]*, A. J. Koning* [4]*, A. J. M. Plompen*[1]

[1] EC-JRC IRMM, B-2440 Geel, [2] INRNE, BG-1784 Sofia, [3] NIPNE-IFIN, RO-76900 Bucharest, Romania, [4] NRG, NL-1755 ZG Petten

The energy range of interest for ADS extends up to a few GeV, neutrons with energy below 20 MeV play a considerable role with regard to hydrogen and helium gas production and the number of displacements per atom. Those effects are caused by (n, xp), (n, xα) reactions, which are extensively studied in the present work. Precise cross sections above 14 MeV are still sparse although these are important for high energy dosimetry, estimation of damage rates and activation level of structural materials of high energy accelerator based neutron fields. The isomeric cross section ratios are of fundamental interest for the investigation of the nuclear spin and structure effects in the formation of isomeric states. The survey of the available data pointed out the needs for extensive studies in order to achieve better understanding of quantitative formation of isomeric states.

Tab. 1: Isotopic abundance (in %) of the used natural and enriched Ni samples.

A	^{61}Ni	^{nat}Zr
58	2	68.077(9)
60	9.89	26.223(8)
61	86.2±0.6	1.14(1)
62	1.81	3.63(2)
64	0.1	0.926(1)

Measurements with the activation technique were done at the 7 MV Van-de-Graaff accelerator with neutrons produced via the T(d, n) reaction at deuteron energies of 1, 2, 3 and 4 MeV. Samples were placed at angles from 0 to 125 degrees to obtain incident neutron energies from 13.3 to 20.5 MeV. Natural metal Co foils with 99.99 % purity were used for (n, 2n) reaction cross sections on ^{59}Co. The samples were prepared by punching discs of 13 mm diameter and 0.125 mm thickness from metallic cobalt sheets. For ^{59}Co(n,2n)^{58}Co^{m,g} isomeric cross-section ratio, measured by complex decay curve of ^{58g}Co, larger samples with 20 mm diameter and 5 m thickness were used, in order to achieve sufficient measurement statistics.
Reaction cross sections on Ni were measured using natural metallic Ni foils 13 mm diameter, 0.1 mm thick with 99.995 % purity (supplied by Goodfellow Metals, Cambridge,

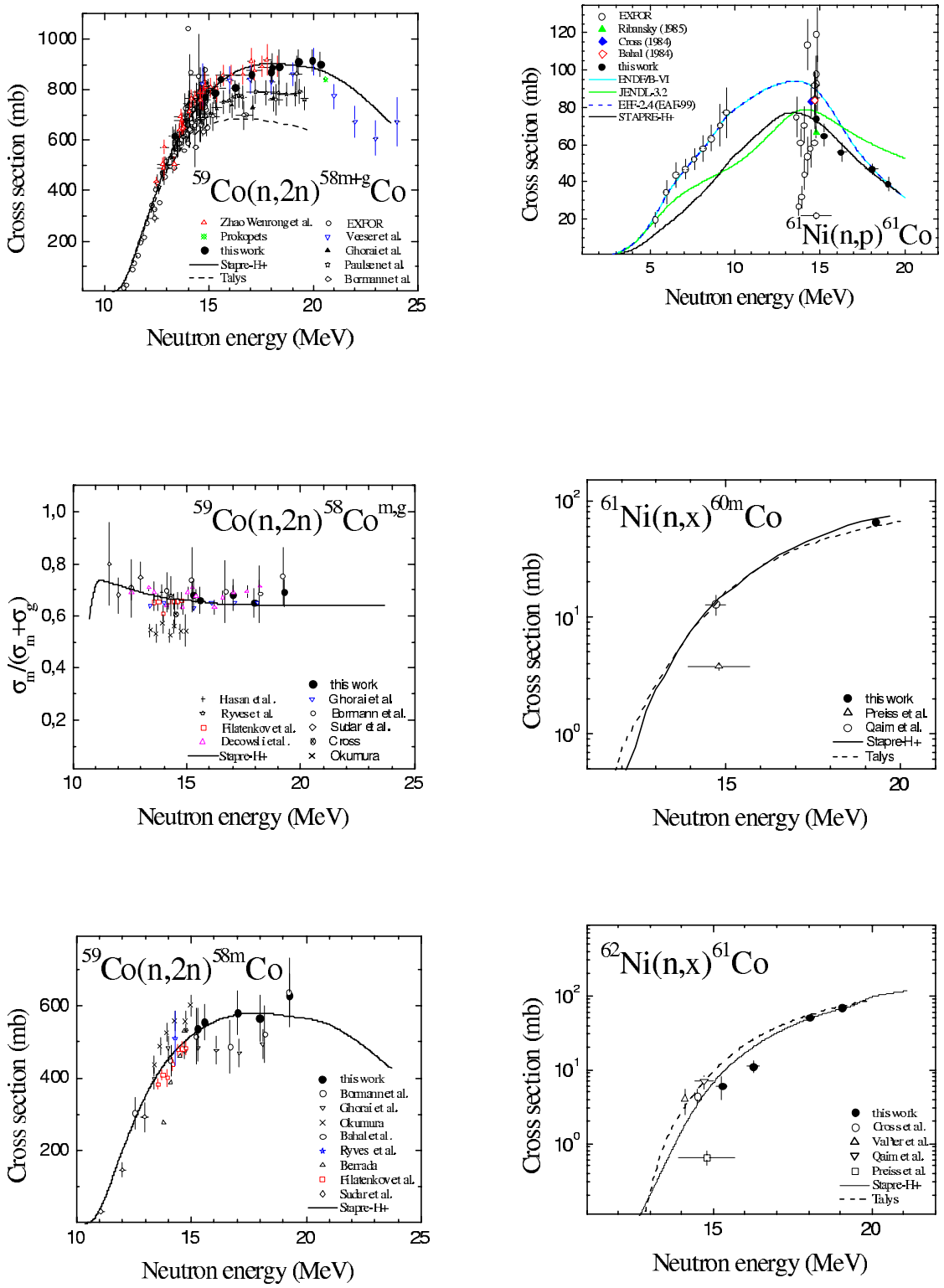

Fig. 1: New measurements for isotopes of Ni and for ^{59}Co compared with available measurements, evaluations and the new model calculations.

UK). In the investigated energy range (n, n'p) reaction channel is open. To distinguish between activities produced by ^{60}Ni(n, p) and ^{61}Ni(n, n'p) and respectively by ^{61}Ni(n, p) and ^{62}Ni(n, n'p), the sample, enriched in ^{61}Ni supplied by JSC "JV ISOFLEX", Moscow, Russia, was used as well. The sample was in a powder form and had a weight of 50 mg. It was filled in Al-container with 13 mm diameter. The container was filled up with filter paper and glued. The isotopic compositions of the used Ni samples are shown in Tab. 1.
The ^{59}Co(n, 2n)$^{58m+g}$Co reaction is recommended as secondary standard for the flux measurements. As can be seen from the graph both experimental data and evaluations differ considerably. Isomeric cross section ratio ^{59}Co(n, 2n)^{58m,g}Co were determined from complex decay curve of the ground state and ^{59}Co(n, 2n)^{58m}Co were deduced from isomeric cross section ratio and total ^{59}Co(n, 2n) reaction cross section.

Experimental data are in a good agreement with STAPRE-H code calculations, see Fig. 1. Very few experimental data exist in the literature for ^{61}Ni(n, x)^{60m}Co and ^{62}Ni(n, x)^{61}Co reaction cross sections, in both cases around 14 MeV. Our data agree relatively well with model calculations. There are big discrepancies between data for ^{61}Ni(n, p)^{61}Co reaction cross section around 14 MeV. Our results above 15 MeV are unique. Our measured data are in good agreement with model calculations.

Neutron activation cross-sections on different isotopes of Zr for 15 to 21 MeV incident energy.

V. Semkova [1,2], *A. J. M. Plompen* [1]

[1] EC-JRC-IRMM, B-2440 Geel, [2] INRNE, BG-1784 Sofia

The neutron spectrum in a fusion reactor or in an Accelerator Driven System (ADS) is extended above the traditional limits for fission reactors. This reflects in general different and more complex radioactivity induced by those neutron fields. This results in a larger number of open reaction channels, i.e. besides elastic, inelastic scattering, radiative capture also the threshold (n, 2n), (n, p), (n, α), (n, np), (n, d), (n, 3n), (n, nα) reactions. This causes both the production of different end products from a given target nuclide or the same end product produced by different routes. Although the energy range of interest for ADS extends up to a few GeV, neutrons with energy below 20 MeV play a considerable role with regards to hydrogen and helium gas production and the number of displacements per atom. Those effects are caused by (n, xp), (n, xα) reactions, which are extensively studied in a present work.
Measurements with the activation technique were done at the 7 MV Van de Graaff accelerator. Quasi-monoenergetic neutrons were produced via the T(d, n) reaction at deuteron energies of 1, 2, 3 and 4 MeV. Samples were placed at angles from 0 ^{o} to 75 ^{o} to obtain incident neutron energies from 15 to 20.5 MeV. In addition to the natural samples, a set of enriched isotopes was also irradiated in order to determine the cross sections for the interfering reactions. The enriched samples were borrowed from Japanese Atomic Energy Research Institute, Tokai-mura, Japan and made by wrapping in small paper envelopes of 1 cm^2 size. The isotopic composition of the used Zr samples is shown in Tab 1. In all cases, the beam intensity variation was measured

Tab. 1: Isotopic abundance a (in %) of the used natural and enriched Zr samples (data supplied from manufacturer).

A	^{90}Zr	^{91}Zr	^{92}Zr	^{Nat}Zr
90	99.36±0.10	3.24±0.01	2.38±0.01	51.45(40)
91	0.3±0.01	94.59±0.10	1.08±0.01	11.22(5)
92	0.17±0.01	1.63±0.01	95.36±0.10	17.15(8)
94	0.12±0.01	0.46±0.01	1.06±0.01	17.38(28)
96	0.04±0.01	0.08±0.01	0.12±0.01	2.8(9)

and corrected for by the use of a BF_3 proportional counter, the count rates of which were stored in multi-channel scaling mode. Neutron attenuation, neutron scattering, sample geometry, and the neutron source angular distribution were accounted for by use of the MCNP-4C code. Depending on the threshold of the reaction studied, use

was made of the ^{115}In(n, n'), ^{58}Ni(n, p), ^{27}Al(n, p), ^{27}Al(n, α), ^{93}Nb(n, 2n), standard cross sections. Normalisation to the data was done relative to the ^{27}Al(n, α)^{24}Na ENDF/B-VI standard cross section. The induced radioactivity was measured using standard gamma-ray spectroscopy.

Results: Results of new activation cross section measurements are presented in Fig. 1 together with those available from literature for the following neutron-induced reactions: ^{90}Zr(n, α)^{87m}Sr [1, 2, 3, 4], ^{90}Zr(n, p)^{90m}Y [2, 3, 5], ^{91}Zr(n, p)^{91m}Y [4, 5], ^{91}Zr(n, x)^{90m}Y [3], ^{92}Zr(n, p)^{92}Y [3], ^{92}Zr(n, x)^{91m}Y [3, 5]. The presented reaction cross sections have been measured for the first time in the investigated energy range and match the previously published data at 15 MeV. The results for ^{90}Zr(n, α)^{87m}Sr, and ^{92}Zr(n, p)^{92}Y, reactions are in a good agreement with EAF-99 and ADL-3 evaluations, respectively.

[1] R. Pepelnik, B. Anders, B.M. Bahal, *Measurement of 14 MeV Neutron Activation Cross Sections*, Int. Conf. On Nucl. Data for Basic and Applied Science, Santa Fe, New Mexico, 13-17 May 1985

[2] A. Marcinkowski, U. Garushka, H. M. Huang, D. Kielan, and B. Zweglinski, *Cross Section of the (n, p) Reaction on Zirconium Isotopes*, NPA 510 (1990) 93

[3] Y. Ikeda, Ch. Konno, K. Oishi, T. Nakamura, H. Miyade, K. Kawade, H. Yamamoto, and T. Katoh, *Activation Cross Section Measurements for Fusion Reactor Structural Materials at Neutron Energy from 13.3 to 14.9 MeV Using FNS Facility*, JAERI 1312, Tokai-mura (March, 1988)

[4] A. Grallert, J. Csikai, Cs. M. Buczko, and I. Shaddad, *Investigations on the Systematics in (n, α) Cross Sections at 14.6 MeV*, INDC(NDS)-286, IAEA, Vienna, November 1993, p.131

[5] A. A. Filatenkov, S. V. Chuvaev, V. N. Aksenov, V. A. Yakovlev, A. V. Malyshenkov, S. K. Vasilev, M. Avrigeanu, V. Avrigeanu, D. L. Smith, Y. Ikeda, A. Wallner, W. Kutschera, A. Priller, P. Steier, H. Vonach, G. Mertens, and W. Rochow, *Systematic Measurement of Activation Cross Sections at Neutron Energies from 13.4 to 14.9 MeV*, IAEA Report INDC(CCP)-402, Vienna, 1997; Khlopin Radium Institute Report RI-252, St. Petersburg, 1999

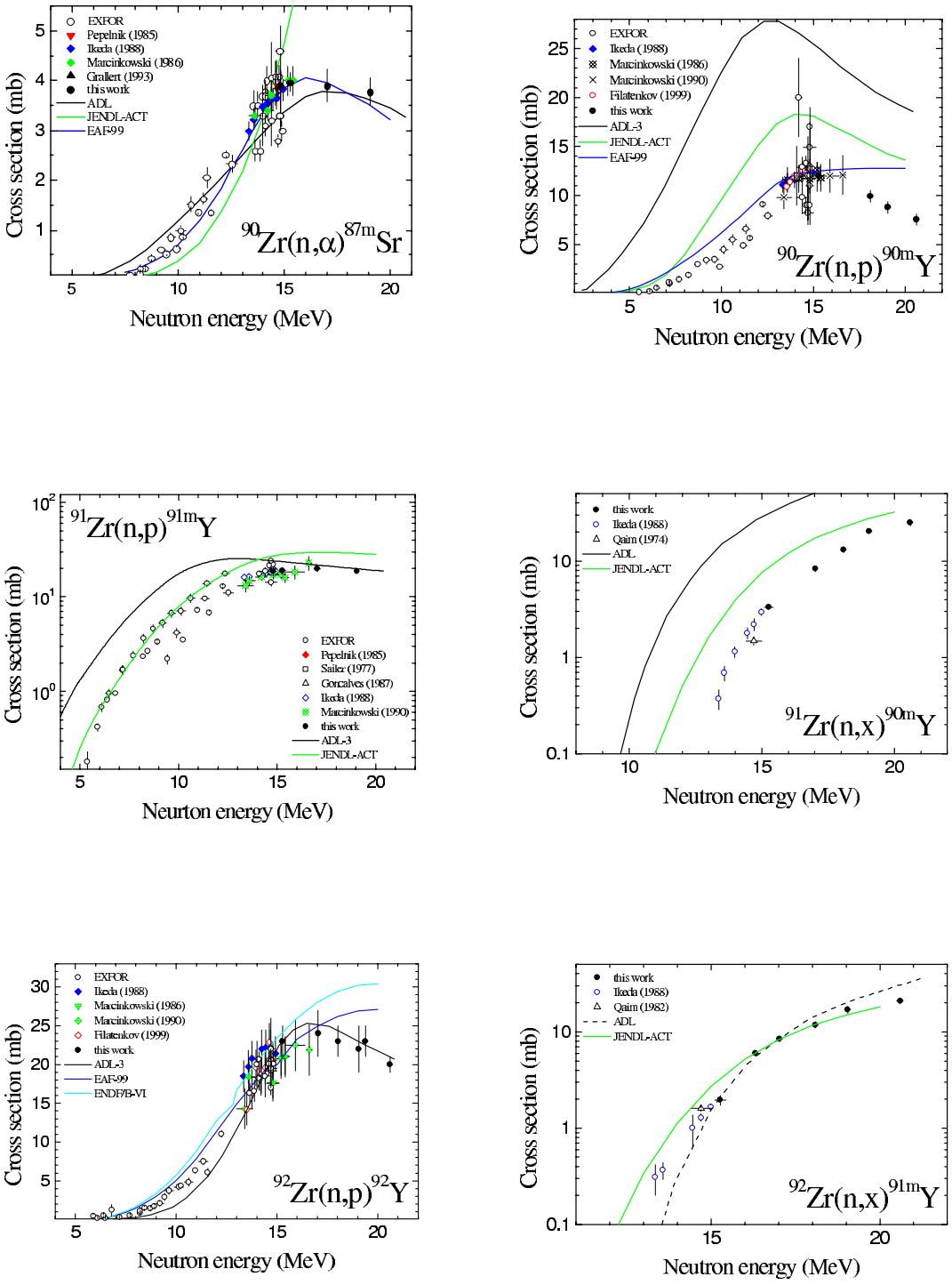

Fig. 1: New measurements for Zr compared with available measurements and evaluations.

Measurements and nuclear model calculations for neutron induced reactions on ^{127}I, ^{129}I isotopes up to 21 MeV

F. Cserpák[1,2]*, S. Sudár*[1,2]*, A. J. M. Plompen*[1]*,*

[1] EC-JRC IRMM, B-2440 Geel, [2] IoEP, University of Debrecen, H-4001 Debrecen,

Abstract

Excitation functions were measured by the activation technique for the ^{127}I(n, 2n)^{126I}, ^{129}I(n, 2n)^{128}I, ^{129}I(n, p)^{129}Te and ^{129}I(n, α)^{126}Sb reactions from 16 MeV to 21 MeV neutron energy. Isomeric cross-section ratios for the ^{129}I(n, p)^{129m,g}Te, ^{129}I(n, α)^{126m,g}Sb reactions were also determined. The irradiations were performed at the Geel Van de Graaff accelerator. Quasi mono-energetic neutrons were produced via T(d, n)^{4}He reaction. The radioactivity of the activation products was determined by high resolution γ-ray spectrometry. For most of the reactions on the radioactive ^{129}I isotope, the present measurement provides the first consistent set of data. Statistical model calculations taking into account the precompound effects were performed for all reactions, and acceptable agreement was found with the measured data.

Introduction

The measurement of cross sections with the activation technique is an efficient method to survey the status of our knowledge with regard to (n, xn), (n, xp) and (n, xα) reactions and of course for reactions leading to activation product.
The special interesting of this measurement is that the ^{129}I isotope is a fission product. This is why only a few experimental data exist for this neutron induced reactions.

Experimental techniques

Cross sections were measured by activation technique, commonly used at Geel.

a. **Samples**
Iodine samples were prepared from nuclear waste in the form of PbI_2 compound, encapsulated in Al or plexi-glass cylinder. The inner diameter of one sample was 14 mm, thickness of the wall was 0.5 mm, the thickness of the sample was about 2.5 mm. The total mass of the encapsulated powder in one sample is near 2 g including PbI_2 and other compounds. It is evident that the samples contain both iodine isotopes ^{127}I and ^{129}I. In addition to the cross-section measurement, detailed investigation was performed to determine the ^{127}I, ^{129}I and Pb content of the samples. Gamma attenuation method and comparative neutron activation technique were used to determine the ^{127}I and Pb content of the sample, while the m(^{129}I)/m(^{127}I) ratio was determined by mass spectrometry at IRMM.

b. **Irradiation**

All samples were irradiated at the Geel 7 MV Van-de-Graaff accelerator. Neutrons from 16 to 20.7 MeV were obtained by use of the T(d, n) reaction with deuteron energies of 1, 2, 3, and 4 MeV and a titanium-tritide target of 2 mg/cm^2. The used irradiation setup is a light weight holder that allows samples to be placed from 1 to 5 cm from the neutron producing target with angles varying from 0 ^{o} to 135 ^{o} with respect to the incident deuteron beam. In this setup the influence of multiple scattering is less then 2 % for the investigated reactions. For the cross section measurements the samples were placed at 0 ^{o} to the beam and about 2 cm distance from the target. Depending on the half life of the reaction product, the irradiation time varied from 1 hour to 3 days. In all cases the beam intensity variation is measured and corrected for by the use of a BF_3 proportional counter, the count rates of which are stored in multichannel scaling mode. For determination of neutron fluences the ^{27}Al(n, p), ^{27}A(n, α) and ^{93}Nb(n, 2n) standard cross sections were used. Monitor foils were attached to the front and the back of the samples. The mean fluences for the samples were calculated by volume integrated method.

c. **Activity determination**

Activities of all irradiated samples and monitors were determined by γ-ray counting. For all measurements the same HPGe detector was used which was calibrated with point sources obtained from PTB and DAMRI. Corrections were made for summing coincidence, self absorption and sample size.

Nuclear model calculations

a. **Calculation with STAPRE code**

Nuclear reaction model calculations were performed using the computer code STAPRE [1]. The preequilibrium emission was taken into account by the exciton model formalism while the width-fluctuation corrected Hauser-Feshbach formula was used for first chance emission from the equilibrated system. Direct interactions were taken into account by using Multi Step Direct reaction cross section calculated by the EMPIRE-II code [2]. The absorption cross section was reduced by the according to the MSD and the (n, n') reaction were corrected by the MSD contribution. The particle transmission coefficients were generated via the spherical optical model using the computer code SCAT 2 [3]. For the energy and mass dependence of the effective matrix element of the internal transition, the $|M|^2$ = FM/(A^3E) formula was used. The FM value was dependent on the used level density formalism. For the preformation factor of the α-particles, a value of 0.25 was used in the formulation of the emission rates. The excited states of the product nuclei were described by the available information on the discrete levels using the ENSDF data files of Brookhaven National Laboratory, USA. At higher energies the levels were treated as a continuum, described by the back-shifted Fermi gas model [4]. The selection method of the level density parameters is described below. The transmission coefficients of photons have considerable significance in

calculations on isomeric cross sections. They were derived from the gamma-ray strength functions. For the E1 radiation, the Brink-Axel model (1952) with global parameters was applied, while for the M1, E2, M2, E3 and M3 radiation the Weisskopf model was used. The unknown branching ratios for the discrete levels were calculated using the gamma transmission coefficients calculated in a way similar to that implemented in the STAPRE for the continuum.

b. **Calculation with EMPIRE-II code**
The version 2.16 of the EMPIRE (Montenotte) code was used for the calculation. The standard library of input parameters were used which include the nuclear masses, optical model parameters, ground state deformations, discrete levels and decay schemes, level densities, moments of inertia (MOMFIT), and strength functions. The particle transmission coefficients were generated via the spherical optical model using the computer code (SCAT2) using the default set of global parameters: Wilmore-Hodgson [5] for neutrons, Bechetti Greenless [6], and for α-particles, Avrigeanu's [7] potential. In the calculation the Multi Step Direct, Multi Step Compound and Hauser-Fesbach model with width fluctuation correction (HRTW) were used. The code conserves particle flux by dividing the absorption cross section of the optical model between the different types of reaction mechanism. For the level densities, the dynamic approach of the EMPIRE-II was used. In this case the formalism of the super-fluid model (BCS) is applied below the critical excitation energies and the Fermi gas model above the critical energy. Selection of the optical model parameters (OMP) for model calculation on ^{127,129}I target nuclei were based on the measured total cross section data of ^{127}I and ^{129}I which were collected from the EXFOR database. Detailed studies were available only for the ^{127}I isotope. The transmission coefficients were calculated by the SCAT-2 optical model (OM) code. Global and local OM parameters were tested for the calculation by comparing the experimental data with the model calculation. The best average deviation between the calculate and measured total cross sections was getting by using the global Wilmore-Hodgson [5] parameters or Koning's [8] local and global OM parameters for both silver and iodine. The level density parameters a for the calculation were selected by interpolating the data of the neighboring isotopes, taking into account the odd-even systematic from the Plyaskin data [9]. The back shift parameter ($\triangle$) was determined individually for all nuclei used in the model calculation. The cumulative plot of the known discrete levels, collected from the ENDSF database, was fitted by the BSFG formula while the level spacing at the neutron biding energy were kept on the experimental value.

Results

a. **^{127}I(n, 2n)^{126}I reaction**
The measured and calculated excitation functions of ^{127}I(n, 2n)^{126}I reaction are shown on Fig. 1. Besides the 14 MeV data more cross sections were measured in wider energy range (Santry, Lu Han Lin, Martin, Bormann). The data

of Santry and Lu Han Lin seems to be agreeing within the error limit. Martin's and Bormann's data significantly lower. The present measurements at IRMM are in agreement with Santry's and Lu Han Lin's data. The model calculation both STAPRE and EMPIRE are near to the experimental data, especially above 16 MeV. Below this energy, the calculations lower than Santry's and Lu Han Lin's data and the EMPIRE gives better values.

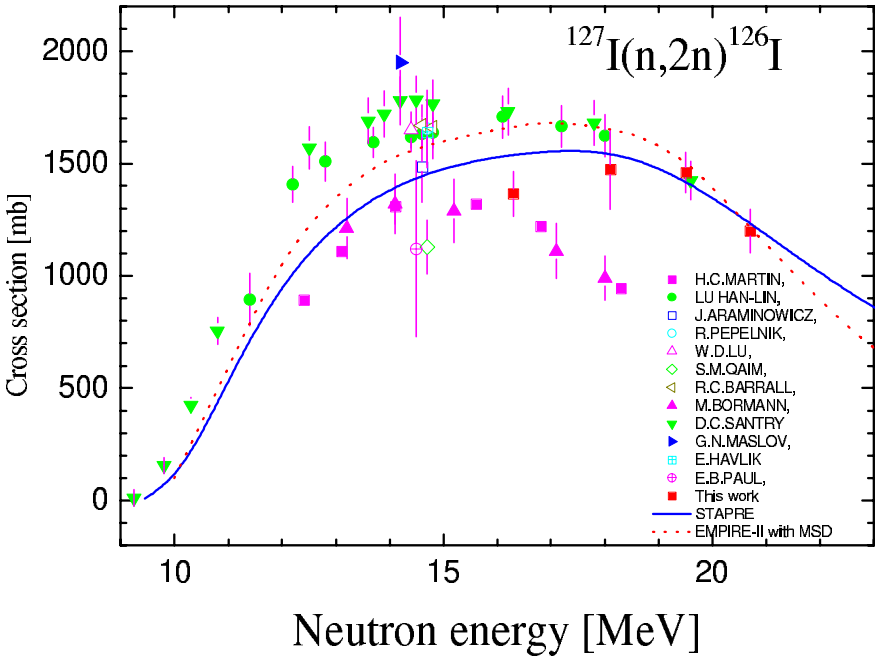

Fig. 1: Measured and calculated excitation functions for the ^{127}I(n, 2n) ^{126}I reaction

b. **^{129}I(n, 2n)^{128}I reaction**

The cross section for the radioactive nuclei, like ^{129}I, was even less studied. Only the ^{129}I(n, 2n)^{128}I reaction was studied in the 14 MeV region earlier. The measured cross section and the calculations are shown on Fig. 2. The latest measured data agree with our measurements and shows relatively lower values than expected from the systematic and the model calculation using the global OM parameters. Both the STAPRE and the EMPIRE overestimate the measured data using these parameter sets. To describe better the experimental data, the parameters of the optical model were modified. The calculation with these parameters is show by the continuous line on Fig. 2. The absorption cross section has also decreased by the new parameters and therefore both the calculated (n, p) and (n, α) cross sections decreased achieving better agreement between the model calculation and experimental data.

c. **^{129}I(n, p)^{129m,g}Te reactions**

The final nucleus of the ^{129}I(n, p)^{129}Te reaction has an isomeric state taking possible to study production both the isomeric and ground states. The Figs. 3 and 4 depict the measured and calculated excitation function of ^{129}I(n, p)^{129g}Te and ^{129}I(n,

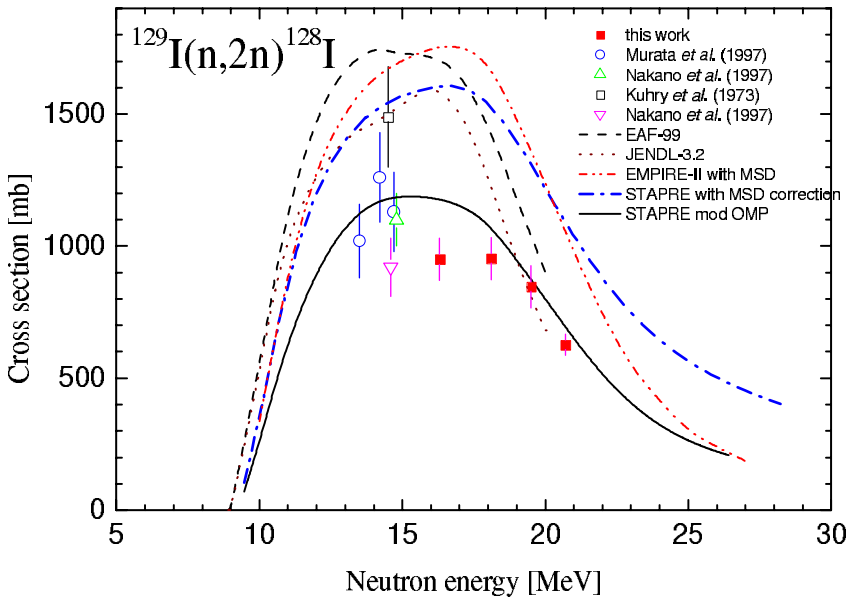

Fig. 2: Measured and calculated excitation functions for the ^{129}I(n, 2n) ^{128}I reaction

p)^{129m}Te reaction respectively. The EMPIRE gives quite low cross section comparing with the experiment, in spite of that the used OMP overestimate the (n,2n) excitation function. The STAPRE with the modified OM parameters in the neutron channel describe the magnitude the cross section quite well, but the shape of the excitation function is not fully agree with the experiment. The STAPRE without precompound emission gives similar values as the EMPIRE, indicating that the main contribution arrives from the precompound emission. The dotted lines show the uncertainties of the calculation based on the estimated uncertainties of the model parameters. (This uncertainty does not include the uncertaintiy connected to the absorption cross section reduction caused by the change of the OMP parameters, which would be quite high.)

d. **^{129}I(n, α)^{126m,g}Sb reactions**

Figs. 5 and 6 present the measured and calculated excitation function of ^{129}I(n, α)^{126g}Sb and ^{129}I(n, α)^{126m}Sb reaction respectively. The EMPIRE code gives quite low cross section comparing with the experiment, similarly to the (n, p) excitation functions. The STAPRE with the modified OM parameters in the neutron channel describe the magnitude the cross section quite well, but the shape of the excitation function is not fully agree with the experiment.

The isomeric cross-section ratios do not depend strongly on the model parameters as the cross section. This can be seen in the left part of Fig. 7, which depict the isomeric cross-section ratio for the ^{129}I(n, p)^{129m,g}Te reaction. The uncertainties caused by the uncertainty of the same model parameters as shown in Figs. 3 and 4 have less effect on the isomeric cross-section ratio than for the excitation functions. Comparing the experimental data and model calculation, in the case of

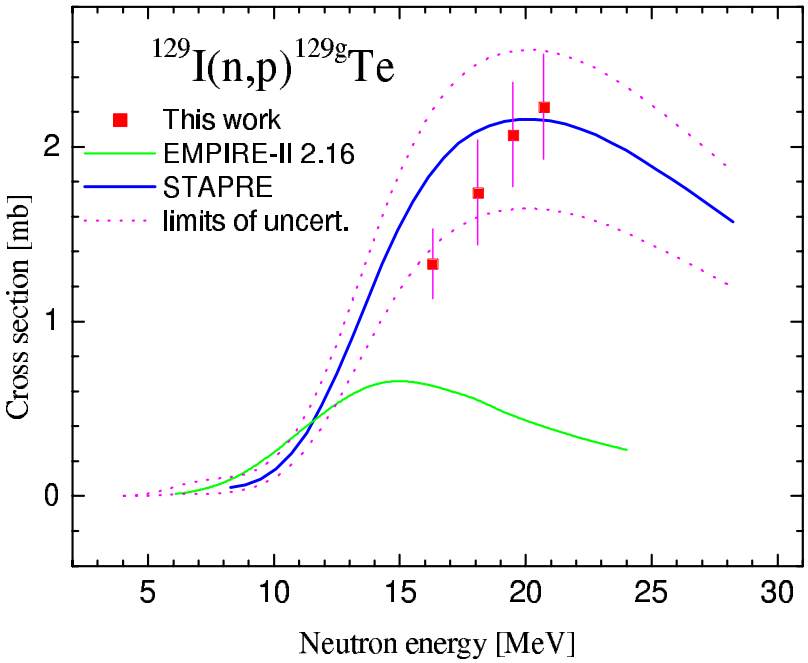

Fig. 3: Measured and calculated excitation functions for the ^{129}I(n, p) ^{129g}Te reaction

the ^{129}I(n, p)^{129m,g}Te reaction only one experimental data point is a bit far from the model calculation. For the ^{129}I(n, α)^{126m,g}Sb reaction the isomeric cross-section ratios from the model and experiment are agreement only at one energy. This indicates that there is some inconsistency in the measurements.

Summary

New experimental cross sections were determined for neutron induced reaction on the iodine isotopes, especially for the radioactive target of ^{129}I. The model calculations with the STAPRE and EMPIRE II show some discrepancy in the high-energy region. The present measurements are in better agreement with the STAPRE. The isomeric cross section ratios are less sensitive for the model parameters than the excitation functions; therefore they give better indication between the inconsistencies of the experimental data.

[1] M. Uhl and B. Strohmaier, *Computer code for particle induced activation cross section and related quantities*, Institut für Radiumforschung und Kernphysik, Vienna, Report 76/01 and Addenda to this report.
See also Strohmaier B. and Uhl M., International Energy Agency Report IAEA-SMR-43 (1980) 313

[2] M. Herman, R. Capote Noy, P. Oblozinsk, A. Trkov and V. Zerki, *Recent Development and Validation of the Nuclear Reaction Code EMPIRE*, Int. Conf. Nuclear Data for Science and Technology, Tsukuba 2001

[3] O. Bersillon, *SCAT 2: Un programme de modele optique spherique*, Centre dEtudes de Bruyres-le-Chtel Report, CEA-N-2227 (1981)

[4] W. Dilg, W. Schantl, H. Vonach and M. Uhl, *Level density parameters for the back-shifted Fermi gas model in the mass range 40<A<250*, Nucl. Phys. A217 (1973) 26

[5] D. Wilmore and P. E. Hodgson, *The calculation of neutron cross-sections from optical potentials* Nucl. Phys. 55 (1964) 673

[6] F. Becchetti, W. Greenless, *Polarisation Phenomena in Nuclear Reactions*, H. H. Barschall, W. Haeberli (Eds.) 682

[7] V. Avrigeanu, P. E. Hodgson, M. Avrigeanu, Report OUNP-94-02(1994) and Phys. Rev. C49 (1994) 2136

[8] A. J. Koning, private communication

[9] V.I. Plyaskin and R.A. Kosilov, INDC(CCP)-424, p.27

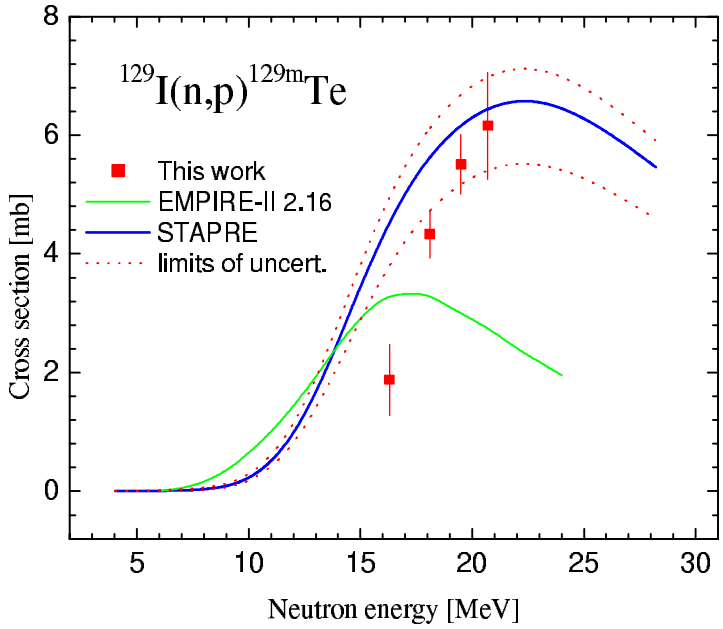

Fig. 4: Measured and calculated excitation functions for the ^{129}I(n, p) ^{129m}Te reaction

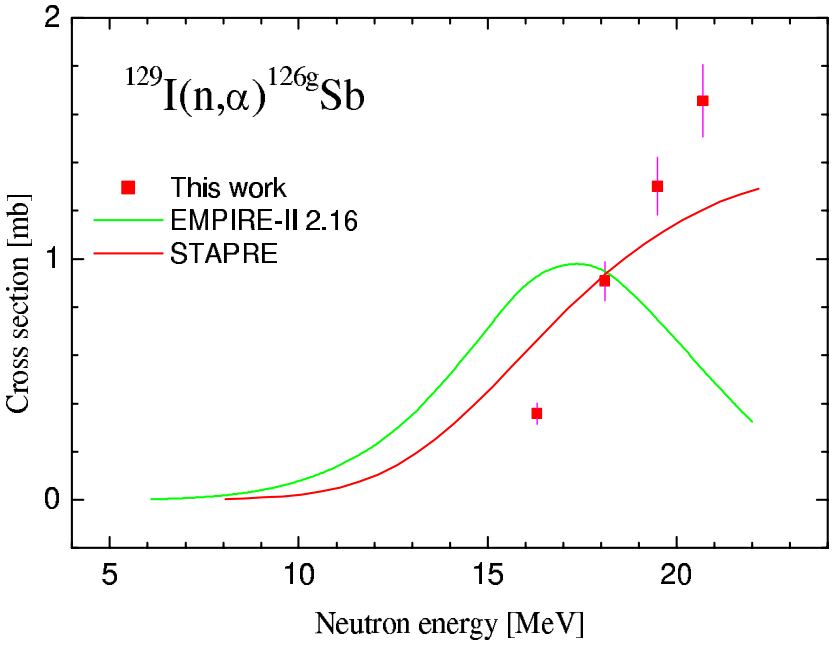

Fig. 5: Measured and calculated excitation functions for the ^{129}I(n, α)^{126g}Sb reaction

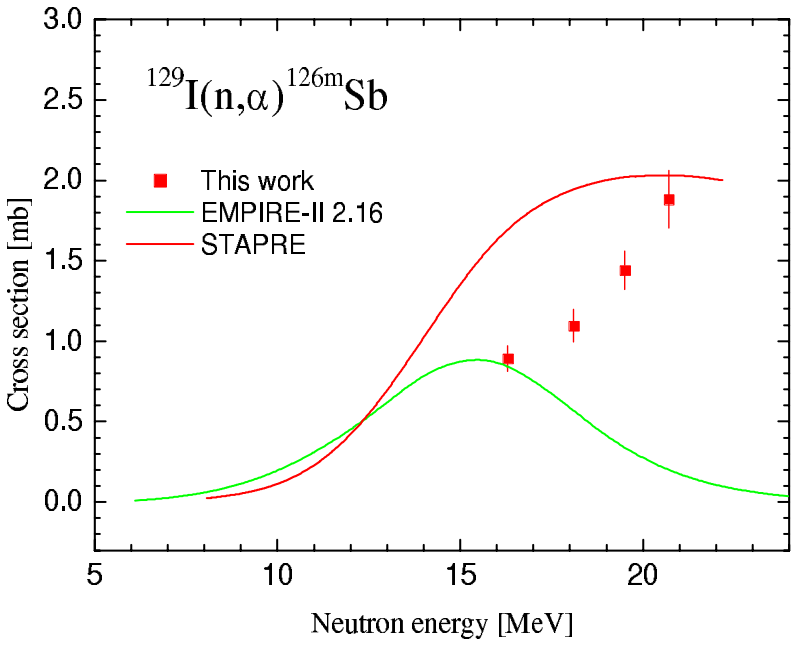

Fig. 6: Measured and calculated excitation functions for the ^{129}I(n, α)^{126m}Sb reaction

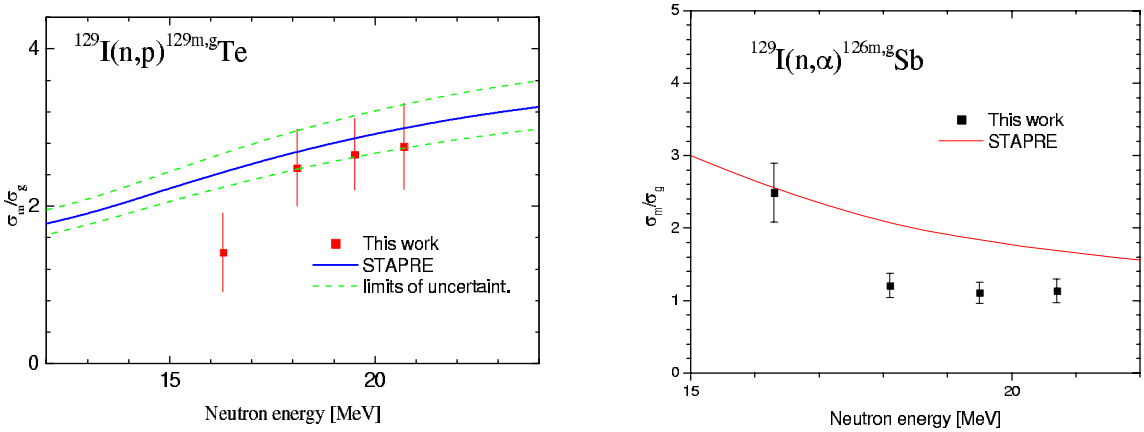

Fig. 7: Measured and calculated isomeric cross-section ratios for the ^{129}I(n, p)^{129m,g}Te and ^{129}I(n, α)^{126m,g}Sb reactions

Measurement of the inelastic neutron scattering cross section for ^{58}Ni at high resolution.

L. Oláh[1,2], *C. Borcea*[1,3], *V. Avrigeanu*[1,3], *A. J. Koning*[4], *J. Lupo*[1], *A. J. M. Plompen*[1], *W. Schubert*[1], *R. Shelley*[1]

[1] EC-JRC IRMM, B-2440 Geel, [2] IEP, University of Debrecen, H-4001 Debrecen, [3] NIPNE, RO-76900 Bucharest, [4] NRG, NL-1755 ZG Petten

Neutron-induced cross sections for structural materials are key ingredients to our understanding of the role of these materials under irradiation in reactors. Since neutron transport is governed by (in)elastic scattering and (n,xn) cross sections it is essential to measure these data for nuclides of interest in reactor applications.
^{58}Ni, the most abundant (68 %) isotope of natural nickel, is applied in various stainless steel alloys that are widely used as reactor structural materials. Here we report high resolution data of new measurements with the (n, n'γ) technique in the energy range from threshold to 18 MeV which are of relevance to inelastic scattering of ^{58}Ni. Measurement details and preliminary results were reported in the annual report for 2001 [1]. Here we report on progress achieved in the meantime.

Time-of-flight measurements were performed at the pulsed neutron source GELINA of IRMM. Strong efforts were made to optimize the experimental setup. Coaxial HPGe detectors were used for prompt gamma-ray detection in order to be able to clearly resolve close lying gamma lines (e.g. 1454.5 keV, 1448.2 keV emitted by the ^{58}Ni sample and 1460.2 keV from ^{40}K). Time resolution better than 8 ns (measured by PilotU-HPGe start-stop measurement with ^{60}Co) was achieved for the HPGe detectors by using slow-risetime rejection. This time resolution combined with the 200 m neutron flight path allows the determination of high-resolution (2 keV at 1.5 MeV, 12.5 keV at 5 MeV, 35.5 keV at 10 MeV) excitation functions of the emission cross sections for the first five excited levels of ^{58}Ni. At flight path N^o 3, 100 m ^{10}B and U filters were used to eliminate overlap neutrons and the intensity of the gamma flash. Data from preliminary measurements indicated the need for further background reduction. This goal was achieved both by reducing the amount of scattering material around the sample, as shown in Fig. 2 of Ref. [1]. and by introducing a more effective, complex collimator shielding (Fig. 1) after the last Cu collimator. However gamma flash events due to the rescattering from the sample still significantly increased the dead time of the acquisition system. Correction for their effect was determined from measured data of LINAC bursts having no detected gamma flash event at the beginning. The size and the position of the beam spot after the collimator were measured by photographic technique. Moreover a scan with a 1.5 cm diameter plastic scintillator showed good uniformity and edge definition of the beam profile. Thus it was verified that the enriched (99.9 %) ^{58}Ni sample completely overlapped the neutron beam and that the gamma-rays emitted by the sample are well represented by a uniform source.

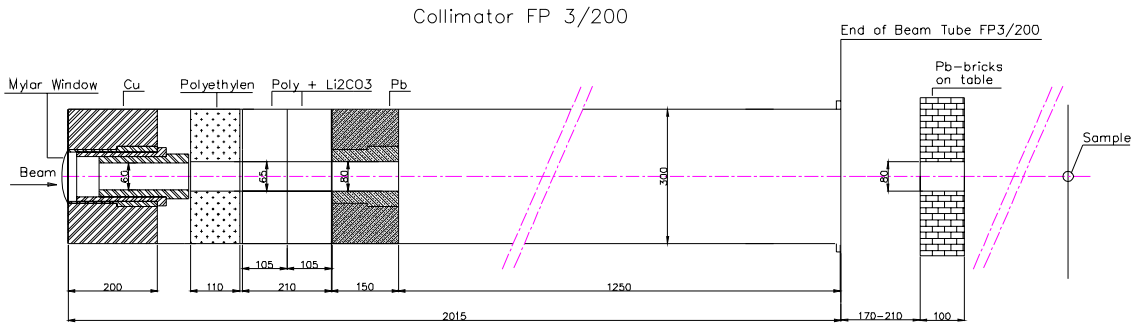

Fig. 1: The improved collimation at the 200 m station.

In comparison with the one detection angle (125°) reported in refs. [2, 1, 4], the use of two detectors at the angles of 70° and 150° increases the precision of the determination of the total cross section further by reducing the influence of the gamma ray angular distribution. Detector efficiencies were determined from measured data of standard

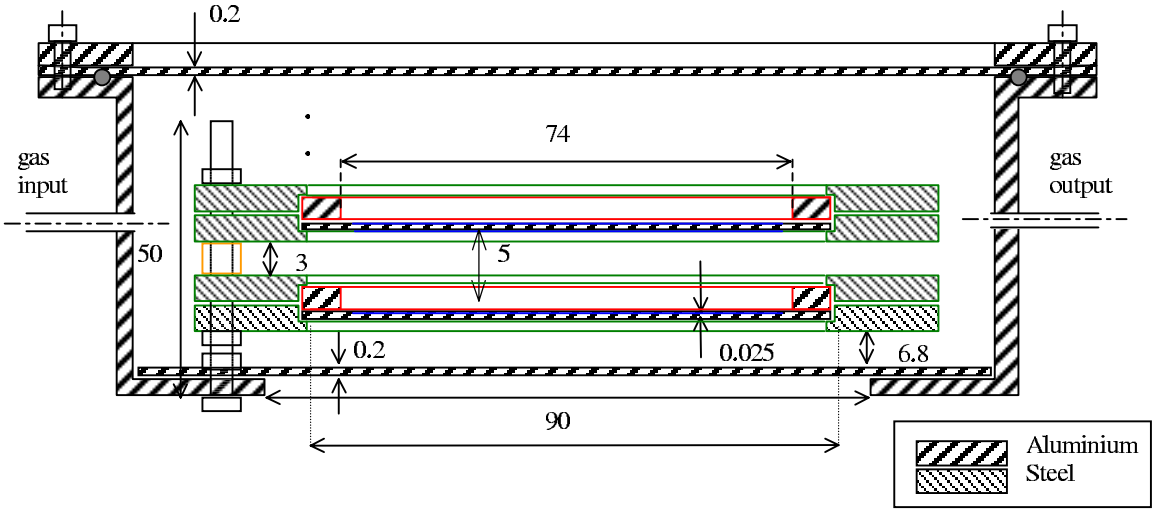

Fig. 2: The new ^{235}U fission chamber at 200 m.

gamma sources in the sample position in the energy range from 245 keV - 1408 keV with corrections deduced from MCNP calculations for pointlike and extended volume sources. The flux of the neutron beam was measured by ^{235}U fission chambers at stations 100 m and 200 m. The latter is a new chamber with 2 single-sided and 3 double-sided fission deposits ($^{235}UF_4$) with 5 mm spacing and a total areal density of 3.066(6) mg/cm^3, (see Fig. 2). This chamber is well calibrated by alpha-particle spectrometry and has good uniformity. Deposit diameters are larger (8 cm) than the beam and thus flux normalizations relies entirely on areal densities of this fission chamber and the sample. The deposits were made at the IRMM SP unit.

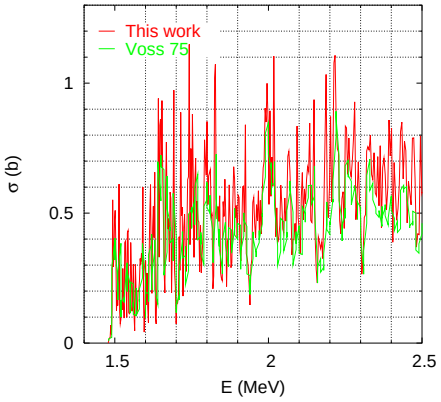

Fig. 3: Gamma-ray production cross section for the 1454 keV transition at high resolution

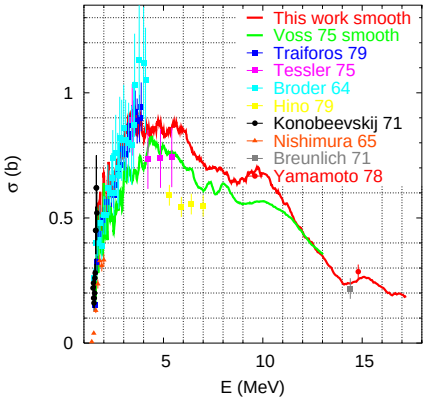

Fig. 4: Gamma-ray production cross section for the 1454 keV transition in the full energy range (320 ns/bin)

Nevertheless due to the small flux (and very low count rate) at station 200 m a long measurement time (1000 h) was necessary to reduce the statistical error of the fission chamber data. Time-of-flight and pulse height data of the HPGe detectors and fission chambers were recorded simultaneously by the DAQ2000 acquisition system and were stored in event list mode on disk. Time sliced and amplitude based sorting/conversion of list mode data and manipulation of large ASCII matrixes were performed efficiently by C codes we have written for this purpose. Gamma production data were normalized by using the neutron flux measured by ^{235}U fission chambers, corrections were applied for beam attenuation and multiple scattering effects calculated by MCNP-4C. The gamma-ray production cross section of the 1454.5 keV line from the $2_1^+ \rightarrow$gs transition exclusively represents the inelastic cross section up to 2459 keV excitation energy, but with the contribution of gamma production cross sections from the higher lying excited states the total inelastic cross section can be extended practically up to 6 MeV. In Fig. 3 the good resolution is shown and compared to the earlier result of Voss et al. Fig. 4 shows the new data smoothed in comparison with earlier measurements [4, 5, 6]. Fig. 5 has the same data compared with model calculations with the Stapre-H95++ and the Talys codes. Additional gamma-ray production cross sections are shown for the 1005, 1321, 1448 and 1523 keV transitions, as well. Overall good agreement is obtained with the bulk of the earlier experimental data and in particular with the model calculations. The total inelastic cross section constructed from the measured data is shown in Fig. 9 and compared with the model calculations shows good agreement as well. This indicates that the experimentally determined lower limit to the total inelastic cross section at energies above 6 MeV is very close to the actual inelastic cross section. This implies that direct feeding to the ground state from the high-lying excited states is small. Notice that the good agreement in Figs. 3 and 4 with the 14 MeV data indicates the first succesful use of the GELINA neutron facility at these energies for the determination of a partial cross section.

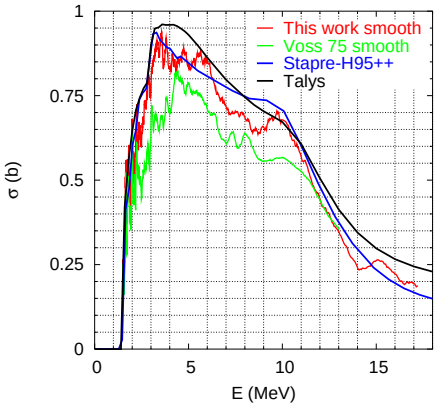

Fig. 5: As above compared with model calculations.

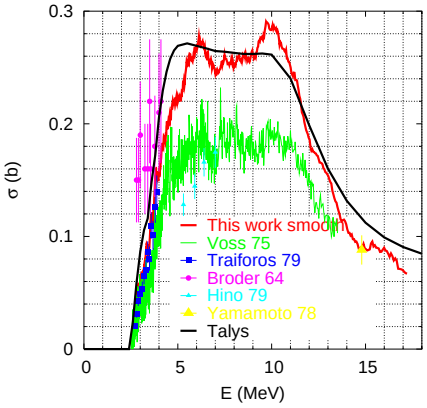

Fig. 6: Model calculations compared to the 1005 keV transition.

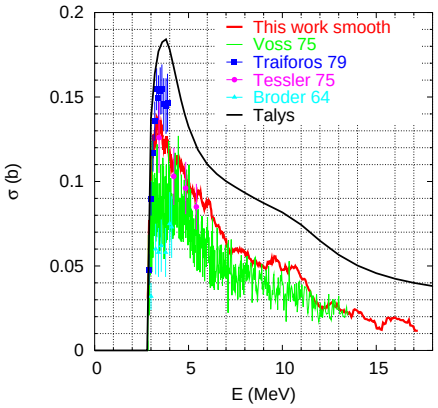

Fig. 7: As in Fig. 5 for the 1321 keV transition.

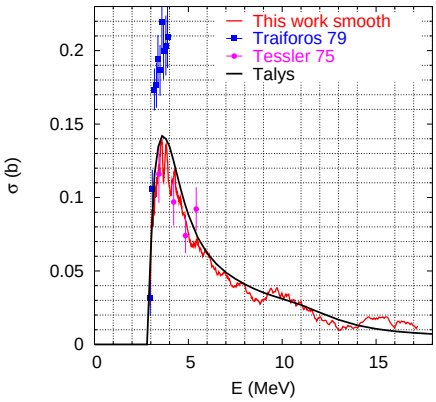

Fig. 8: As in Fig. 6 for the 1448 keV transition.

Gamma production cross sections with a unique resolution and energy range are presented here for the first four excited state of ^{58}Ni (gamma production cross sections for higher excited states were also determined with less resolution) as well as the deduced total inelastic cross section.

The fairly good agreement with most of the available data of other measurements shows the reliability of our system. Measurements with a very similar setup for the ^{52}Cr were completed and data-analysis is in progress and measurements for ^{209}Bi and ^{206}Pb are in preparation for 2003. ^{207}Pb and ^{208}Pb will follow in 2004-2005.

The present results were reported at the PHYSOR 2002 conference, Seoul, Korea, October 7-10, 2002. The total inelastic cross section and individual level cross sections will be inferred up to 6 MeV from the measured gamma production data and will be sent to the EXFOR database to NEA. A possible further step in the improvement

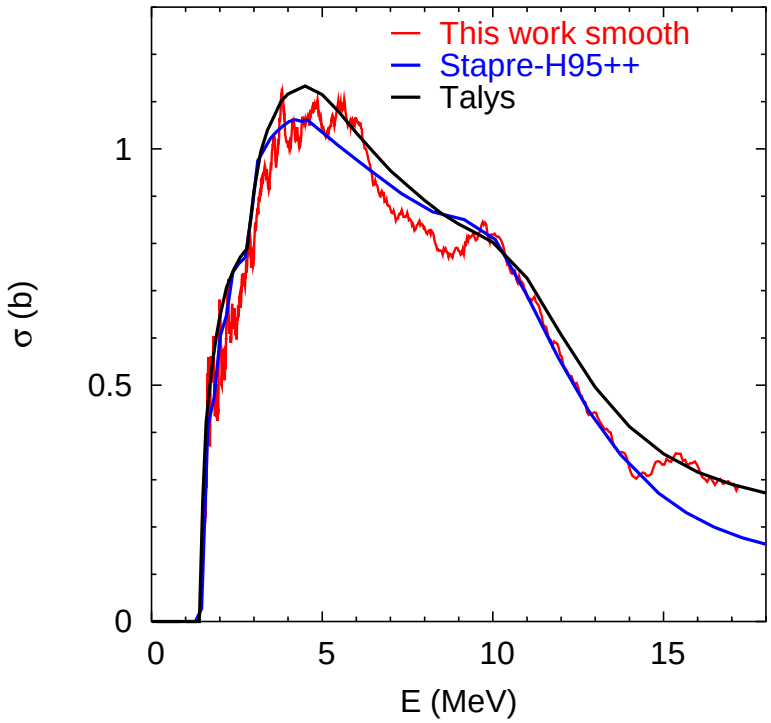

Fig. 9: Total inelastic cross section (320 ns/bin).

of our measurement system is to apply fast signal digitizers instead of conventional electronics. This way entirely digital data acquisition/processing can be achieved in the future with the goal to eliminate the large impact of slow rise-time rejection on detection efficiency below 600 keV, and the dead-time generated by pile-up of the gamma-flash with neutron-induced events (currently about 20-50 % of the GELINA pulses result in a detected gamma-flash).

[1] L. Oláh *et al.*, Report EUR20412 EN, IRMM Neutron Physics Unit, Scientific Report, (2001)

[2] S. Traiforos *et al.*, Nucl.Sci.Eng. 72 (1979) 191

[3] H. Vonach *et al.*, Phys.Rev. 50 (1994) 1952

[4] ”EXFOR, Nuclear reaction data”, www.nndc.bnl.gov, www.nea.fr, or www-nds.iaea.org (2002)

[5] F. Voss *et al.*, EXFOR 20744, Proc.Conf. Nuclear cross sections and technology, NBS 425 (1975) 916

[6] G. Tessler and S. Glickstein, EXFOR 10439, Proc.Conf. Nuclear cross sections and technology, NBS 425 (1975) 934

Determination of the total and capture cross section in the low energy region for stable fission products

A. Borella[1], *E. Berthoumieux*[2], *A. Brusegan*[1], *A. Leprêtre*[2], *W. Mondelaers*[1], *P. Schillebeeckx*[1], *P. Siegler*[1]

[1] EC-JRC IRMM, B-2440 Geel, [2] CEA Saclay, F-91191 Gif sur Yvette

Improved capture cross sections for various stable fission products, with a high capture probability are on the NEA High Priority Nuclear Data Request List [1, 2] and are requested by both the British [1] and the French industry [3]. Improved data for stable fission products are motivated by the objective to optimise the use of present nuclear power plants. The requests concentrate mainly on the thermal energy and the energy region covering the first strong resonance(s) [4, 5, 6]. Improved capture data for certain lanthanides, in both the thermal and fast region, are also required for fuel cycles using reprocessed fuel [2].

To improve the above mentioned data, we started a collaboration with the CEA Saclay. In 2002 we performed a feasibility study to determine the capture and total cross section of stable fission products in the low energy region at GELINA. We performed transmission measurements (at 50 m) and capture measurements (at 14 m) for ^{103}Rh. In addition to the ^{103}Rh experiments, we also performed transmission and capture measurements on Au. These data are used to verify the various procedures to deduce the cross section data: optimum background filters, energy calibration and normalisation of the capture data. The results of the transmission measurements indicate that the background in the energy region between 0.02 eV and 0.4 eV can be well defined by using a 6 mm thick Eu filter.
As in ref. [7], the neutron energy scale for the capture measurements in the meV-region is verified by means of the prominent Bragg-reflection cuts in Be at 5.24 and 6.84 meV. An example of the energy calibration for the flux measurements, as part of the capture normalisation procedure, is shown in Fig. 1. In Fig. 2 we compare the result of the capture measurements for a 0.3 mm thick ^{103}Rh target, with the results for a 0.5 mm thick ^{208}Pb target and the response to the ambient background. The position of the 2.85 keV black resonance of ^{23}Na is also indicated in Fig. 2. The ^{208}Pb run provides a good estimate of both the so-called ”open beam” background and of the contribution due to scattered neutrons. Fig. 2 reveals that the largest background contribution originates from the ambient background. Using proper shielding conditions, we can reduce this time independent background component by almost a factor 10. The signal to background can also be improved by operating the accelerator with a larger burst width. A larger burst width ($\leq$ 10 ns) is justified, since the natural line width and the Doppler effect dominate the total observed line width of the low-energy resonances.

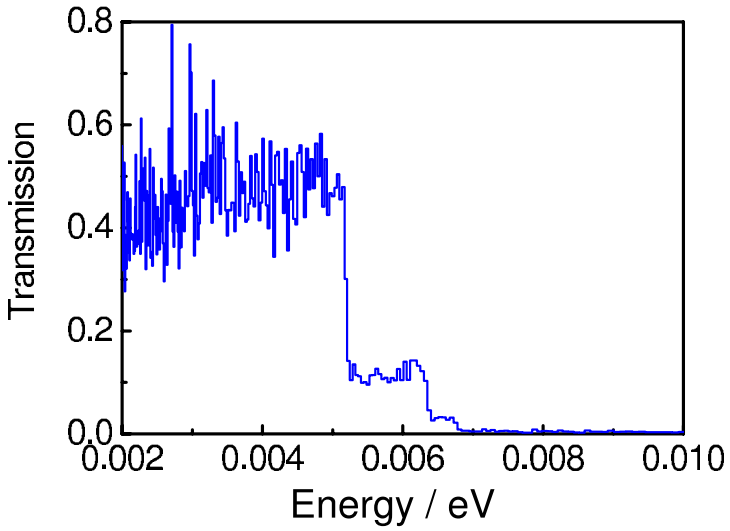

Fig. 1: Verification of the neutron energy scale, for the neutron flux measurement system, with the Bragg-reflection cuts in Be.

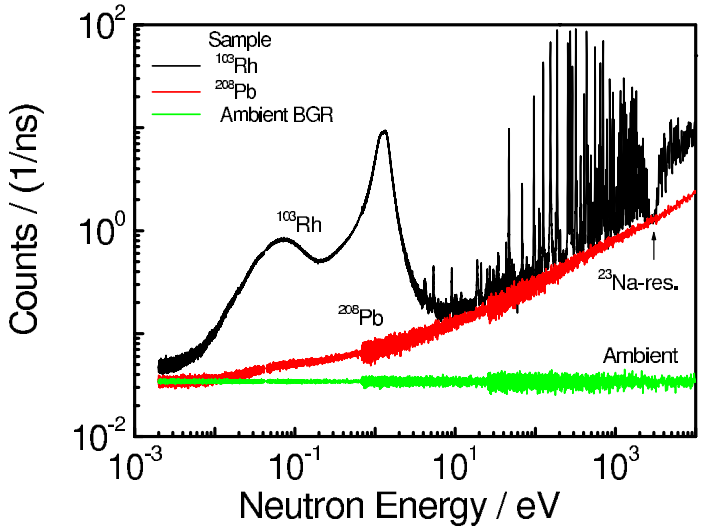

Fig. 2: The response of the capture detection system for measurements with ^{103}Rh and ^{208}Pb is compared with the ambient background.

[1] High Priority Request List issued by OECD-NEA Data Bank (Fukahori, Editor) (2001)

[2] M. Salvatores, *Future Nuclear Power Systems and Nuclear Data Needs*, Journal of Nuclear Science and Technology, Supplement 2 ND2001, 4-12

[3] F. Storrer et al., *Priority Nuclear Data Needs for Indsutrial Applications*, Journal of Nuclear Science and Technology, Supplement 2 ND2001, 1357-1360

[4] O. Bouland, *Progress Report on Main FPs: recommendations for:* ^{103}*Rh,* ^{152g}*Eu and* ^{153}*Eu*, JEFDOC-912, JEFF Meeting 24-26 April 2002

[5] C. Chabert, A. Courcelle, B. Roque and O. Serot, *Progress Report on FPs: recommendations for:* ^{149}*Sm,* ^{143}*Nd,* ^{154,155}*Eu*, JEFDOC-885, JEFF Meeting, 19-21 November 2001

[6] A. Santamarina et al., *Experimental Validation of JEF2 Fission Products. Required Improvements in the JEFF3 Evaluations*, JEFDOC-851, JEFF Meeting, 04-06 December 2000

[7] C. Wagemans, P. Schillebeeckx, A.J. Deruytter and R. Barthélémy, *Subthermal fission cross-section for* ^{233}*U,* ^{235}*U, and* ^{239}*Pu*, Proc. Int. Conf. on Nuclear Data for Science and Technology, Mito (Japan), JAERI (1988) 91-95

Branching ratio measurements of neutron capture in ^{209}Bi

G. Aerts[1], *E. Berthoumieux*[1], *A. Borella*[2], *A. Brusegan*[2], *F. Gunsing*[1], *A. Letourneau*[1], *F. Marie*[1], *P. Mutti*[3], *L. Perrot*[1], *P. Schillebeeckx*[2], *G. Simpson*[3]

[1] CEA Saclay, F-91191 Gif sur Yvette, [2] EC-JRC IRMM, B-2440 Geel, [3] ILL, F-38042 Grenoble

Future high power spallation sources may consist of liquid lead-bimuth targets. Therefore, for the operation and safety assessment of Accelerator Driven Systems the ^{209}Bi(n, γ)^{209m}Bi and ^{209}Bi(n, γ)^{210g}Bi cross-sections are important nuclear data. These two reactions contribute significantly to the short- and long-term radiotoxicity of the target via the production of ^{210}Po ($T_{1/2}$ = 138.376 d) and ^{210m}Bi ($T_{1/2}$ = 3.04$\times$10^{6} y), both alpha-emitters. The reaction probabilities for the population of the ground state and the meta-stable state, and corresponding branching ratio are crucial data for operational safety reasons and long-term disposal aspects.

Existing data are very scarce and no direct experimental data exist for the branching ratio. An experimental program has been proposed, as part of a collaboration between the CEA Saclay (F) and the IRMM, to determine the ^{209}Bi(n, γ)^{210m}Bi and ^{209}Bi(n, γ)^{210g}Bi cross sections. We planned to determine these cross sections in the thermal energy region at the ILL and the differential cross sections at GELINA, by measuring all gamma rays populating both states with high resolution γ-ray spectroscopy. A detailed description of this technique can be found in Ref. [2].

A first experiment has been carried out successfully at the ILL Grenoble and is reported in Ref. [2]. We find for the total capture cross-section 35.0 (1.8) mb, which is in good agreement with existing results. The branching ratio 51 (5) %, deduced from the partial cross sections (σ(n, γ)$_g$ = 17.9 (2.0) mb and σ(n, γ)$_m$ = 17.1 (2.0) mb), is by 25 % smaller than the values reported in the evaluated libraries.

[1] C. Coceva, Nuovo Cimento, A107 (1994) 85.

[2] A. Letourneau et al., *Thermal neutron capture branching ratio of ^{209}Bi using a gamma-ray technique*, 11th International Symposium on Capture Gamma-ray Spectroscopy and Related Topics, September 2-6 2002, Prague, Czech Republic.

The nuclear fission process

Fission cross-section evaluation in the frame of the multi-modal fission model for ^{235}U(n, f)

F.-J. Hambsch[1)], *S. Oberstedt*[1)], *G. Vladuca*[2)], *A. Tudora*[2)]

[1] EC-JRC IRMM, B-2440 Geel, [2] Bucharest University, RO-76900 Bucharest

Neutron-induced fission of ^{235}U is of great importance for applications. This nuclide is the major standard, and the knowledge of its cross-section is of utmost importance. Based on the successful calculations for the compound system ^{238}Np [1], where all reaction channels could be reproduced, the next challenge tackled was to repeat the fission cross-section evaluation for ^{235}U(n, f). Again the statistical model code STATIS

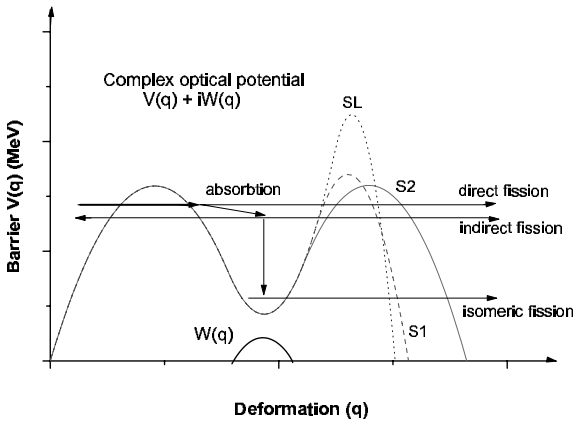

Fig. 1: Schematic view of the double humped fission barrier and the possible fission processes.

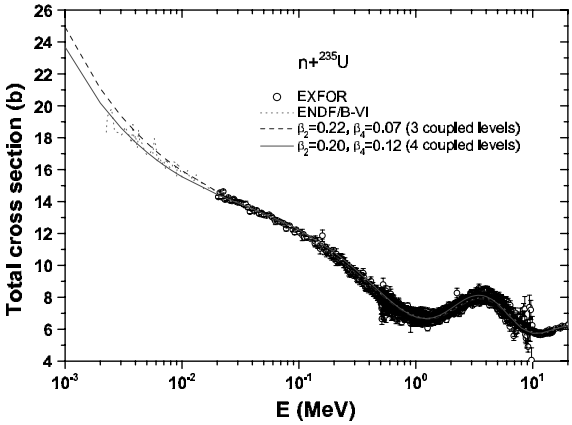

Fig. 2: The total reaction cross-section for ^{235}U.

[2] was used to calculate the contribution of each fission mode in competition with the other open channels. Also for this nuclide it was shown from fission mode calculations based on the MM-RNR model [3] that the bifurcation point is close to the second minimum of the double-humped fission barrier. Consequently, the inner barriers and the isomeric wells were taken the same for all modes, and the outer fission barrier for each fission mode was taken different. For each mode the sub-barrier effects, the direct, indirect and isomeric fission cross-sections are taken into account. A schematic view of the double-humped barrier and the different possible decay paths of the fissioning system are shown in Fig. 1. For the neutron-induced reactions of actinides in the incident energy range, where only one compound nucleus is formed, the competitive processes

are the elastic and inelastic scattering, the radiative capture and fission. In case of fission only the three most dominant and experimentally confirmed fission modes, S1, S2 and SL have been taken into account. The neutron transmission coefficients are provided by the direct interaction mechanism calculations using the coupled channel code ECIS-95 [4]. This code provides the total cross section, the direct contributions of the neutron elastic and inelastic cross-sections of the rotational levels coupled to the ground state and the neutron transmission coefficients needed in the compound nucleus calculations. To give an idea of the quality of the calculations the total reaction cross section in the incident energy range 0.001 to 20 MeV obtained by the coupled channel calculations is shown in Fig. 2.

The "experimentally" separated fission mode cross-sections are obtained by multiplying the ENDF/B-VI evaluated cross-section with the experimentally determined branching ratios [5] and are shown as full symbols in Fig. 3. The purpose is to describe these fission cross-sections in the frame of the statistical model. For the studied reaction, the calculations are done in the incident energy range between 0.01 MeV (where the statistical model assumptions become valid) and 5.5 MeV, where the first fission chance is still dominant. The resulting fission cross-sections for the S1, S2 and SL modes and the total fission cross-section in comparison with the "experimental" modal cross-sections and available experimental fission cross-section data from EXFOR are given in Fig. 3.

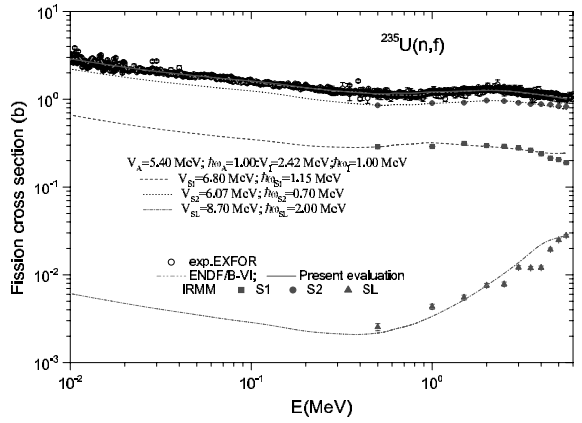

Fig. 3: ^{235}U(n,f) fission cross section: Experimental data (open symbols) from EXFOR. Mode separated data (full symbols) based on IRMM experiments and lines based on the present calculations.

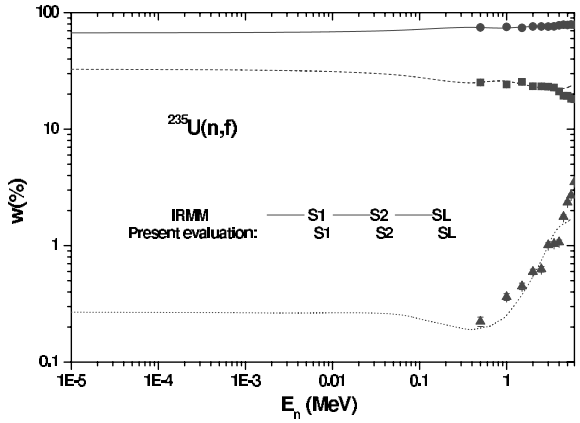

Fig. 4: Theoretically deduced branching ratios (different lines) as a function of incident neutron energy compared to experimental results (full symbols).

Another problem consists of verifying if the Hauser-Feshbach statistical model describes as reasonably well the calculated fission cross-sections as it can be expected for a fissile nucleus. Surprisingly enough, as it can be seen in Fig. 4, the Hauser-Feshbach statistical cross section calculations (doted curves for S1, S2 and SL modes and dash-dotted for the sum of the modes) are obviously higher then the results given by the STATIS code. We conclude that for the "modal cross-sections" the sub-barrier effect calculations and the width fluctuation are still very important. The explanation can

be, that the barrier heights for S1 and SL are higher than the neutron binding energy of ^{236}U and the barrier height for S2 is comparable with it. Consequently, the Hauser-Feshbach statistical model is not recommended for such calculations. The statistical computer code STATIS provides also the cross sections of all competitive processes. A detailed description of the results and the theoretical procedures are given in ref. [5].

[1] G. Vladuca et al., Nucl. Phys. A (2002) 995

[2] G. Vladuca et al., Annals of Nucl. Energy 27 (2000) 995

[3] S. Oberstedt et al., Nucl. Phys. A644 (1998) 289

[4] J. Raynal, private communication

[5] G. Vladuca et al. IRMM Int. Report GER/NP/07/2002/07 and Nucl. Phys. A720 (2003) 274

Prompt fission neutron multiplicity and spectra evaluation in the frame of the multi-modal fission model for ^{235}U(n, f)

F.-J. Hambsch[1)], *S. Oberstedt*[1)], *G. Vladuca*[2)], *A. Tudora*[2)], *I. Ruskov*[3)]

[1] EC-JRC IRMM, B-2440 Geel, [2] Bucharest University, RO-76900 Bucharest, [3] INRNE, BU-1784 Sofia

The prompt fission neutron multiplicity and spectra of the actinides are nuclear data of crucial importance for energy and non-energy nuclear applications. For this reason new evaluations of these quantities with higher degree of accuracy are required. Especially for ^{235}U, being the standard nucleus for evaluated nuclear data files, new evaluations concerning the prompt fission neutron multiplicity and spectra, based on modern approaches, with more physical effects and assumptions, are welcome.
In this work, as a continuation of last years effort [1], an attempt to improve the evaluation of the prompt fission neutron multiplicity and spectra for ^{235}U(n, f), within the multi-modality of the fission concept is made. A superposition of the three most dominant fission modes, S1, S2 and SL is taken into account for ^{235}U. The prompt fission neutron spectra and multiplicities for each mode are calculated using an improved Los Alamos (LA) model [2] with the consideration of the compound nucleus cross section of the inverse process. For the determination of the model parameters the experimental fission fragment yield, Y(A), the total kinetic energy, TKE(A), for the neutron induced fission of ^{235}U (at 12 incident energies) as measured at IRMM are used.

From the experimental data the branching ratios w_m, the average fission fragment mass $<$A$>$, the standard deviation of the fragment mass distribution σ_A and the average total kinetic energy $<$TKE$>$ are deduced for each mode. Up to now for the calculation of the input model parameters the ”7 point approximation” was used in the frame of single-mode fission spectrum models [2]. Taking into account that the mass distribution Y(A) and TKE(A) experimental data are for the full range of fission fragments, an new method for the determination of the multi-modal model parameters was developed. This method is more adequate than the ”7 point approximation” because the full fission fragment mass range is taken into account. That means A_H from 118 to 160 and A_L from 118 to 76 for (n + ^{235}U). For each fission fragment mass pair A_{Lj}, A_{Hj} two isobars per fragment mass are taken into account, with values for the charge Z that are the nearest integer values above and below the most probable charge ZUCD. Consequently the number of fission fragment pairs is 86 for ^{235}U. For each fission fragment pair (Z_{Li}, A_{Li}, Z_{Hi}, A_{Hi}) the level density parameter is calculated using the Ignatiuk super-fluid model [3].

The resulting total multiplicity of ^{235}U(n, f) is obtained in good agreement with the experimental data (see Fig. 1). Also the prompt fission neutron spectra are obtained in

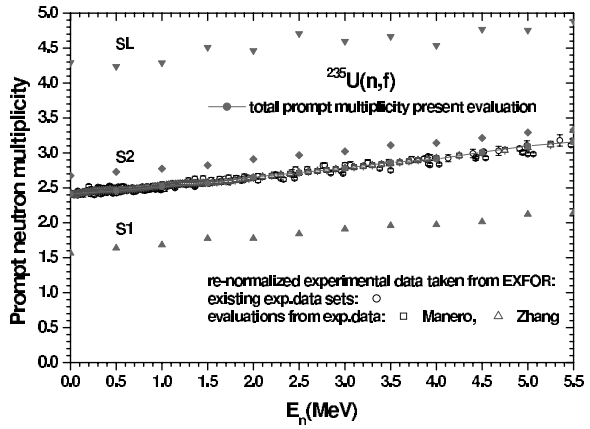

Fig. 1: Average prompt fission neutron multiplicity for ^{235}U(n, f) compared to experimental data from EXFOR and disentangled into the contributions of the different modes.

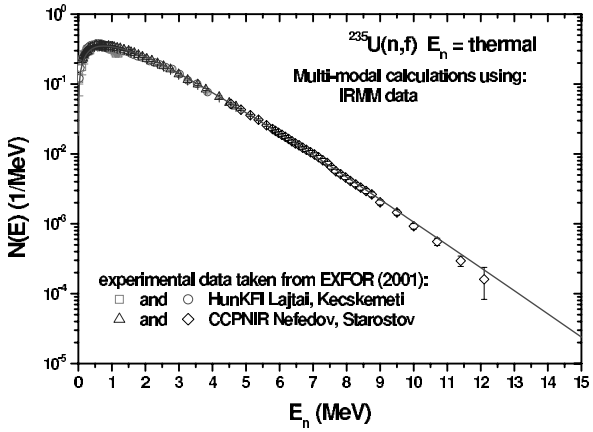

Fig. 2: Prompt fission neutron spectrum for ^{235}U(n, f) at thermal incident neutron energy compared to experimental data from EXFOR and disentangled into the different contributions from the different modes.

good agreement with the existing experimental data as exemplified in Fig. 2 for thermal neutron-induced fission of ^{235}U. The same example is given in Fig. 3 as ratio to the ENDF/B-VI evaluation, in order to emphasize the agreement with the experimental data. It is obvious from Fig. 3 that especially, at lower fission neutron energy, the available experimental data tend to be higher than the evaluations. Since the results have been obtained under the assumption that all fission neutrons are emitted from fully accelerated fragments, the inclusion of anisotropy effects [4] seems to be compelling.
In order to do so, equivalent single-mode calculations are made, since we do not know the anisotropy parameter of each mode. As can be seen in Fig. 4 at thermal incident neutron energy, the agreement with the experimental data is considerably increased, especially, in the lower fission neutron energy region of the spectrum using an anisotropy parameter b = 0.2. The same considerably improved agreement with experimental data is obtained at E$_n$ = 0.5 MeV (see Fig. 5).

[1] F.-J. Hambsch et al., NP unit Scientific Report 2001, 44 (2002) EUR 20412 EN.

[2] D. G. Madland, J. R. Nix, Nucl. Sci. Eng. 81 (1982) 213.

[3] A. Ignatiuk, IAEA-RIPL, TECDOC-1034, 1998.

[4] J. Terrel, Phys. Rev. 113 (1957) 527.

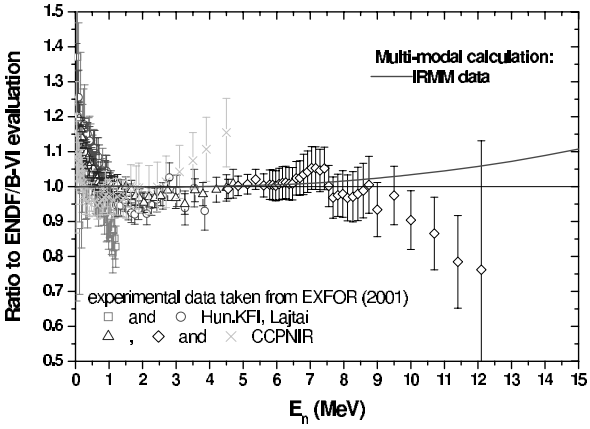

Fig. 3: Prompt fission neutron spectrum at thermal incident neutron energy compared to experimental data, shown as ratio to the ENDF/B-VI evaluation.

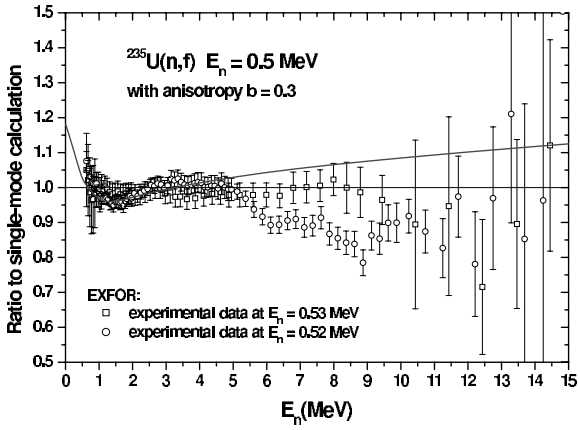

Fig. 4: Prompt fission neutron spectrum at thermal incident neutron energy with the anisotropy effect taken into account, presented as ratio to the ENDF/B-VI evaluation.

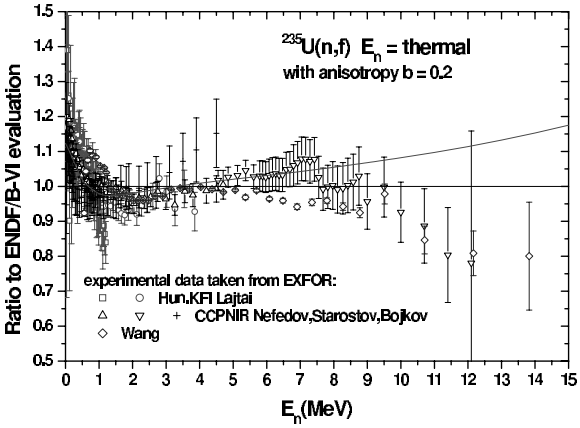

Fig. 5: Prompt fission neutron spectrum at E_n = 0.5 MeV, with the anisotropy effect taken into account, presented as ratio to the ENDF/B-VI evaluation.

Prompt fission neutron multiplicity and spectra evaluation in the frame of the multi-modal fission model for ^{252}Cf(sf)

F.-J. Hambsch[1)], *S. Oberstedt*[1)], *G. Vladuca*[2)], *A. Tudora*[2)], *I. Ruskov*[3)]

[1] EC-JRC IRMM, B-2440 Geel, [2] Bucharest University, RO-76900 Bucharest, [2] INRNE, BU-1784 Sofia

For ^{252}Cf - spontaneous fission (SF) much more effort than for other nuclei was devoted to the measurement and interpretation of the prompt fission neutron spectrum because this spectrum is also used as a neutron spectrum shape standard. This led to the fact that the prompt fission neutron spectrum could be evaluated on the basis of experimental data ("free of model") only, by Mannhart [1]. The evaluation resulted in a chi-square per degree of freedom of nearly unity and indicated no real inconsistencies between the various experiments [1].

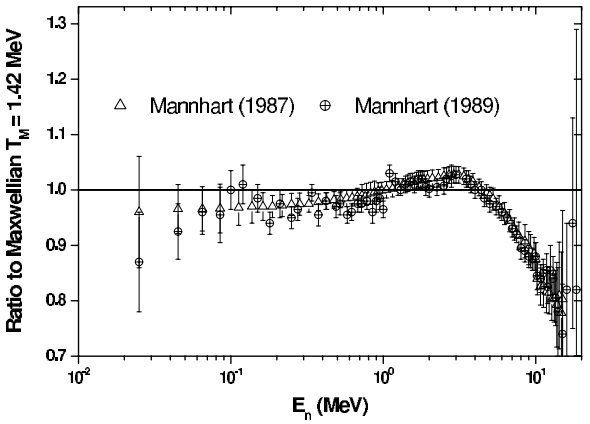

Fig. 1: The prompt fission neutron spectrum standard evaluation of Mannhart [1] represented as ratio to the Maxwellian spectrum with T_M = 1.42 MeV.

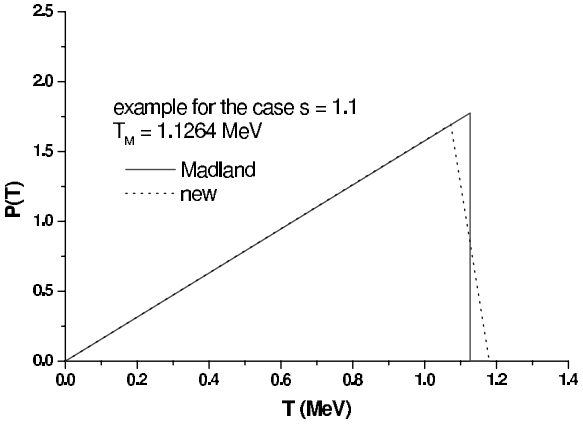

Fig. 2: Fission fragment residual nuclear temperature distribution with T_M = 1.1264 MeV. Solid line the P(T) shape used in the classical LA model [2], dashed line the new shape of P(T).

Based on this evaluation, the ^{252}Cf spectrum was established as an internationally accepted reference standard for metrological applications. Mannhart's "point-wise" evaluation [1] is shown in Fig. 1 as ratio to the well-known Maxwellian spectrum of ^{252}Cf. This Maxwellian spectrum with the temperature T_M = 1.42 MeV was the first model evaluation applied to ^{252}Cf(SF). In the past two decades several attempts (see e.g. [2, 3]) have been made to give a theoretical description of the prompt fission neutron spectrum of ^{252}Cf(SF). These models were based on the assumption that the mechanism of neutron emission is the evaporation after fully accelerated fission fragments (FF).

In the present work an attempt to improve the ^{252}Cf(SF) prompt fission neutron spectrum evaluation is made taking into account the multi-modal fission concept. A more generalized form of the FF residual nuclear temperature distribution and a possible anisotropy effect are considered, too.
It has been found [4] that a triangular temperature distribution (see Fig. 2) accounts satisfactory for the CMS spectrum but at higher neutron energy the experimental spectrum is slightly larger than the calculated one. This discrepancy could arise because the triangular temperature distribution eliminates the high-energy contributions to the spectrum that would otherwise be present from temperatures larger than T_M. In the present work we propose therefore another shape for the FF residual temperature distribution with a broader high-temperature cutoff (see Fig. 2, dotted line).
The hypothesis of isotropic neutron emission in the center-of-mass system (CMS) covers no more than 90 - 95 % of the total number of prompt neutrons per fission. The remaining part of prompt fission neutrons showing itself as an increased neutron yield in the low energy region, in the laboratory system, can be considered as an effect of the anisotropy [5]. Using the input multi-modal data obtained at IRMM, the prompt fission neutron spectrum of ^{252}CF(SF) was calculated in first instance without anisotropy effect and using original residual temperature distribution from ref. [2].

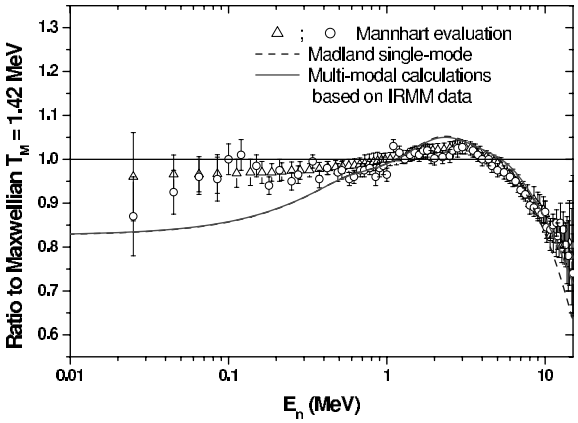

Fig. 3: The present calculations as ratios to the Maxwellian spectrum with T_M = 1.42 MeV in comparison with the "experimental" evaluation of Mannhart and those of Madland, respectively. Only the lower energy part is shown.

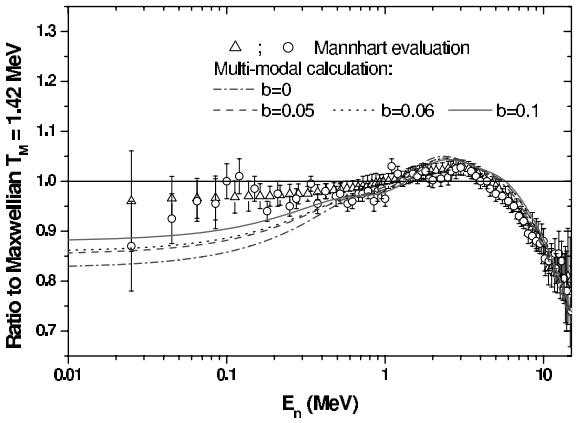

Fig. 4: The prompt fission neutron spectrum of ^{252}Cf was calculated, in the frame of the multi-modal model with the following values of the anisotropy parameter: b = 0.05, b = 0.06 and b = 0.1.

The result is given in Fig. 3 where the present calculations are represented as ratios to the Maxwellian spectrum with T_M = 1.42 MeV in comparison with the "experimental" evaluation of Mannhart and those of Madland, respectively, showing only the lower energy part. Concerning the lower energy part (E $\leq$ 0.3 MeV) both present calculations and Madland's evaluation underestimate Mannhart's evaluation (see Fig. 3). It should be mentioned that there are no evaluations based on models which are in good

agreement with the ”experimental” evaluation of Manhart in the lower energy part of the spectrum.
The conclusion arising from the above calculation is that the use of the multi-modal approach in the frame of the LA model with multi-modal model parameters calculated taking into account the entire FF range and based on the IRMM modal data, leads to an improved agreement of the prompt fission neutron spectrum evaluation with the Mannhart's data except in the lower part of the neutron energy region.
A number of papers in the last ten years (see e.g. [5] and refs. in [6]) have treated the inclusion of the anisotropy into the models build on the assumption that all prompt neutrons are emitted from the fully accelerated FF. For instance statistical calculations done only for the few most important FF appearing in the spontaneous fission of ^{252}Cf, using both the current phenomenological approximation of the anisotropy parameter b = 0.1 and b depending on the neutron energy in CMS, show mainly an increase of the neutron yield in the region of low (E $\leq$ 0.5 MeV) and high energies in the LS. The same behavior of the LS spectrum, when the anisotropy is taken into account, is pointed out in e.g. ref. [5] from where also possible values for the anisotropy parameter were extracted: b = 0.05. Consequently the prompt fission neutron spectrum of ^{252}Cf was calculated, in the frame of the multi-modal model with the following values of the anisotropy parameter: b = 0.05, b = 0.06 and b = 0.1.
The results are given in Fig 4. It is evident from this figure that the anisotropy account leads to an increased agreement of the present calculations with Mannhart 's evaluation especially in the region of low neutron energies (in LS).
The chi-square calculations gives, that the best agreement with the Mannhart data is obtained with the phenomenological usual value of the anisotropy parameter b = 0.1.

Up to now we can conclude that the inclusion of the anisotropy effect in the LA model (with the classical P(T) distribution with sharp cutoff as of eq.(1)) used in the frame of the multi-modal fission approach leads to a substantial improvement of the agreement of the calculated spectra with the Mannhart standard spectrum.
A further inclusion of the modified P(T) distribution gives an additional improvement compared to Mannhart's evaluation for b = 0.1 and s = 1.1. More details will be found in ref. [6].

[1] Mannhart W., IAEA-INDC(NDS) 220 (1989) 305.

[2] D. G. Madland, J. R. Nix, Nucl. Sci. Eng. 81 (1982) 213.

[3] Mrten H., Ruben A., Seeliger D., IAEA-INDC(NDS) 220 (1989) 245.

[4] Kapoor S.S., Ramanna R., Rama Rao P.N., Phys.Rev. 131 (1963) 283.

[5] Budtz-Jrgensen C., Knitter H.-H., IAEA-INDC(NDS) 220 (1989) 181.

[6] A. Tudora et al., to be published

Measurement of the ^{234}U(n, f) cross section as a function of the neutron energy

C. Wagemans[1)], *J. Wagemans*[2,†)], *J. Heyse*[2)], *Kang Wei Chou*[1)], *L. De Smet*[1)], *J. Van Gils*[2)]

[1] University of Gent, Dept. of Subatomic and Radiation Physics, Proeftuinstraat 86, B-9000 Gent, [2] EC-JRC IRMM, B-2440 Geel

A high-resolution measurement of the ^{234}U(n,f) cross section is being performed at a 30 m long flight path of GELINA, using a Frisch-gridded ionisation chamber with very pure methane as detector gas. The ^{234}U sample has a thickness of 101.7 μg/cm^2 and was electrolytically deposited on a 20 μm thick aluminum substrate. The sample material has a ^{234}U enrichment of 99.868 at.%, the ^{235}U content only being 0.076 at.%. The linac was operated at a 800 Hz repetition frequency, the pulse width being 1 ns.

Fig. 1 shows an interim result in the neutron energy region from 540 to 600 eV. A comparison of the resonance doublets at about 560 eV and 585 eV clearly demonstrates that an improved energy resolution is obtained as compared to the corresponding data of James *et al.* [1].

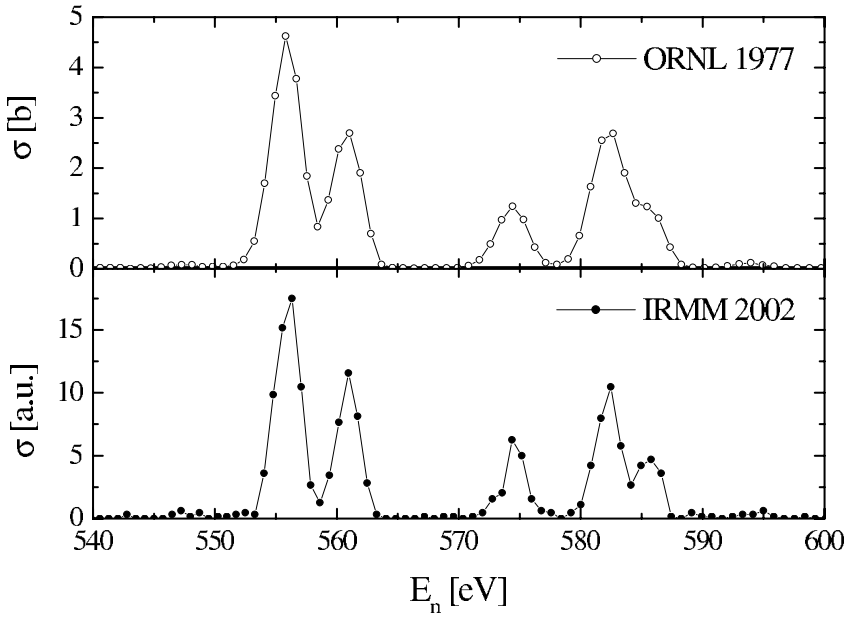

Fig. 1: The ^{234}U(n,f) cross section measured by James *et al.* [1] (upper part) compared to our interim result (lower part) in the neutron energy region from 540 to 600 eV.

[†]present address: SCK•CEN, B-2400 Mol

[1] G. James, *et al.*, Phys. Rev. C15 (1977) 2083

Investigation of the triton and α-emission in ternary fission

C. Wagemans[1)], *J. Heyse*[2)], *O. Serot*[3)], *J. Wagemans*[2,†)], *P. Janssens*[1)], *P. Geltenbort*[4)], *J. Van Gils*[2)]

[1] University of Gent, Dept. of Subatomic and Radiation Physics, Proeftuinstraat 86, B-9000 Gent, [2] EC-JRC IRMM, B-2440 Geel, [3] CEA Cadarache, F-13108 Saint-Paul-lez-Durance, [4] ILL, F-38042 Grenoble

In most cases, a fissioning nucleus splits into two heavy fragments, which is called binary fission. In 0.2 - 0.3 % of the events however, both heavy fission fragments are accompanied by the emission of a light charged particle, mostly an α-particle or a triton. This is called ternary fission. The triton emission in ternary fission appears to be the major source of radioactive tritium production in reactors and used fuel elements.

An interesting characteristic of the ternary fission process is the influence of the excitation energy on the emission probability of the ternary particles. We have investigated this phenomenon for the fissioning system ^{248}Cm in its ground-state (spontaneous fission) and at 6.2 MeV excitation energy (the thermal neutron induced fission of ^{247}Cm). The measurements with thermal neutrons were performed at the high flux reactor of the ILL in Grenoble, the spontaneous fission was studied using a dedicated setup at the IRMM. The results were surprising: for the ternary α's the emission probability per binary fission event **decreased** from (0.00230 $\pm$ 0.00010) for ^{248}Cm(SF) to (0.00185 $\pm$ 0.00010) for ^{247}Cm(n$_{th}$,f), despite the increased excitation energy. For the triton emission however this was not the case, since we obtained an emission probability of (0.000179 $\pm$ 0.000011) for ^{248}Cm(SF) and (0.000184 $\pm$ 0.000011) for ^{247}Cm(n$_{th}$,f) [1]. This slight increase of the emission probability with increasing excitation energy is what one expects a priori. The "anomalous" behaviour of the ternary α-particles is probably due to a strong α-cluster-preformation probability, which decreases with increasing excitation energy. This phenomenon is now being investigated for the similar fissioning systems ^{246}Cm(SF) and ^{245}Cm(n$_{th}$,f).

Another interesting problem in ternary fission is the shape of the energy distribution of the ternary particles, which can be well described by a Gaussian distribution, except for the α's. The origin of the non-Gaussian low-energy tail is believed to be the decay of short-living ternary ^{5}He particles, but this was recently put into doubt by Kopatch *et al.* [2], who investigated ^{5}He particles emitted in the ternary fission of ^{252}Cf. Now we are confronted with two facts: (a) a non-Gaussian low-energy tailing for the ternary α's has been observed by several authors and for various nuclides; however, none of the experiments was optimised for detecting low-energy α's [2]; (b) the yields of the other ternary particles are usually determined relative to the ternary α-yield, so a reliable

[†] present address: SCK•CEN, B-2400 Mol

extrapolation towards E = 0 of the ternary α-spectrum is needed.

So, an experiment was performed at a very intense beam of the high flux reactor of the ILL in Grenoble to determine the ^{235}U(n$_{th}$,f) ternary α-spectrum, aiming at an optimal measurement of its low-energy part. The basic idea is to limit energy loss phenomena and radioactive α-decay of the sample. For ^{235}U samples, most of the α-activity is generally due to ^{234}U impurities (T$_{1/2}$ = 7.038$\times$10^8 y for ^{235}U and 2.455$\times$10^5 y for ^{234}U). We used highly enriched sample material, containing 99.9724 at.% of ^{235}U and only 0.0053 at.% of ^{234}U impurities. With a layer thickness of 10 μg/cm^2, evaporated over a diameter of 15 mm on a 20 μm thick aluminum substrate, the total sample activity is less than 2 Bq. This makes it possible to measure without an absorber foil in between the sample and the ΔE-E detector, so the α's reach the detector without losing energy. Moreover, a 15 μm thick ΔE detector was used to make the detection threshold as low as possible. Fig. 1 shows the preliminary energy distribution of the ternary α's obtained, clearly demonstrating a non-Gaussian low-energy tail, confirming the results reported in [2]. The full line represents a Gaussian fit to the data points above 12.5 MeV.

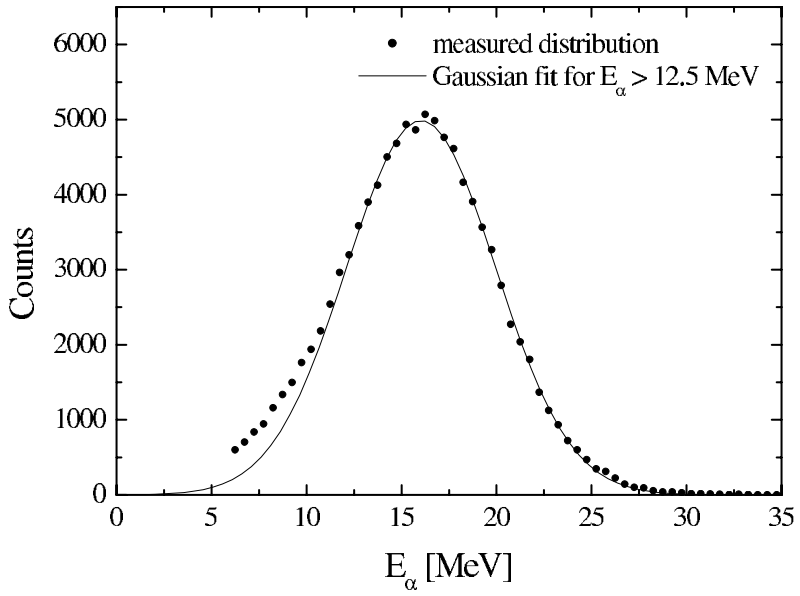

Fig. 1: Energy distribution of the ^{235}U(n$_{th}$,f) ternary α's. The full line represents a Gaussian fit to the data points above 12.5 MeV.

[1] O. Serot *et al.*, Proc. Int. Conf. on Fission and Properties of Neutron-Rich Nuclei, Sanibel Island, Florida, USA (2002), in print

[2] Y. Kopatch *et al.*, Phys. Rev. C65 (2002) 044614

[3] C. Wagemans, The Nuclear Fission Process, CRC Press, Boca Raton, USA (1991)

[4] N. Larson, report ORNL/TM-9179/R4 (1998)

^{239}Pu at resonance energies and its multi-modal interpretation

F.-J. Hambsch 1, H. Bax 1, I. Ruskov[2]*, L. Demattè*[3]

[1] EC-JRC IRMM, B-2440 Geel, [2] INRNE, BU-1784 Sofia, [3] CINECA, Casalechio di Roma, Italy

The activity already described in the last scientific report [1] has been continued and finalised. In addition to the results mentioned in ref. [1] the statistical significance of the observed fluctuations in the different fission fragment observables has been tested with the Kolmogorov-Smirnov (K-S) test [2]. The K-S test provides an alternative to

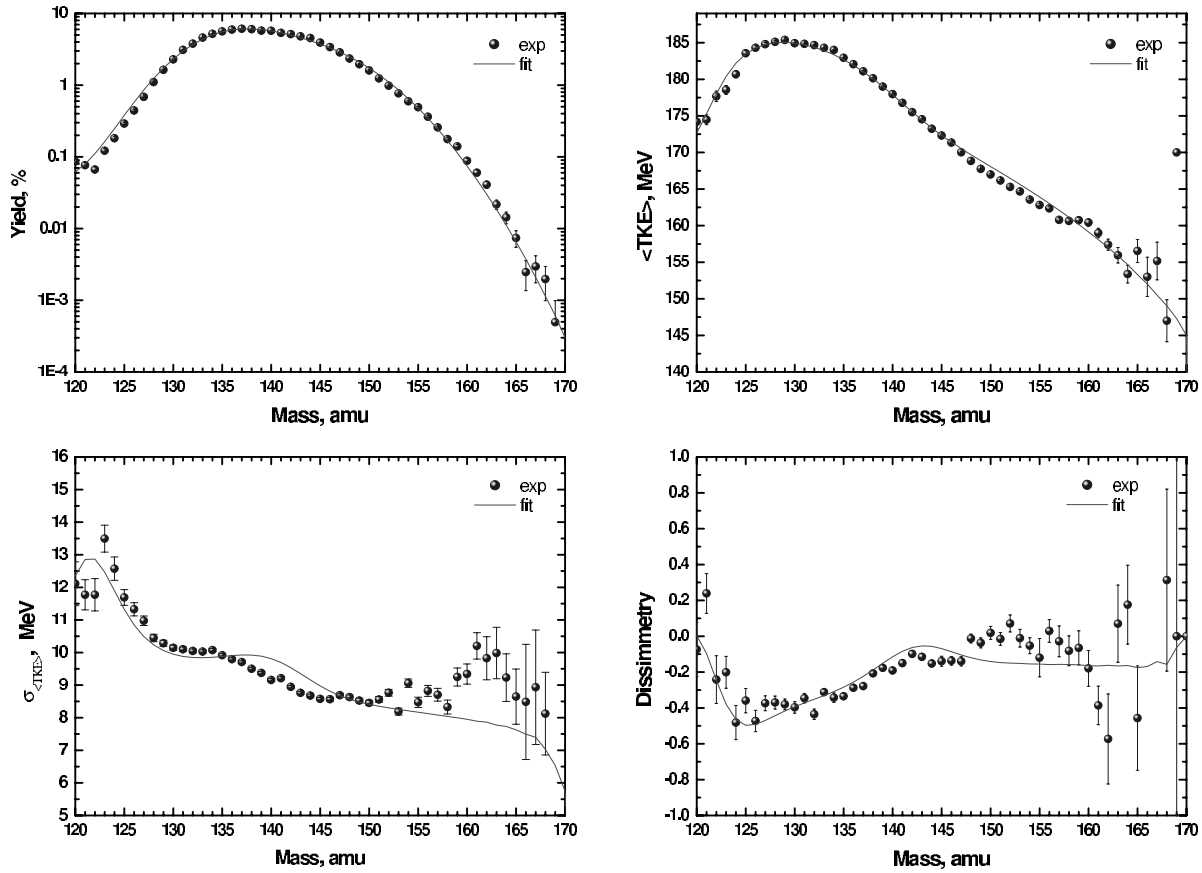

Fig. 1: Comparison between fit and experiment at thermal energy for the mass distribution (upper left), the TKE distribution (upper right) and the higher moments of the TKE distribution, variance (lower left) and dissymmetry (lower right).

the better known χ^2-test, but is usually superior to it for several reasons, one of them being that this test works well with data having low statistics. Details about this test will be presented in Ref. [3]. In conclusion it has shown that for all $J^\pi = 1^+$ resonances

the mass yield differs compared to the mass yield at thermal fission. The kinetic energy distribution for all 1^+ resonances is also different compared to the thermal one, with one exception being the 0.296 eV resonance, which shows a heavy fragment energy distribution similar to the one at thermal energy. The Y(A,TKE) distributions for 0^+ resonances differ compared to the Y(A,TKE) distributions for 1^+ resonances, but insignificantly from the Y(A,TKE) distribution at thermal energy. The mass distributions deduced from in-between resonance energies are closer to the mass distribution of the 0.296 eV resonance, but the energy distributions are different from the one at thermal energy with 95% confidence. This can be understood as a result of the influence of the high-energy tail of the 0.296 eV resonance, which is quite a broad resonance.
In addition for each resonance the experimental two dimensional Y(A,TKE) distributions have been decomposed into the three main modes, two asymmetric modes, called standard I and II (S1 and S2), and one symmetric superlong (SL) mode. The mass distribution of each mode being of Gaussian shape and the TKE distribution of skewed Gaussian shape. Details can be found in Ref. [3]. In Fig. 1 the quality of the

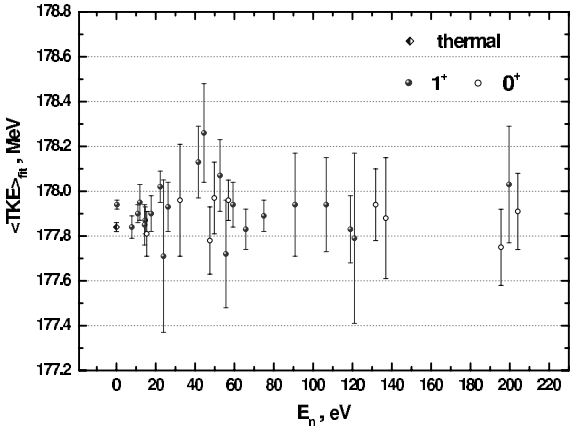

Fig. 2: Resulting TKE from the fit as a function of resonance energy.

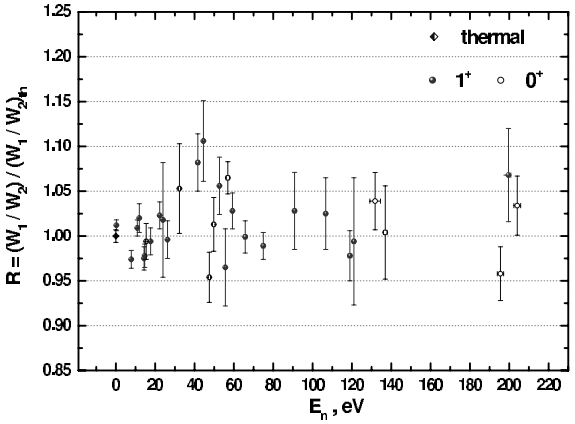

Fig. 3: Resulting branching ratio of the two asymmetric modes as a function of resonance energy.

fit is demonstrated by comparison of the fitted results to the experimental mass and TKE distributions at thermal energy as well as the higher moments of the TKE distribution (variance and skewness). Since strong variations in statistical significance are present in the data, only a slightly smoothed Y(A,TKE) distribution yielded convergent fit results. In Fig. 2 the variation of the fitted TKE and the branching ratios of the two asymmetric modes S1 and S2 are given, the latter relative to the respective thermal value. An up to 10 % change in the branching ratio is obvious from the right part of Fig. 2. Also a bump like structure is evident in both figures with a maximum at about 40 eV. If this is compared to the results from the resonance fission of ^{235}U [4], it is evident that the structure is similar, except that the magnitude is more pronounced and the neutron energy of the position of the bump is about half in case of ^{235}U(n, f). To further elaborate on the results, the correlation has been investigated between the different observables available for the resonance fission of ^{239}Pu. In Fig. 3 the correlation between

the branching ratio and the relative changes in TKE is shown. A strong correlation is obvious, which is also understood from energetics point of view. If the mass distribution is changed, an immediate consequence is that also the mean TKE averaged over all masses is changing. The prompt neutron multiplicity is also subject to changes, if

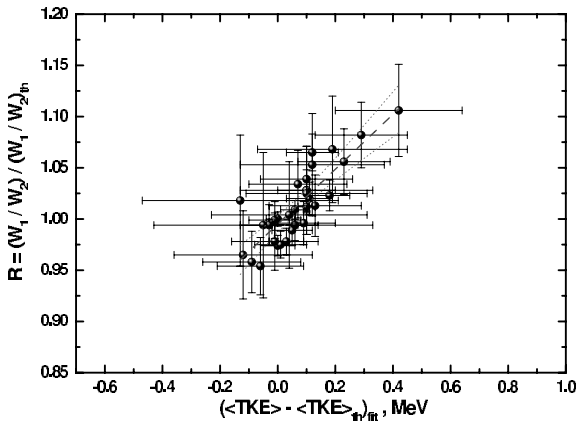

Fig. 4: Correlation between branching ratio and relative TKE.

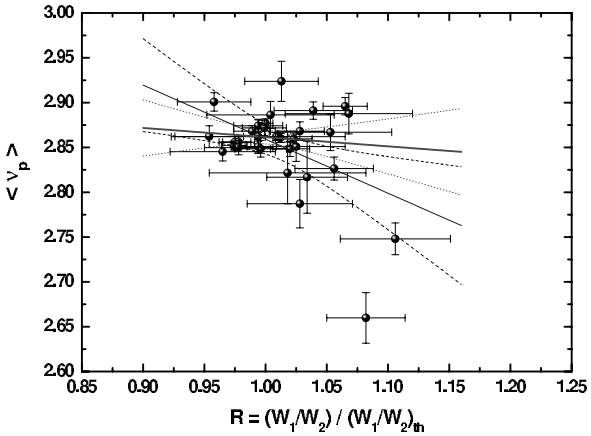

Fig. 5: Correlation of the branching ratio with ν_p.

the mass and TKE distributions are varying. Again this is obvious from the energy balance. In Fig. 4 the corresponding anti-correlation with the TKE shows only a moderate correlation, if all the resonances are included. If the two 1^+ resonances at 41.66eV and 44.53eV, which have the smallest ν_p-values, are omitted, the correlation becomes insignificant. As it was already mentioned, in contrast to resonance neutron induced fission of ^{235}U [4], less pronounced fluctuations in the mass yield and TKE-distributions for ^{239}Pu(n,f) were observed. A possible explanation for the rather weak fluctuations of the fission fragment parameters is to be found in a new theoretical approach by Furman [5]. In ^{239}Pu, for each spin state J^π only one possible K-channel, above the outer fission barrier, can be open, whereas for ^{235}U a mixture of two to three K-channels can take place [4, 5]. If the quantum number K is considered to be a "good" quantum number, i.e. if it is conserved from saddle to scission, the scission configuration should have the same K. In this way, the fission fragment properties, for a given fission mode and K quantum number, should be "fixed". Hence, the superposition of different transition states with different K-quantum numbers (as in ^{235}U) and thus, different fission fragment property distributions can make them fluctuating from resonance to resonance. In case of ^{239}Pu, with only a single transition state, such fluctuations should be absent or be less pronounced, as it is observed.

[1] Neutron Physics Unit, Scientific Report 2001, EUR 20412EN, 2001

[2] W. T. Eadie, D. Drijard, F. James, M. Roos, B. Sadoulet, "Statistical Methods in Experimental Physics", North-Holland, 1971

[3] I. Ruskov, F.-J. Hambsch, L. Demattè, to be published

[4] F.-J. Hambsch, H.-H. Knitter, C. Budtz-Jrgensen and J.P. Theobald, Nucl. Phys. A491 (1989) 56

[5] W. Furman, Proc. FJ/OH Spring Session 99, May 17-21, 1999, Geel Belgium (1999) 124

Corrigendum to:
Light charged-particle emission in thermal neutron-induced fission of $^{252}Cf^{*}$ - first detection of LCP emission with A = 36

S. Oberstedt[1], *A. Oberstedt*[2], *D. Rochman*[3] *F. Gönnenwein*[4] *I. Tsekhanovich*[3] *J. Becker*[2,5], *A. Sartz*[2], *H. Bax*[1] *F.-J. Hambsch*[1] *S. Raman*[6]

[1] EC-JRC IRMM, B-2440 Geel, [2] Örebro Universitet, SE-70182 Örebro, [3] ILL, F-38042 Grenoble, [4] Eberhard-Karls Universität Tübingen, D-72076 Tübingen, [5] FB Physik, Bergische Universität GH Wuppertal, D-42097 Wuppertal, [6] Oak Ridge National Laboratory, Oak Ridge, Tennessee 37831

Due to a re-evaluation of the nuclear-charge calibration for the particle telescope used in the experiment ^{251}Cf(n$_{th}$, f)LCP reported in EC-JRC IRMM Scientific Report (2001) 53 the particle identification for A = 36 had to be revised. The full text has been submitted for publication:

High resolution measurements of light charged particles (LCP) emitted in thermal neutron-induced fission of $^{252}Cf^{*}$ (E^{*} = 6.2 MeV) have been performed with the recoil mass-separator LOHENGRIN. For this compound nuclear system emission yields of LCPs, their mean kinetic energies and widths have been obtained for 8 isotopes with nuclear charges $Z \geq 2$. For 13 further isotopes the emission yields were estimated on the basis of systematics on their kinetic energy distributions. ^{34}Al and ^{36}Si emission has been observed for the first time in thermal neutron-induced fission.

Tab. 1: *LCP mean energy obtained from Gaussian-type functions fitted to the experimental energy distributions. Values with a † are estimates from existing systematics. Our results are compared to values existing only for the reaction ^{252}Cf(SF) published in refs. [2, 3, 4], and for the reaction ^{249}Cf(n$_{th}$, f) [1]. Arrows indicate data obtained from mass-integrated energy distributions.*

	$\overline{E}$ (MeV)				
	this work	ref. [2]	ref. [3]	ref. [4]	^{250}Cf* [1]
^{6}He	11.0±0.9	11.6±0.6	12.2±1.9	11.6±0.2	-
^{8}He	9.5±0.5	10.2±1.0	10.2±1.0	10.1±0.4	-
^{7}Li	-	↑	-	15.0±0.7	-
^{8}Li	11.9±0.6	14.3±1.0	-	13.5±1.4	15.1±1.4
^{9}Li	14.1±0.5	↓	-	12.1±1.5	12.5±0.9

Tab. 1: (continued)

^{9}Be	17.8±1.2	↑	-	-	-
^{10}Be	18.7±0.3	17.5±1.0	-	-	17.5±0.4
^{12}Be	16.4±0.6	↓	-	-	15.1±1.1
^{11}B	-	↑	-	-	-
^{12}B	23.8±1.8	21.2±1.0	-	-	21.8±0.8
^{15}B	19±1†	↓	-	-	16.8±1.9
^{14}C	-	↑	-	-	27.0±0.3
^{15}C	24.4±0.8	26±1	-	-	25.1±0.5
^{17}C	23.7±0.7		-	-	21.3±1.7
^{18}C	24.3±1.5	↓	-	-	20.4±2.8
^{24}O	27±2†	-	-	-	-
^{24}F	32±2†	-	-	-	26.3±2.8
^{24}Ne	31±9	-	-	-	33.9±2.9
^{27}Na	35±6	-	-	-	38.4±8.2
^{30}Na	35±4†	-	-	-	31.7±8.6
^{30}Mg	38.4±6.8	-	-	-	34.9±3.7
^{34}Al	40±6†	-	-	-	-
^{34}Si	49±5†	-	-	-	-
^{36}Si	42±5†	-	-	-	-

Tab. 2: *LCP full width at half maximum (FWHM) obtained from Gaussian-type functions fitted to the experimental energy distributions. Values with a* † *are estimates from existing systematics. For quoted references see Tab 1. Arrows indicate data obtained from mass-integrated energy distributions. Data with a* $^{*)}$ *are quoted as preliminary in ref. [1].*

	FWHM (MeV)				
	this work	ref. [2]	ref. [3]	ref. [4]	^{250}Cf* [1]
^{6}He	9.6±0.5	10.5±0.9	10.4±1.8	10.1±0.1	-
^{8}He	8.9±0.6	10.2±1.0	8.0±2.4	10.5±0.2	-

Tab. 2: (continued)

^{7}Li	-	↑	-	15.5±0.8	-
^{8}Li	12±2†	14.3	-	13.8±1.7	16.7±3.1
^{9}Li	12.4±2.1	↓	-	12.1±2.0	13.0±2.4
^{9}Be	11.8±2.1	↑	-	-	-
^{10}Be	17.4±0.9	18	-	-	18.1±1.4
^{12}Be	12.0±1.2	↓	-	-	16.7±2.6
^{11}B	-	↑	-	-	-
^{12}B	20.2±4.4	19.3	-	-	19.3±4.2
^{15}B	17±1†	↓	-	-	16.5±2.4
^{14}C	-	-	-	-	23.3±1.2
^{15}C	18.6±1.9	-	-	-	21.0±1.6
^{17}C	20±2†	-	-	-	19.5±2.1
^{18}C	16.5±2.0†	-	-	-	20.0±3.3
^{24}O	24±2†	-	-	-	22±8$^{*)}$
^{24}F	27±3†	-	-	-	28.5±4.7
^{24}Ne	30±3†	-	-	-	33.4±4.5
^{27}Na	32±4†	-	-	-	38±11
^{30}Na	30±4†	-	-	-	28±14
^{30}Mg	33±4†	-	-	-	30.6±4.2
^{34}Al	34±4†	-	-	-	-
^{34}Si	37±5†	-	-	-	27±3$^{*)}$
^{36}Si	36±5†	-	-	-	-

Tab. 3: *LCP emission yields from the thermal neutron-induced fission of ^{252}Cf. For quoted references see Tab 1. Arrows indicate data obtained from mass-integrated energy distributions. Data with a $^{*)}$ are quoted as preliminary in ref. [1].*

	$Y_{LCP}/Y_{^{10}Be}$				
	this work	ref. [2]	ref. [3]	ref. [4]	^{250}Cf* [1]

Tab. 3: (continued)

^{6}He	2.9±0.7	3.3±0.6	7.8	2.2	>1.4
^{8}He	0.20±0.04	0.26±0.05	0.33	0.14	-
^{7}Li	-	↑	↑	0.09	-
^{8}Li	0.05±0.01	0.54±0.06	0.65	0.05	0.069±0.014
^{9}Li	0.17±0.03	↓	↓	0.14	0.10±0.02
^{9}Be	0.11±0.03	↑	↑	-	-
^{10}Be	1	≈1.3	≈1.3	1	1
^{12}Be	0.10±0.01	↓	↓	-	0.073±0.014
^{11}B	-	↑	↑	-	-
^{12}B	0.04±0.01	0.07±0.04	0.13	-	0.04±0.01
^{15}B	$(5\pm1)\times10^{-3}$	↓	↓	-	$(2.4\pm1.0)\times10^{-3}$
^{14}C	-	-	↑	-	0.34±0.03
^{15}C	0.16±0.02	-	1.3	-	0.14±0.02
^{17}C	$(1.7\pm0.3)\times10^{-2}$	-		-	$(2.0\pm0.5)\times10^{-2}$
^{18}C	$(8\pm1)\times10^{-3}$	-	↓	-	$(6.4\pm1.6)\times10^{-3}$
^{24}O	$(1.2\pm0.9)\times10^{-3}$	-	-	-	$1.5\times10^{-3*)}$
^{24}F	$(1.2\pm0.9)\times10^{-3}$	-	-	-	$(2.2\pm1.0)\times10^{-4}$
^{24}Ne	$(6.0\pm1.2)\times10^{-3}$	-	-	-	$(6.3\pm1.2)\times10^{-3}$
^{27}Na	$(2.9\pm0.5)\times10^{-3}$	-	-	-	$(2.2\pm0.8)\times10^{-3}$
^{30}Na	$(2.5\pm1.7)\times10^{-4}$	-	-	-	$(6\pm6)\times10^{-4}$
^{30}Mg	$(2.4\pm0.6)\times10^{-3}$	-	-	-	$(2.5\pm1.0)\times10^{-3}$
^{34}Al	$(9\pm7)\times10^{-4}$	-	-	-	-
^{34}Si	$(1.0\pm0.6)\times10^{-3}$	-	-	-	$5\times10^{-4*)}$
^{36}Si	$(4\pm3)\times10^{-4}$	-	-	-	-
^{37}Si	-	-	-	-	$5\times10^{-5*)}$
^{36}S	$<1.2\times10^{-4}$	-	-	-	-
^{37}S	-	-	-	-	$1.2\times10^{-4*)}$
^{38}S	$<1.2\times10^{-4}$	-	-	-	-
^{40}S	$<10^{-4}$	-	-	-	$<9\times10^{-5}$

[1] M. Davi, PhD thesis, Johannes Gutenberg Universität, Mainz (1997), unpublished
I. Tsekhanovich, Z. Büyükmumcu, M. Davi, H. O. Denschlag, F. Gönnenwein and S. F. Boulyga, Phys. Rev. C67 034610 (2003)

[2] M. Mutterer, P. Singer, Y. N. Kopach, M. Klemens, A. Hotzel, D. Schwalm, P. Thirolf, M. Hesse, 3^{rd} Int. Conf. on Dynamical Aspects of Nuclear Fission, Castá-Papernicka, Slovak Republic, Aug. 30 - Sept. 4 (1996) 250

[3] C. Wagemans, Chap. 'Ternary Fission' in The Nuclear Fission Process, CRC Press (1991) 553

[4] Z. Dlouhy, J. Svanda, R. Bayer, I. Wilhelm, Proc. Int. Conf. on Fifty Years Research in Nuclear Fission (Berlin, 1989), eds. D. Hilscher et al (Berlin: Hahn-Meitner Institut) Report HMI-B 464, p.43

Nuclear reaction mechanisms and standards

Study of the (n, p) and (n, α) reactions on ^{26}Al and ^{36}Cl

L. De Smet[1)], *C. Wagemans*[1)], *J. Wagemans*[2,†)], *G. Goeminne*[1)], *J. Heyse*[2)], *J. Van Gils*[2)]

[1] University of Gent, Dept. of Subatomic and Radiation Physics, Proeftuinstraat 86, B-9000 Gent, [2] EC-JRC IRMM, B-2440 Geel

An interesting problem in astrophysics is the origin of ^{26}Al in the interstellar medium of our galaxy. Its presence is clearly established, e.g. by recent observations of the 1.8 MeV γ-line emitted in its decay, with the Compton γ-ray observatory. These observations support the idea that ^{26}Al is still produced in our galaxy (e.g. during supernova explosions) and ejected in the interstellar medium at a rate of two solar masses of ^{26}Al per million year. A good understanding and a quantitative description of the corresponding nucleosynthesis scenario's require accurate cross section data for the production and destruction of ^{26}Al. Key reactions in this respect are ^{26}Al(n,p)^{26}Mg and ^{26}Al(n,α)^{23}Na.

Last year, these reaction cross sections have been determined with thermal neutrons at the high flux reactor of the ILL (Grenoble, France), using a sample containing 2×10^{17} atoms of the very rare ^{26}Al [1]. Measurements with higher neutron energies (up to 150 keV) are ongoing at a 8 m flight path of GELINA, using a Frisch-gridded ionisation chamber with very pure methane as detector gas. Partial results permit already the identification of four resonances in the ^{26}Al(n,α)^{23}Na cross section not observed so far.

Although the bulk of the elements between C and Fe are produced in thermonuclear fusion reactions in stars, some rare, neutron rich isotopes such as ^{36}S are bypassed by these reactions. These isotopes are created by neutron capture on nuclides produced during He and C burning, and their formation can be described by the weak component of the s-process. The corresponding network comprises several (n,p) and (n,α) reactions, such as ^{36}Cl(n,α)^{33}P and especially ^{36}Cl(n,p)^{36}S.

The ^{36}Cl(n,α)^{33}P and ^{36}Cl(n,p)^{36}S reaction cross sections have previously been determined at a thermal neutron beam of the ILL in Grenoble [2] and were now investigated

[†] present address: SCK•CEN, B-2400 Mol

at a 30 m flight path of GELINA up to 350 keV neutron energy, using a Frisch-gridded ionisation chamber with very pure methane as detector gas. The ^{36}Cl sample used contains 1.4×10^{19} atoms. The reaction cross sections as a function of the neutron energy have a much better energy resolution than the corresponding data of Koehler *et al.* [3], as shown in Fig. 1. About 20 resonances have been observed, several of them for the first time. The determination of the resonance parameters is being done using the R-matrix code SAMMY [4].

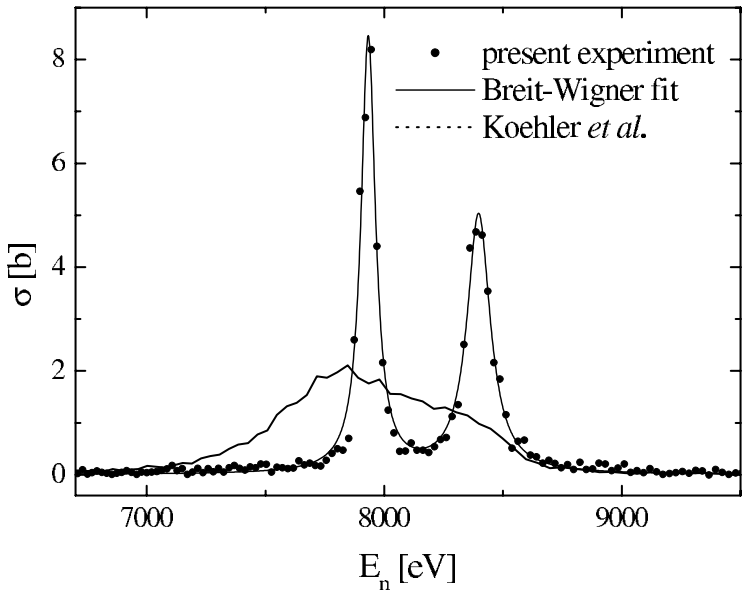

Fig. 1: The ^{36}Cl(n,p) resonance doublet at about 8 keV. Our data are represented by points, the full line is a Breit-Wigner fit to these data and the dotted line represents the data of Koehler *et al*. [3].

[1] J. Wagemans *et al.*, Nucl. Phys. A696 (2001) 31

[2] C. Wagemans *et al.*, Phys. Rev. C54 (1996) 188

[3] P. Koehler *et al.*, Phys. Rev. C47 (1993) 2107

[4] N. Larson, report ORNL/TM-9179/R4 (1998)

Determination of average resonance parameters from average capture measurements using the characteristic function model

A. Lukyanov[1)], *N. Koyumdjieva*[1)], *N. Janeva*[1)], *K. Volev*[1)], *A. Brusegan*[2)], *P. Schillebeeckx*[2)], *G. Lobo*[2)], *F. Corvi*[2)]

[1] INRNE, BG-1784 Sofia, [2] EC-JRC IRMM, B-2440 Geel

In the Unresolved Resonance Region (URR) only statistical modelling can reveal the resonant cross section structure, and accurately describe the average cross-sections and their functionals in all energy intervals. Various schemes for the calculation of resonance-averaged cross sections in the URR are known [1]. They are mainly based on the Hauser-Feshbach formula. Since the fine structure is described in a single level Breit-Wigner approximation, such a scheme is in principle only valid for isolated resonances. Several procedures have been proposed to account for a significant resonance level overlap within the Hauser-Feshbach formalism. However, these schemes do not supply general analytical expressions for resonance-averaged cross-section functionals. They have to be calculated by Monte-Carlo simulations.

The model proposed in [2] not only provides the resonance-averaged cross sections but also their functionals. The model is based on the idea of introducing the characteristic function of the R-matrix element distribution. For the parameterisation of the cross-section the Reich-Moore R-matrix approximation is used. Applying this model, reliable average resonance parameters can be deduced from transmission, capture and self-indication measurement data obtained in the URR. To investigate the discrepancies between the average capture cross-section for ^{232}Th(n,γ) reported in [3] and [4], we analysed the GELINA capture data [3] together with the results of the self-indication measurements of [5].

Average resonance parameters for ^{232}Th, in the URR below the inelastic scattering threshold, are deduced by fitting experimental average capture data with theoretical expressions. The free parameters in the fitting procedure are: the average reduced neutron width ($\bar{\Gamma}^l_n$), the average radiation width ($\bar{\Gamma}_\gamma$), the mean level spacing ($\bar{D}$) and the effective scattering radius (R'). The parameters $\bar{\Gamma}^l_n$, $\bar{\Gamma}_\gamma$ and $\bar{D}$ are adjusted only for s- and p-wave neutrons. The radius R' is considered to be independent of the orbital angular momentum of the incoming neutron. The average parameters for d-wave neutrons are fixed and taken from JENDL 3.2. The resulting parameters and the initial values from JENDL 3.2 are summarised in Table 1. To verify the results, we also performed a fit of the GELINA data together with the data from self-indication measurements of [5]. The average parameters from this simultaneous analysis are given in the last column of Tab. 1 and are in good agreement with the data deduced from the capture measurements.

Tab. 1: Average resonance parameters for ^{232}Th in E_n = (4 - 40) keV.

		JENDL 3.2	Fitted average resonance parameters	
			$\overline{\sigma}_{\gamma\,exp}$	$\overline{\sigma}_{\gamma\,exp}, f_{\gamma\,exp}$
$\overline{\Gamma}_n^l$ / meV	l=0, J$^\pi$=0.5	1.730	1.90	1.83
	l=1, J$^\pi$=0.5	3.650	3.91	3.69
	l=1, J$^\pi$=1.5	1.807	1.95	1.84
	l=2, J$^\pi$=1.5	0.922		
	l=2, J$^\pi$=2.5	0.616		
$\overline{\Gamma}_\gamma$ / meV	l=0, J$^\pi$=0.5	21.20	25.37	26.19
	l=1, J$^\pi$=0.5	21.20	24.24	25.22
	l=1, J$^\pi$=1.5	21.20	24.24	25.22
	l=2, J$^\pi$=1.5	21.20		
	l=2, J$^\pi$=2.5	21.20		
$\overline{D}$ / eV	l=0, J$^\pi$=0.5	18.464	18.03	18.42
	l=1, J$^\pi$=0.5	18.464	18.03	18.42
	l=1, J$^\pi$=1.5	9.217	9.02	9.21
	l=2, J$^\pi$=1.5	9.217		
	l=2, J$^\pi$=2.5	6.159		
R' / fm	l=0,1,2	10.010	8.94	8.99

[1] F. Fröhner, *Evaluation and Analysis of Nuclear Resonance Data*, JEFF Report 18 (2000)

[2] N. Koyumdjieva, N. Janeva and A. A. Lukyanov, Z. Phys. A253 (1995) 31

[3] G. Lobo, F. Corvi, P. Schillebeeckx, N. Janeva, A. Brusegan, P. Mutti, *Measurement of the Th neutron capture cross-section in the region 5 keV-150 keV*, J. of Nucl. Science and Techn., Supplement 2 ND2001 429

[4] K. Wisshak, F. Voss and F. Kappeler, *Neutron capture cross section of ^{232}Th*, Nucl. Science and Eng. 173 (2001) 183

[5] H. Oigawa, Y. Fujita, K. Kobayashi, S. Yamamoto, I. Kimura, *Self-shielding factors for neutron capture reactions of Uranium-238 and Thorium-232 in energy range of 1-35 keV*, J. of Nucl. Science and Techn., 28 (1991) 879-893

Fast-neutron total and capture cross sections of ^{58,60}Ni and ^{59}Co isotopes

V. Avrigeanu[1,2]*, A. J. M. Plompen*[2]*, and H. Weigmann*[2]

[1] Association EURATOM-MEC, NIPNE, RO-76900 Bucharest, [2] EC-JRC IRMM, B-2440 Geel

Various discrepancies exist between the recent GELINA total neutron cross sections of ^{58,60,61}Ni isotopes [1] and other data sets as well as optical model potential (OMP) predictions. There are also large discrepancies between the average radiative widths $\Gamma_{\gamma 0}$ of the s-wave neutron resonances measured recently at IRMM [2] and the evaluated data within RIPL [3]. In order to provide accurate calculated total neutron cross sections the SPRT method [4] was involved for the analysis of some frequently used OMP parameter sets. The OMP parameter sets of Kawano *et al.* [5] were validated for the isotopes ^{58,60,62,64}Ni, while parameters were modified [6] for ^{61}Ni and ^{59}Co (Fig. 1).

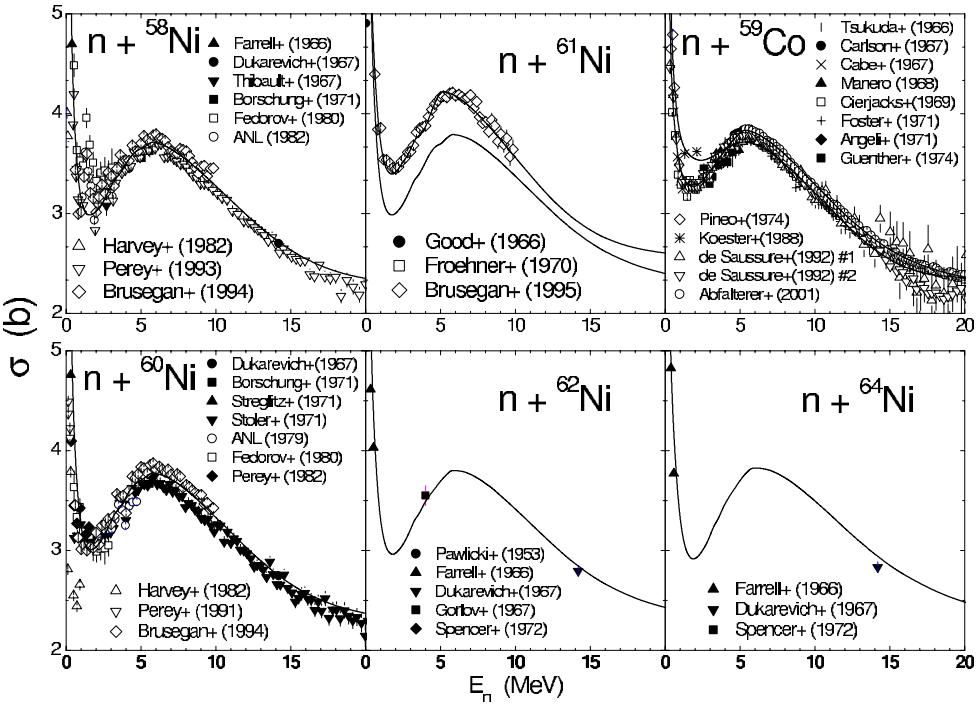

Fig. 1: Calculated vs. measured $^{58,60-62,64}$Ni and ^{59}Co neutron total cross sections.

These OMPs were employed in calculations of the fast-neutron capture cross sections with the Hauser-Feshbach-Moldauer model. The key ingredients of such calculations, the γ-ray transmission coefficients, are fixed by the γ-ray strength functions $f_{XL}(\varepsilon_\gamma)$. Here the dominant electric dipole transition strength function $f_{E1}(\varepsilon_\gamma)$ was obtained

from the modified energy-dependent Breit-Wigner (EDBW) model [7]. By analysing the experimental $\Gamma_{\gamma 0}^{exp}$ systematic EDBW-model correction factors were established in the range A=41-105 assuming that they are given by the ratio $F_{SR}=\Gamma_{\gamma 0}^{exp}/\Gamma_{\gamma 0}^{EDBW}$. The method was validated by comparison of calculated and experimental capture cross sections of ^{59}Co and ^{58,60}Ni in the neutron energy range from few keV to 2-3 MeV. The RIPL values for $\Gamma_{\gamma 0}^{exp}$ lead to γ-ray strength functions that are too large while recent IRMM [2] and ORNL values [8] provide good agreement with the experimental capture data (Fig. 2).

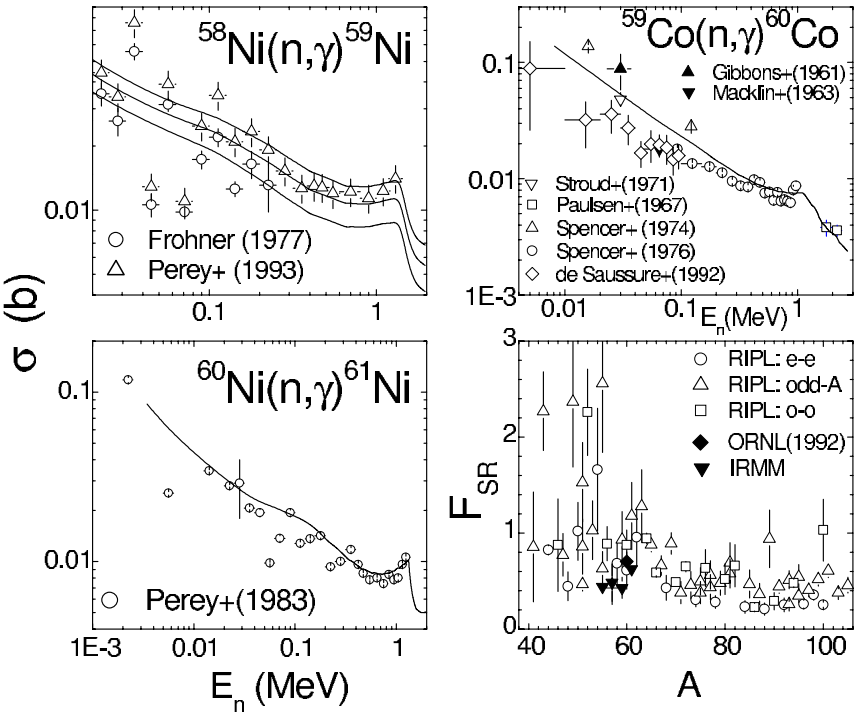

Fig. 2: Calculated vs. measured ^{58,60}Ni and ^{59}Co neutron-capture cross-sections.

Besides the considerable interest for reactor design of neutron total and capture cross sections themselves, their accurate description provides also a basis for fast-neutron activation cross sections and especially isomeric cross-section ratio analysis. On the other hand there are quantities involved in such calculations, *e.g.* nuclear level densities, which are still uncertain in spite of many decades of their study or even basic interest like in the case of the nuclear moment of inertia. It is why the present work has been one unavoidable step for the development of improved methods for calculation of activation cross sections.

[1] A. Brusegan *et al.*, in *Proc. Int. Conf. on Nuclear Data for Science and Technology, Gatlinburg, May 1994*, edited by J.K. Dickens (American Nuclear Society, La Grange Park, 1994), p. 224; EXFOR data file Entry 22315, dated 1997-02-14

[2] F. Corvi *et al.*, as [1]a, p. 221; F. Corvi *et al.*, Nucl. Phys. A697 (2002) 581

[3] *Handbook for calculations of nuclear reaction data. Reference Input Parameter Library*, Report IAEA-TECDOC-1034, Vienna (1998); http://iaeand.iaea.or.at/ripl

[4] J.P. Delaroche, Ch. Lagrange, and J. Salvy, in *Nuclear theory in neutron nuclear data evaluation*, Report IAEA-190 (IAEA, Vienna, 1976), vol. 1, p. 251

[5] T. Kawano *et al.*, in *Proc. Int. Conf. on Nuclear Data for Science and Technology, Jülich, May 1991*, edited by S.M. Qaim (Springer-Verlag, Berlin, 1992), p. 974

[6] M. Avrigeanu *et al.*, in *Workshop on Activation Data EAF 2003, Prague, June 2002*

[7] D.G. Gardner and F.S. Dietrich, LLNL Report UCRL-82998, Livermore, 1979; M. Avrigeanu *et al.*, Rev. Roum. Phys. 32 (1987) 837

[8] G. de Saussure *et al.*, Ann nucl. Energy 19 (1992) 393

Isomeric cross section ratio of the ^{58}Ni(n, p)^{58}Co^{m,g} and ^{59}Co(n, 2n)^{58}Co^{m,g} reactions

V. Avrigeanu[1,2]*, A. J. M. Plompen*[1]*, and V. Semkova*[1]

[1] EC-JRC IRMM, B-2440 Geel, [2] NIPNE, RO-76900 Bucharest

The cross sections analysis of activation reactions on the ^{58,60}Ni and ^{59}Co isotopes in the energy range from threshold up to 20 MeV has been reported based on (i) unitary use of the common model parameters for different mechanisms concerned at once, (ii) use of consistent sets of input parameters which are determined by analyses of various independent experimental data [1], and (iii) unitary account of a whole body of related experimental for isotope chains of neighboring elements [2, 3]. Calculated excitation functions have been finally provided for the reactions ^{58}Ni(n,n'γ) including population of first excited state, ^{58}Ni(n,p)^{58}Co^{m,g}, ^{58}Ni(n,α)^{55}Fe, ^{58}Ni(n,pα)^{54}Mn, ^{58}Ni(n,xα), ^{58}Ni(n,n'p)^{57}Co, ^{58}Ni(n,2n)^{57}Ni, ^{59}Co(n,p)^{59}Fe, ^{59}Co(n,α)^{56}Mn, ^{59}Co(n,xα), ^{59}Co(n,2n)^{58}Co^{m,g} (e.g. Fig. 1), ^{60}Ni(n,p)^{60}Co^{m,g} (Fig. 2) and ^{60}Ni(n,α)^{57}Fe.

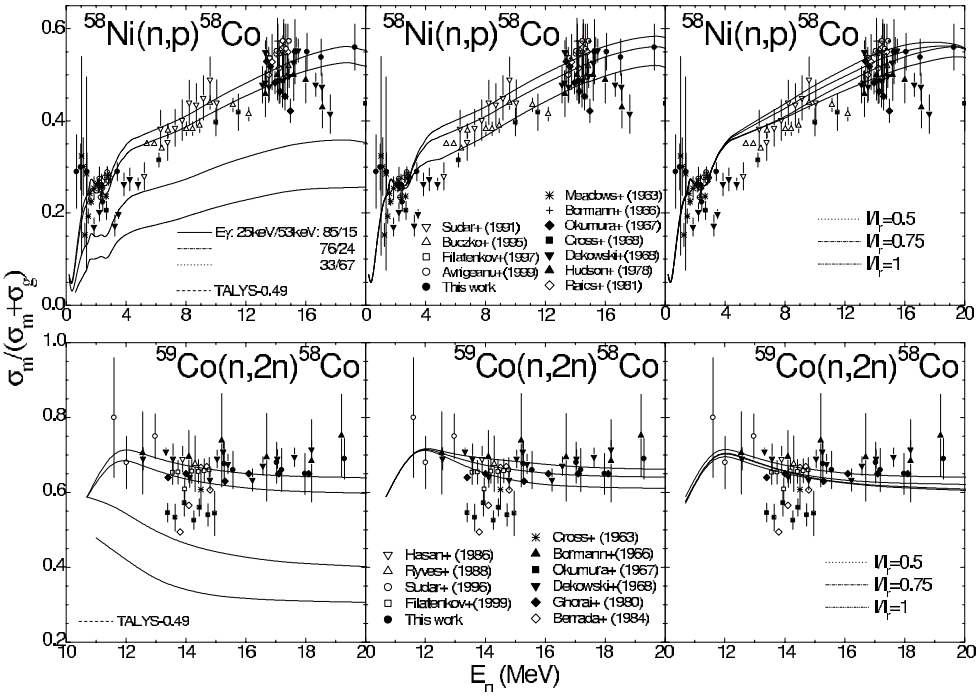

Fig. 1: Calculated vs. measured isomeric cross section ratios for ^{58}Co^{m,g} population.

Recently Gul [4] reported results of calculation of the excitation functions and isomeric cross section ratio of ^{58}Ni(n,p)^{58}Co^{m,g} reactions, and noted that an anomaly of the branching ratio of the 52.8 keV (4^+) state to the isomeric 24.9 keV state (5^+) has been resolved by using more precise formalism of the gamma-ray transition probabilities for the continuum and discrete levels. In order to analyse the correctness of

our previous calculation of this reaction [5] we have discussed at the same time the energy dependence of the isomeric cross-section ratio for both ^{58}Ni(n,p)^{58}Co^{m,g} and ^{59}Co(n,2n)^{58}Co^{m,g} reactions. They were well reproduced by using the same common parameters, as well as actually all activation cross sections [2] of fast-neutron induced reactions on the target nuclei ^{59}Co and ^{58}Ni. Additional questions risen in the meantime concerning the suitable effective moment of inertia I of the nucleus, *i.e.* spin distribution of the nuclear level density, have had to be solved too. However, at present, measurement uncertainties and question marks associated with the decay scheme of ^{58}Co preclude a definitive conclusion about the appropriate value of the effective moment of inertia (Fig. 1).

The calculation and description of both the ground and isomeric states of ^{60}Co through the (n,p) reaction on the target nucleus ^{60}Ni have been easier since the more well known decay scheme of ^{60}Co. The agreement with the experimental data for reaction cross sections as well the isomeric cross section ratio has been found satisfactory especially when it has been analysed the effect of the various I/I_r-values on the calculated excitation functions (Fig. 2). Thus, the reaction cross sections have been better described by the value I/I_r=0.75, while the limits 0.5 and 1.0 are proved to be not suitable. However, the isomeric cross section ratio obtained by using the variable moment of inertia describes better the experimental data in the whole incident energy range.

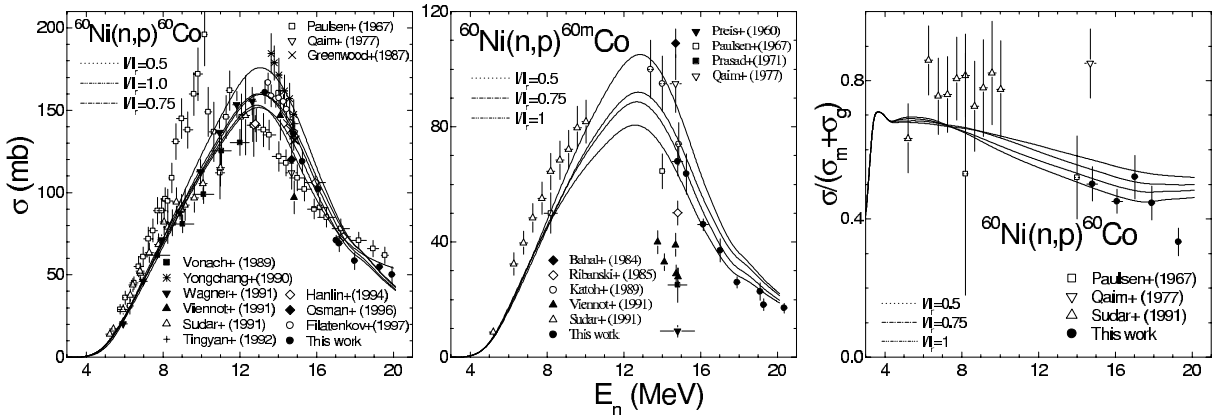

Fig. 2: Calculated vs. measured ^{60}Co^{m,g} population cross sections and their ratio.

[1] M. Avrigeanu *et al.*, in *Workshop on Activation Data EAF 2003, Prague, June 2002*

[2] A.J.M. Plompen, V. Avrigeanu, C. Borcea, L. Olah, and V. Semkova, in *Proc. Int. Conf. PHYSOR-2002, October 7-10, 2002, Seoul, Korea* (in press)

[3] V. Avrigeanu *et al.*, in *Fast Neutron Physics Int. Workshop, Dresden, Sept. 5-7, 2002* (in press); Report EFF-Doc-835, Dec. 2002

[4] K. Gul, Phys. Rev. C62, 067603 (2000)

[5] V. Avrigeanu, S. Sudár, Cs.M. Buczkó, J. Csikai, A.A. Filatenkov, S.V. Chuvaev, R. Dóczy, V. Semkova, and V.A. Zelenetsky, Phys. Rev. C60, 017602 (1999)

The neutron total and capture cross-section of ^{84}Kr below 120 keV

A. Brusegan[1)], *H. Beer*[2)], *F. Corvi*[1)], *P. Mutti*[3)]

[1] EC-JRC IRMM, B-2440 Geel, [2] FZ Karlsruhe, Institut fur Kernphysik, P. O. Box 3640, D-76021 Karlsruhe, [3] ILL, F-38042 Grenoble

The ^{82,84,86}Kr isotopes lie in one of the most sensitive, complicated and therefore interesting region of the s-process nucleosynthesis. This mass region, in fact, receives substantial contributions from both the weak and the main component of the s-process, which are associated to different stellar sites in stars of different size. In fact, isotopes between Fe and Sr are mainly synthesised by the weak s-process component through the activation in massive stars of the ^{22}Ne(α, n)^{25}Mg neutron source during the core-He or shell-C burning evolutionary phases [1, 2]. Also the main s-process component, responsible for the production of the elements from Y up to Bi, contributes to their abundance. According to the most recent double pulse s-process model [3], the main component takes place in He shell burning of low mass AGB stars during the thermal instabilities which characterise the shell-He burning phase. In order to improve the knowledge of capture cross section of the stable isotopes ^{82,84,86}Kr, high-resolution measurements have been performed at the 58 m flight path of the Geel Linear Accelerator (GELINA) in the energy range from 1 eV up to 120 keV. Transmission measurements of the 99.9 % enriched ^{84}Kr sample have been carried out at 49.3 m flight distance. The R-Matrix analysis of the total cross section is completed. The present measurements extend the known region up to 120 keV, well above the 1.6 keV of the existing measurements, providing for 150 resonances neutron energies, neutron scattering widths and in some case parity and spin assignments. The fitted value of the potential scattering radius, 7.93$\pm$0.10 fm, is in good agreement with the 7.46 fm of ENDF, but is much larger than the value of 4.9 fm obtained from deformed optical model calculations [4]. The s-wave neutron strength function, calculated from the 23 resonances lying in the energy region below 120 keV is S_0 = (1.21$\pm$0.36)$\times 10^{-4}$ and very similar to the value of 1.12×10^{-4} given in ref. [4]. In Fig. 1 the plot of the cumulative distribution of number of levels as a function of the reduced neutron widths for s-wave resonances is shown. From the fit to the distribution, shown in the same figure, it was possible to estimate an average level spacing D_0 = 4.2 keV, which has to be compared to D_0 = (5.37$\pm$0.60) keV calculated from the observed number of resonances. The fit is an attempt to correct for missed levels. For the capture data the final analysis will follow after a normalisation test. In Fig. 2 the capture yield and the transmission spectrum are shown for ^{84}Kr in the energy range below 50 keV. The execution of the planned transmission measurements for the ^{82}Kr isotope depends on the availability of a sample.

[1] C.M. Raiteri, M. Busso, R. Gallino, G. Picchio and L. Pulone, Ap.J.367 (1991) 228

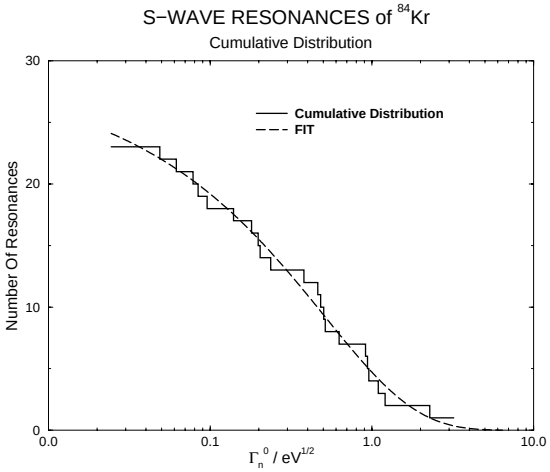

Fig. 1: Cumulative distribution of the number of s-wave levels in function of the reduced neutron widths.

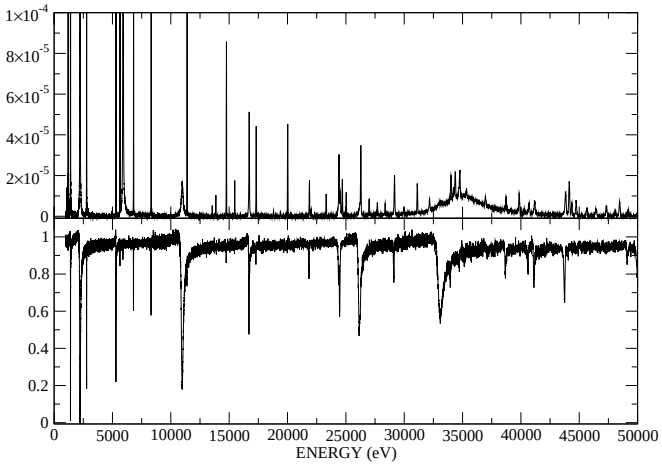

Fig. 2: Plot of the ^{84}Kr capture and transmission (below) spectra in the energy range up to 50 keV.

[2] C.M. Raiteri, M. Busso, R. Gallino, G. Picchio, Ap. J. 371 (1991) 665

[3] O. Straniero, R. Gallino, M. Busso, A. Chieffi, C.M. Raiteri, M. Salaris and M. Limongi, Ap. J. L85 (1995) 440

[4] S.F. Mughabghab, Neutron Cross Section and Technology, Knoxville, Tenn. (1971) 386

The effect of particle leaking and its implications for measurements of the (n, α) reaction on light elements using ionisation chambers

G. Giorginis[1)], *V. Khriatchkov*[2)]

[1] EC-JRC IRMM, B-2440 Geel, [2] IPPE RU-249020 Obninsk

The effect of particle leaking has been discovered at IRMM in 2002 by using a 1-D TPC for the measurement of the ^{10}B(n, α)^{7}Li reaction. Particle leaking arises from the simultaneous emission of reaction products in forwards angles and the inability of the detector to resolve multiple particles. It is an inherent property of all GIC spectrometers used for the study of (n, charged particle) reactions on light-element solid targets. There are implications for all measurables. Forwards angular distributions are truncated at large emission angles and look like depleted of reaction products in a region between a kinematically determined angle (critical angle) and 90^{o} (incomplete distributions). The cross sections $\sigma(\alpha_0)$ and $\sigma(\alpha_1)$ and their ratio $\sigma(\alpha_0)/\sigma(\alpha_1)$ (branching ratio) can not be measured in the depleted angle region. Only the cross section $\sigma(\alpha)$= $\sigma(\alpha_0$ +

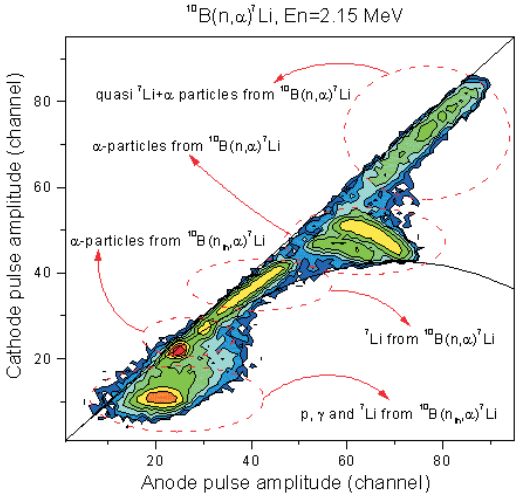

Fig. 1: Two-dimensional pulse amplitude spectrum of the cathode versus the anode for the ^{10}B(n, α)^{7}Li reaction at E$_n$ = 2.15 MeV showing regions of identified particle signatures. The effect of particle leaking induces in the energy spectrum a migration of α and ^{7}Li particles and their detection as quasi 7Li+α particles.

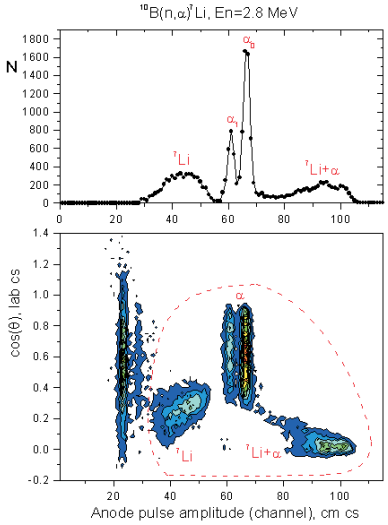

Fig. 2: Two-dimensional spectrum of the cos(θ) (laboratory coordinate system) versus particle energy (centre-of-mass coordinate system) for the ^{10}B(n, α)^{7}Li reaction at E$_n$ = 2.8 MeV (lower part) and the corresponding energy spectrum (upper part) after suppression of the thermal-neutron component.

α_1) can be determined in the full forward hemisphere and strongly benefits from particle leaking but low cross-section values are obtained, if this effect is overlooked.

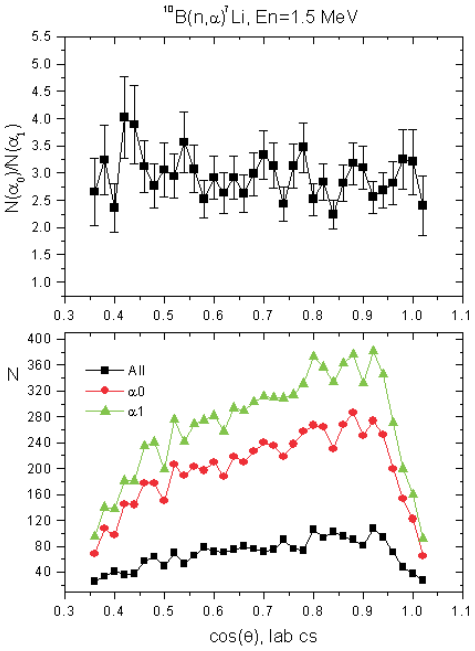

Fig. 3: Incomplete angular distributions of the α_0 and α_1 particle groups emitted by the ^{10}B(n, α)^{7}Li reaction at E_n = 1.5 MeV (lower part) and forwards α_0/α_1 ratio as function of angle (upper part) in the laboratory coordinate system. The cut-off at about cos(θ) = 0.35 is due to particle leaking.

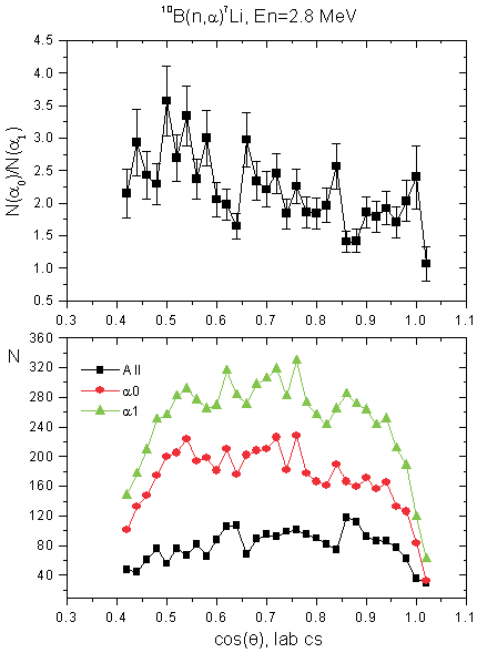

Fig. 4: The same as Fig. 3 but at E_n = 2.8 MeV. The angle cut-off due to the kinematical effect of particle leaking is at cos(θ) = 0.42.

Measurement of the excitation function of the ^{10}B(n, α)^{7}Li reaction by using a 1-D TPC

G. Giorginis[1)], *V. Khriatchkov*[2)]

[1] EC-JRC IRMM, B-2440 Geel, [2] IPPE RU-249020 Obninsk

Cross section values for the ^{10}B(n,α)^{7}Li reaction have been obtained at 37 energy points between 1.5 MeV and 4.5 MeV after a preliminary off-line analysis of the data measured at the IRMM Van de Graaff accelerator in the time from September 2002 to November 2002 by using a 1-D TPC (more than 60 GB recorded data). Fig. 1 shows

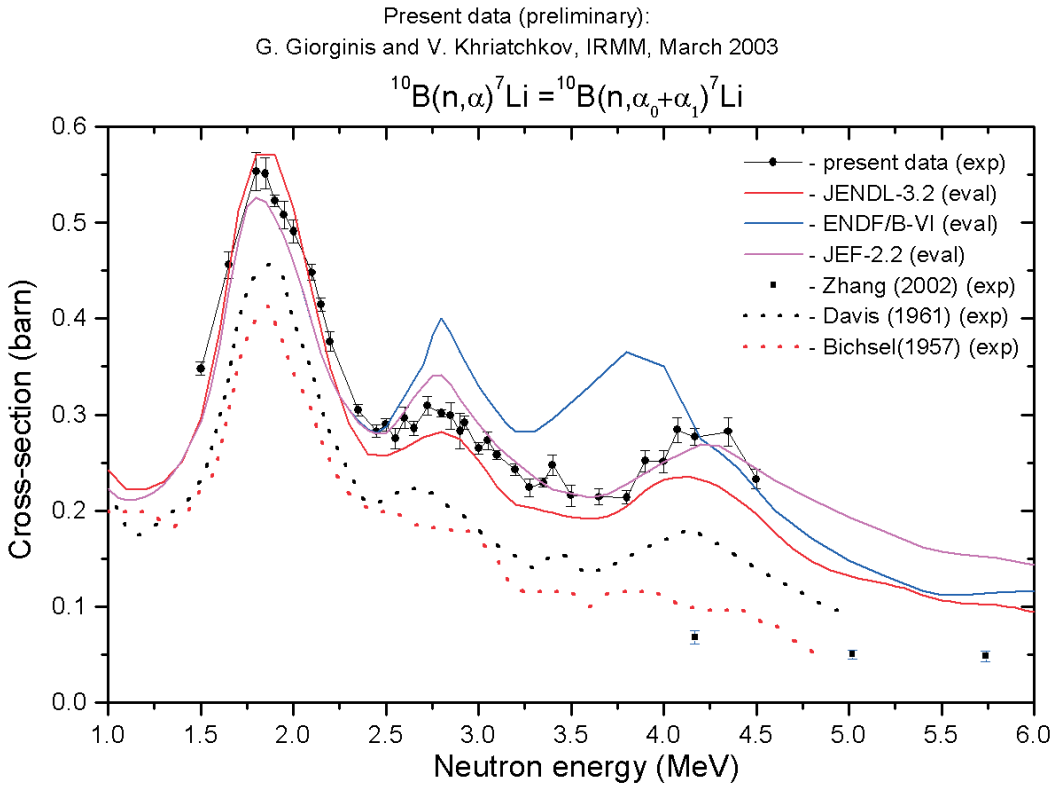

Fig. 1: Comparison of the IRMM excitation function of the ^{10}B(n, α)^{7}Li reaction obtained by using a 1-D TPC with data from the JENDL-3.2, ENDF/B-VI and JEF-2.2 evaluations, and measured cross sections from refs. [1, 2, 3]

the IRMM excitation function (cross section as function of neutron energy) together with evaluated and measured data. Compared to data evaluations the IRMM excitation function is in agreement with JEF-2.2 above 3.05 MeV. In the energy range from 2.55 to 3.05 MeV the IRMM data are between JENDL-3.2 (lower bound) and JEF-2.2 (upper bound). For energies from 2.1 MeV to 2.5 MeV there is again agreement with JEF-2.2

(coinciding with ENDF/B-VI). Our results for E_n = 1.65 MeV to 2.1 MeV are between JEF-2.2 (coinciding with ENDF/B-VI) (lower bound) and JENDL-3.2 (upper bound), and for energies between 1.5 MeV and 1.65 MeV are slightly larger than all three evaluations, which coincide in this energy region. The IRMM cross sections are larger than the other experimental values. The largest difference is between the present data and the most recent data published by G. Zhang et al. [1]. Particle leaking, which has been discovered at IRMM in 2002, and has not been considered in [1], can only partly explain the large discrepancy. Other reasons such as inaccuracies in the neutron-flux determination and number of the ^{10}B-target atoms have to be investigated by the Zhang group.

[1] G. Zhang et al., Nucl. Sci. Eng., 142 (2002) 203

[2] E. A. Davis et al., Nucl. Phys., 27 (1961) 448

[3] H. Bichsel et al., Phys. Rev., 108 (1957) 1025

Doppler broadening of neutron resonances

P. Siegler[1]*, K. Dietze*[2]*, A. Porada*[1]*, P. Ribon*[3]*, H. Riemenschneider*[1]

[1] EC-JRC IRMM, B-2440 Geel, [2] EC-JRC IE, NL-1755 LE Petten, [3] OECD, NEA, F-92130 Issy-les-Moulineaux

The experimentally observed neutron resonance width is a combination of the natural line width and the broadening due to the resolution of the detector and the Doppler effect. It is obvious, that for an exact determination of the resonance parameters the resolution function and the Doppler broadening should be well known. By cooling the samples under investigation, down to temperatures of a few Kelvin, the Doppler broadening is significantly reduced. Fitting the transmission data obtained at different temperatures with a solid state based model for the Doppler broadening, results in an improved definition of its resonance parameters and an accurate description of the resonance shape at different temperatures.

Doppler experiments for the transmission measurements are performed using a Li-glass detector at a 25 m flight path of GELINA with the cooled sample changer located at 10 m. The sample temperatures can be chosen between 15 K and 300 K.

Measurements for natural hafnium were performed for several thicknesses and temperatures. The results for the thick samples (1 mm - 15 mm) were compared to average cross sections obtained by calculations [1] based on different nuclear data libraries and have been published at the ND2001 conference [2]. Thin samples of natural hafnium were used for the determination of the first resonances. The experiments are finalized and the resonance shape analysis is ongoing.

With regard to the renewed interest in Pu reprocessing, high fuel burn-up and reactor fuel with high Pu content, the large resonances of ^{240}Pu (1 eV) and ^{242}Pu (2.7 eV) are of major importance for the determination of temperature coefficients in modern reactors. Both resonances have a small natural resonance width resulting in a large contribution of the Doppler broadening to the total width. A measurement campaign with highly enriched Pu isotopes has been started for thin samples at 15 K, 77 K, and 300 K. Two different thicknesses have been used to cover the first resonances and the resonance region up to 200 eV. A final measurement run, covering the large 1 eV resonance of ^{240}Pu, is foreseen in the fall of 2003.

Recent modifications to the resonance analysis tool SAMMY [3] allow for the treatment of Doppler broadening by using a crystal-lattice model. Currently, tests are performed to reproduce data from measurements on ^{238}U[4]. To use SAMMY for a wide range of compounds, it is necessary to include specific phonon spectra representing the movements of the individual atoms in the crystal. Studies are ongoing to calculate phonon spectra for several materials like UO_2, U_3O_8, UO_3, PuO_2, etc.

[1] J.-Ch. Sublet, P Ribon, CALENDF-2001, Journal of Nuclear Science and Technology, ND2001 proceedings, Aug. 2002, 856.

[2] P. Siegler, K. Dietze, P. Ribon, Journal of Nuclear Science and Technology, ND2001 proceedings, Aug. 2002, 936.

[3] N.M. Larson, Updated users' guide for SAMMY, ORNL/TM-9179/R5 (2002).

[4] A. Meister et al., Conf. Proceedings Vol. 59, Nuclear Data for Science and Technology 1997, Trieste, Italy, 435.

New instruments and methods

Neutron Resonance Capture Analysis (NRCA) of Materials

H. Postma[1)], *M. Blaauw*[1)], *R. Perego*[1)], *P. Schillebeeckx*[2)], *W. Mondelaers*[2)], *A. Borella*[2)], *P. Siegler*[2)]

[1] IRI, NL-2629 JB Delft, [2] EC-JRC IRMM, B-2440 Geel

Resonances in the capture cross section appear at energies particular for each isotope. Therefore, these resonances can be used as ”fingerprints” to identify and quantify elements. This is the basis of a new method ”Neutron-Resonance-Capture-Analysis” (NRCA) having been developed recently [1] to determine the elemental composition of samples. It is a non-destructive method that is applicable to almost all stable isotopes, determines the bulk elemental composition, does not require any sample taking or surface cleaning, and results in a negligible residual radioactivity. In addition, already during data taking a qualitative assessment of the elemental bulk composition of the object can be made.

NRCA is based on the detection of prompt gamma rays, emitted after neutron capture, as a function of the neutron energy. The best way to observe resonances over a wide energy range is to use a ”white” beam of neutrons from a pulsed, accelerator-driven neutron source applying the Time-Of-Flight (TOF) technique. We have applied the technique at the GELINA facility to study the elemental composition of bronze artefacts originating from different origins and time periods. In fig. 1 we show an example of a capture spectrum for a fragment of a cauldron from the 7th century BC excavated in *Satricum* 60 km south of Rome [2]. The composition deduced from the resonances in table 1 reveals that the detection limit for certain elements is at the 10 ppm level. This detection limit depends on the neutron capture cross section and the resonance energy. From the ratio of resonances of the same isotope we can also estimate the thickness of the sample [2] and account for self-shielding effects in the sample. We have validated the method [3] by a comparison of the elemental composition of a bronze arrowhead obtained by NRCA with the results from more conventional Instrumental Neutron Activation Analysis (INAA). The results of this exercise are given in table 2. To obtain a comparable uncertainty due to counting statistics the INAA procedure (including irradiation, waiting time and counting) lasted 3 days compared to 17 h for the NRCA measurements. Thus NRCA compares favourably with INAA considering the time for data taking and the non-destructive nature of NRCA. Taking into account that the quoted uncertainties are only due to counting statistics, we can conclude that there is a good agreement between results from NRCA and INAA.

Tab. 1: The elemental composition resulting from NRCA on a fragment of a 7^{th} century BC cauldron excavated at *Satricum*

Element	**Fractions (%)**	**Isotope**	**Resonance (eV)**
Cu	77.76 (0.11)		
		^{63}Cu	579.0
		^{65}Cu	230.0
Sn	20.85 (0.10)		
		^{112}Sn	94.8
		^{116}Sn	111.2
		^{117}Sn	38.8
		^{118}Sn	45.7
		^{119}Sn	222.6
		^{120}Sn	427.5
		^{122}Sn	1756.0
		^{124}Sn	62.0
As	0.34 (0.01)		
		^{75}As	47.0
Sb	0.196 (0.021)		
		^{121}Sb	6.24
		^{123}Sb	21.4
Ag	0.090 (0.01)		
		^{107}Ag	16.3
		^{109}Ag	5.2
Fe	0.770 (0.09)		
		^{56}Fe	1147.4
In	0.0061 (0.0003)		
		^{115}In	1.46

Tab. 2: Comparison of the elemental composition of an arrowhead as obtained by NRCA and INAA. The indicated uncertainties represent counting statistics only.

	INAA	**NRCA**	**NRCA/INAA**
Ag	$8.20\ 10^{-5}$ (4.0%)	$7.50\ 10^{-5}$ (1.7%)	0.915 (4.0%)
As	$3.24\ 10^{-3}$ (1.3%)	$2.99\ 10^{-3}$ (0.6%)	0.923 (1.3%)
Au	$6.15\ 10^{-5}$ (1.3%)	$6.10\ 10^{-5}$ (2.5%)	0.992 (3.0%)
Cu	$9.00\ 10^{-1}$ (3.0%)	$8.65\ 10^{-1}$ (0.2%)	0.961 (3.0%)
Sb	$3.70\ 10^{-4}$ (1.3%)	$3.50\ 10^{-4}$ (1.7%)	0.946 (2.0%)
Sn	$4.40\ 10^{-2}$ (2.0%)	$4.80\ 10^{-2}$ (1.4%)	1.091 (3.0%)

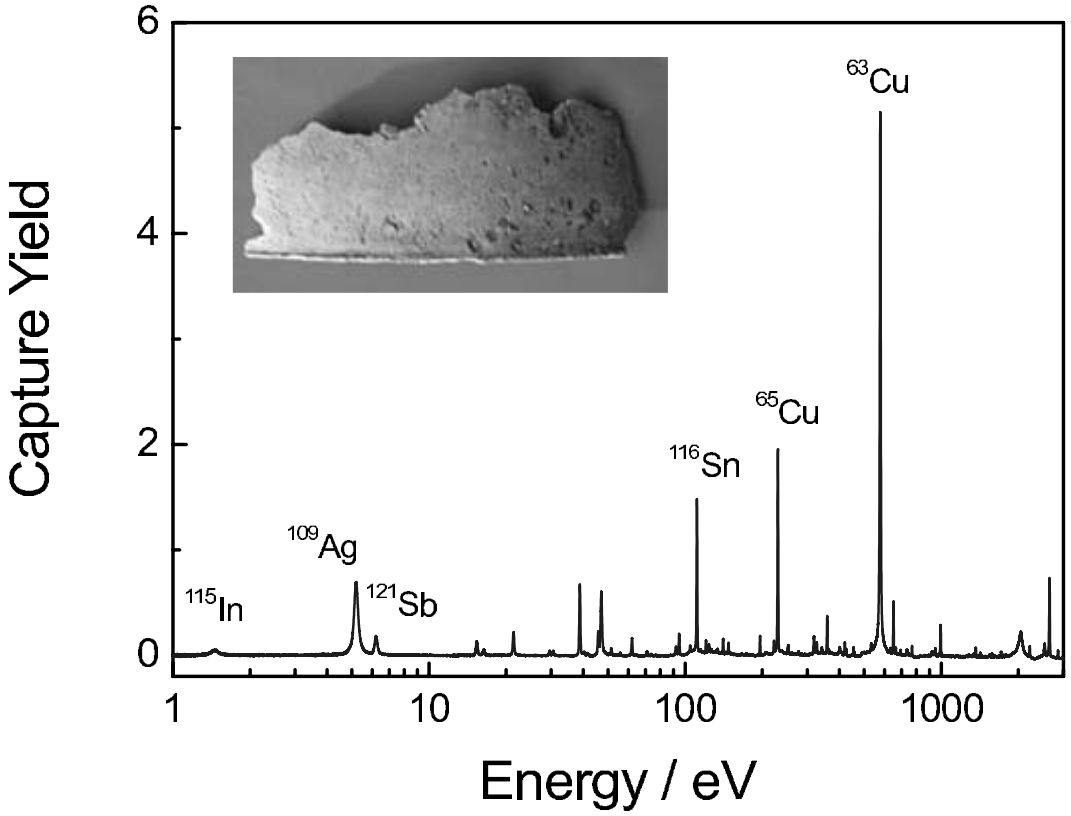

Fig. 1: A capture spectrum for a fragment of a 7^{th} century BC cauldron excavated a *Satricum*

[1] H. Postma, M. Blaauw, P. Bode, P. Mutti, F. Corvi, and P. Siegler, *Neutron-resonance capture analysis of materials*, Journal of Radioanalytical and Nuclear Chemistry, Vol. 248 No. 1 (2001) 115-120

[2] H. Postma, M. Blaauw, P. Schillebeeckx, G. Lobo, R.B. Halbertsma and J.A. Nijboer, *Non-Destructive Elemental Analysis of Copper-Alloy Artefacts with Epithermal Neutron-Resonance Capture*, 14^{th} Radiochemical conference, 14-19 April 2002, Marianske Lazne, Czech Republic, Czech. J. Phys. 52 (2003) A97-A104 (in course of publication)

[3] M. Blaauw, H. Postma, and P. Mutti, *Quantitative Neutron Resonance Analysis Verified with Instrumental Neutron Activation Analysis*, to be published in NIM A

High resolution γ-detection in a (n, n'γ) reaction obtained with a 12 bit flash ADC

S. Lukic[1], *P. Baumann*[1], *C. Borcea*[2], *E. Jericha*[3], *S. Jokic*[4], *L. Oláh*[2], *A. Pavlik*[5], *A. Plompen*[2], *G. Rudolf*[1]

[1] IReS, IN2P3, F-67037 Strasbourg, [2] EC-JRC IRMM, B-2440 Geel, [3] TU Wien, A-1040 Wien, [4] Vinca Institute, Belgrade (Serbia and Montenegro), [5] Universität Wien, A-1010 Wien

In Accelerator Driven Systems, an external flux of neutrons is provided by a spallation source. The energy spectrum of these neutrons extends to hundreds of MeV. This implies that data above 1 MeV which were of lower importance in the conventional thermal reactors become crucial. While capture reactions are not concerned by this extension, fission and (n, xn) reactions have cross sections approaching 1 b at given energies above 10 MeV. The consequences on the predictions of the codes will be strongest for (n, xn) reactions, which have a threshold increasing with x.
Actually, data bases for (n, xn) reactions are fed for many isotopes by model predictions only. This is due to the difficulty to measure their cross sections and to the lack of high energy neutron beams. No universal method applicable to all isotopes exists. With a white beam like that of Gelina on-line γ-ray spectroscopy is the only method which seems possible. The measurement of (n, xn) reactions with this method has been performed since long for x = 1, and has more recently been applied for x = 2 to 13 at WNR (Los Alamos) [1, 2, 3]. It is applicable whenever one or a few transitions in the final nucleus are strongly fed and easily separated in the spectrum. This is the case for many light nuclei, and for even-even isotopes of heavy final nuclei.
Germanium detectors are mandatory because of their high energy resolution. However, this resolution can only be obtained with long shaping times of the electronics, i.e. with a dead time of several tens of μs. With a constant intensity beam, counting rates are thus limited typically to 10^4 Hz. At Gelina, even at a flight path of 200 m, this means that γ-rays produced by the interaction of neutrons with energy of several MeV are not correctly detected with a good resolution when a γ-ray produced by the flash has given a signal in the detector. Our objective is therefore to develop a new technique, based on digital electronics. Since spectroscopy measurements need precise digitalization, the flash ADC must convert on at least 12 bits, and a software which allows obtaining energy and a time resolutions comparable to what can be achieved with conventional electronics has to be developed. Actually, the problem is exactly the same for (n, n'γ) reactions above a few MeV. Therefore, we could test the use of a commercial 12 bit flash ADC and our algorithm for the pulse analysis by simply picking up during a few hours the output of a large volume coaxial HPGe detector used in an experiment aiming at the measurement of the ^{58}Ni(n, n') cross section. The result is shown in Fig. 1. Clearly, it has been possible to obtain a good energy resolution with the so-called trapezoidal [4] method. The parameters which were used here yield a dead time of about 5 μs. Shorter dead time can be obtained at the expense of an

energy resolution slightly worsened, which means, that a compromise would have to be found if neutrons of 20 MeV have to be detected.
We plan to improve the method by using 14 bit digitizers developed at IReS as well as a reduction of the dead time by means of a more efficient algorithm.

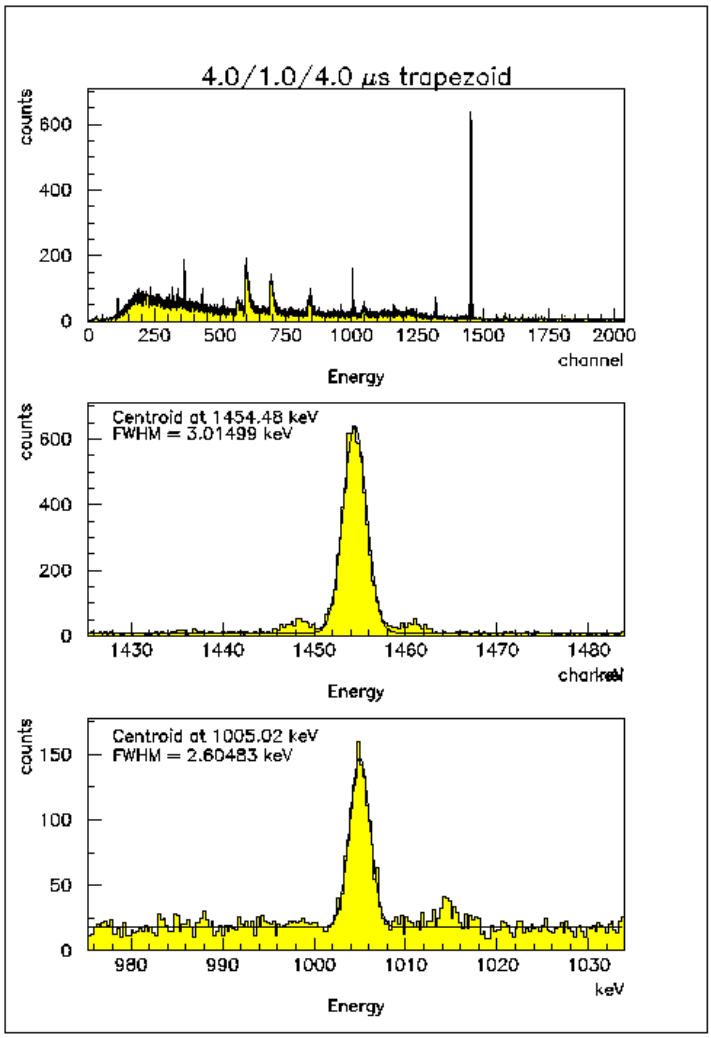

Fig. 1: γ-transitions consecutive to (n, n'γ) reactions on ^{58}Ni, detected by a coaxial HPGe detector, and digitized by a 62.5 MS/s and 12 bit flash ADC.

[1] H. Vonach et al., Phys. Rev. C50 (1994) 1952

[2] A. Pavlik et al., Phys. Rev. C57 (1998) 2416

[3] L.A. Bernstein et al., Phys. Rev. C57 (1998) R2799

[4] V. T. Jordanov and G. F. Knoll, Nucl. Instr. And Meth. A345 (1994) 337
and references therein

VERDI - a study of design parameters

S. Oberstedt, V. Fritsch, F.-J. Hambsch

EC-JRC IRMM, B-2440 Geel

In the course of a feasibility study on VERDI (VElocity foR Direct particle Identification) , a high mass-resolving fission-fragment (FF) detector, Monte-Carlo type simulations of the design parameters have been performed. VERDI is based on the time-of-flight (TOF) technique and allows in conjunction with the measurement of the particle kinetic energy to identify the particle nuclear mass A. The final application for VERDI will be the fission-fragment mass-resolved measurement of delayed-neutron pre-cursor yields.

A double velocity measurement already provides information about the pre-neutron masses of the two complementary fission-fragments assuming that prompt neutron emission from the fragments is essentially isotrope:

$$\begin{aligned} (A_1^*)^2 + 2\Psi A_{CN}(A_1^*) &= \Psi A_{CN}^2 \\ A_{CN} &= A_1^* + A_2^* \end{aligned} \qquad (1)$$

with $\Psi = v_2^2/(v_1^2 - v_2^2)$, where v_1 and v_2 are the velocities of two fragments.
From a subsequent high energy-resolving measurement of the fragment kinetic energy the post-neutron masses are obtained, too:

$$A_i \sim E_i/v_i^2 \qquad \text{with} \quad i = 1, 2. \qquad (2)$$

Therefore, from a 2(v, E)-measurement the prompt-neutron multiplicity is known as a function of the initial fragment mass.

VERDI will consist of a two-arm TOF-section for the velocity measurement of each individual fission fragment followed by a high-resolution energy detector. Today's available technology, like e. g. micro-channel plate (MPC) detectors, provides time pick-off devices with a timing resolution better than 90 ps. Supposing a minimum FF mass A = 80, maximum kinetic energy E_k = 140 MeV and a flight-path lengths of about 50 cm, the flight time t = 27.2 ns giving a timing resolution of better than 0.5 %. This situation improves for higher fragment masses with typically much lower kinetic energies. An alternative device could be based on the PPAC technique, whose features will have to be compared to those of a MCP-detector.
Modern energy-sensitive detectors, e. g. PIPS-detectors, have excellent energy resolution for heavy ions, e. g. ΔE(FWHM)/E = 0.6 % for α-particles at E_α = 5.7 MeV. However, the energy resolution may deteriorate for heavy fission fragments due to the surface dead layer. The capabilities of standard available PIPS detectors, which are dedicated to the detection of heavy ions will be the main subject to a detailed investigation.

From the above parameters a mass resolution of VERDI A/$\triangle$A = 140 should be achievable. Taking a flight-path length L = 500 mm and a typical Si strip-detector of S = 58$\times$58 mm^2 (commercially available detector size) the resulting geometrical efficiency ϵ = 10^{-3}, which would be about 300 times higher than that of the former COSI-FAN-TUTTE spectrometer at ILL [1].

[1] P. Koczoñ, PhD-thesis, IKDA 88/11, TH Darmstadt (1988)

Accelerators: Instrumentation and development

The IRMM Van-de-Graaff accelerator

G. Lövestam, C. Chaves, M. Conti, T. Gamboni, R. Jaime

EC-JRC IRMM, B-2440 Geel

The IRMM 7 MV Van-de-Graaff (VdG) accelerator is, with a few exemptions, dedicated for the production of quasi-monoenergetic neutrons. The accelerator is a vertically mounted belt charged machine with a radio frequency ion source for the production of protons, deuterons or Helium ions. Two analysing magnets arranged in sequence guide the ion beam to one of the two shielded target halls. Intense mono-energetic neutron fields are produced at either of six beam line targets using the nuclear reactions ^{7}Li(p, n)^{7}Be, T(p, n)^{3}He, D(d, n)^{3}He and T(d, n)^{4}He. The available neutron energy range covers 0 - 24 MeV with a gap at about 10 - 12 MeV as shown in Fig. 1. The typical neutron fluence for experimental conditions is about 10^{8} neutrons/cm^{2}/s at a distance of about 10 mm from the target.

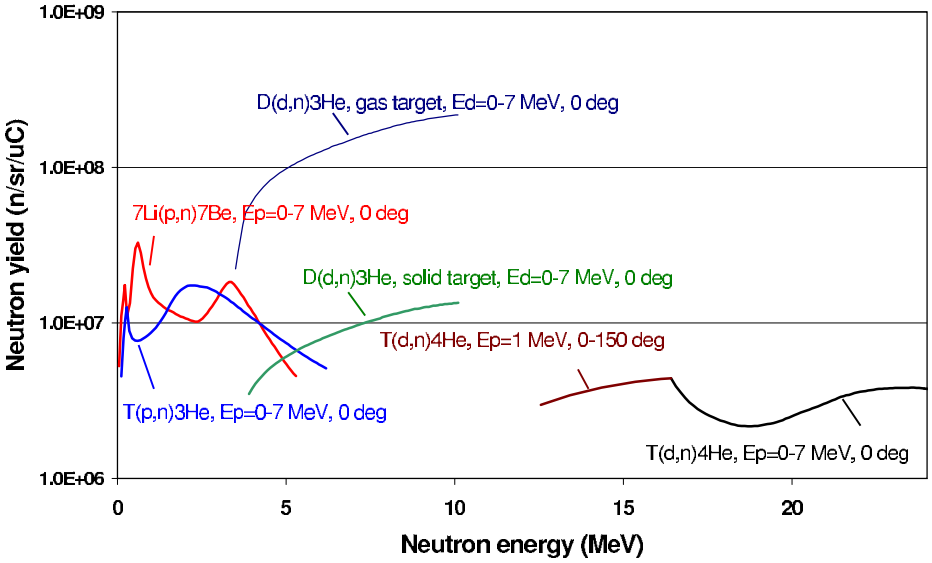

Fig. 1: Available neutron energies and fluencies for the respective neutron reactions utilised at the IRMM Van-de-Graaff laboratory. All targets are solid unless noted.

Either DC or pulsed ion beams are generated with a current of up to 60 μA on target in DC mode and up to 5 μA in pulsed mode. When pulsing, a pulse repetition-rate of 2.5,

1,25 or 0.625 MHz and ion pulses of 2.5 - 1.25 ns FWHM depending on the ion energy may be obtained. The accelerator is very stable and may be operated uninterrupted for more than a week without degraded performance.

Accelerator operation

During 2002, the accelerator was operated for 3372 hours and closed down during July-August for the installation of a new safety and security system. The detailed operation statistics is shown in Fig. 2. Eight ion-source bottles were consumed of which problems were encountered with three having life-times less than 100 h. The problem was traced to a new production technique at the manufacturer. The average life-time of the working bottles was 440 h.
The need for longer experimental measurement campaigns has necessitated accelerator operation on non-office hours including weekends. This has been accomplished without increasing the number of staff by running the accelerator unattended while important machine parameters are logged for remote inspection, via the internet, by the experimentalist in charge. Also, the γ- and neutron-doses around the building are monitored continuously and an automatic stop of the machine is issued whenever doses exceed a preset high limit.

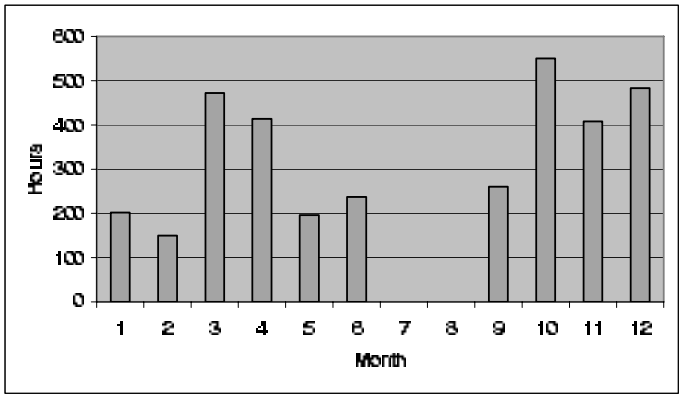

Fig. 2: Operation statistics for 2002 of the IRMM 7 MV VdG accelerator. The accelerator was not in operation during July and August due to the installation of the new safety system.

Accelerator and beam line modernisation and development

In 2002 several actions were taken to improve the high stability and high ion-beam current performance of the accelerator and beam lines. This included:

- The exchange of turbo- and pre-vaccuum pumps for accelerator and beam lines to oil-free pumps was continued. In addition, the computer controlled vacuum automation system was finalised and the system is now fully operational. The objective of installing oil-free pumps was to reduce the oil moisture in the vacuum system to get a cleaner laboratory environment. The oil is also believed to cause build up of carbon on targets, which cause a lower-energetic neutron background in generated spectra.

- A speed controller that regulates the speed of the belt charging the high-voltage terminal was installed. The operation in unattended mode during non-office hours has necessitated considerable efforts to facilitate long-term stable operation of the machine without interventions of the operators. A cause of instability is possible variations in the speed of the belt movement, which in turn is caused by voltage and frequency variations in the network power. The problem is believed to be remediable using the speed controller, which also facilitates a soft accelerating start of the belt and, thus, puts less mechanical tension on the belt when starting up. The performance of the controller concerning accelerator stability will be evaluated during 2003.

- The new fibre optics system for controlling and reading of parameters at the high voltage terminal in the accelerator was successfully laboratory tested. A pilot study in the accelerator will be performed in 2003.

- The level 0 analysing magnet was re-aligned using a low -energy proton beam. A certain misalignement was suspected after the installation of a new accelerator tube 1999. The magnet was moved about 10 mm.

- A new PC-based digital logging and data-base system was developed for logging of accelerator settings, recorded run-time parameters, ion sources and targets.

A new safety and security system

Due to the high neutron fluxes generated in the VdG laboratory a sophisticated safety and security system is instrumental to ensure safe operation. In 2002 the previous in-house built system was replaced by a new computerised industry standard system. The aim of this safety and security system is to:

- protect people in target halls and buildings against too high radiation,

- protect the environment of the laboratory buildings against too high radiation,

- inform VdG operators on alarms, anomalies and safety situation,

- stop VdG in case of unforeseen emergency.

The high intensity beam line

A new high intensity beam line was constructed in the lower level target-hall (see Fig. 3). The objective was to facilitate a continuous high-intensity ion-beam and neutron generation for more than a week uninterrupted. This is a pre-requisite for some low neutron-induced reaction cross-section measurements like the ^{233}Pa neutron-induced fission cross-section measurement campaign that continued during 2002. Long-term stable beam currents up to 50 μA were obtained during 2002.

Neutron fluence and dose measurements

Neutron fluxes and energy spectra are monitored and characterised using proton recoil

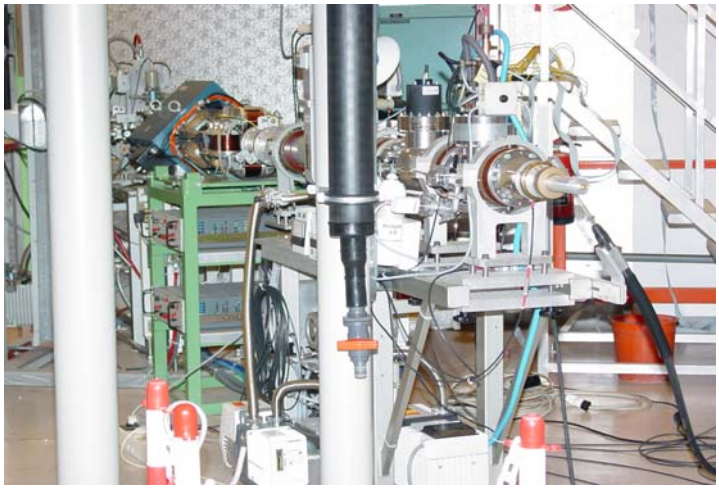

Fig. 3: The new high intensity beam line as viewed from the target.

telescope counters, proportional counters, BF_3 counters, Bonner multiple sphere systems, fission chambers and activation foils and discs. During 2002, the Bonner sphere system was particularly evaluated and a project to test different spectrum unfolding programmes was initiated. Also, following recommendations from ICRP, the Belgian authorities reduced in 2001 the dose limits for radiological and non-radiological staff. To comply with the new regulations, a new neutron shield consisting of a 0.5 m concrete wall was built around the VdG-laboratory in 2001. A project to study the performance of this wall was initiated during 2002. Neutron fluence measurements were made in the surrounding environment as well as in office areas using a portable neutron monitor, the Bonner sphere system and activation discs followed by low-background γ-ray measurements. The measured data will be evaluated during 2003.

New software

Mono-energetic fast neutrons produced by nuclear reactions from accelerated ions are usually accompanied by a contribution of neutrons elastically and inelastically scattered from the target housing and support. To simulate the complete neutron spectrum at a given measurement point, including neutron production, transport and scattering processes in the target, the Monte-Carlo code TARGET was written in 1983 by H. Lesiecki at the Physikalisch-Technischen Bundesanstalt (PTB) in Braunschweig, Germany. Although updated since several times, the programme has only been compiled for the DEC VMS environment. During 2002, the TARGET code was adopted for PC and MS windows environment by the VdG group.

An important feature at the VdG laboratory is the possibility of immediate calculation of accelerator settings related to ion beam parameters (ion, energy and current), neutron production (nuclear reaction and target) and neutron fluence (neutron energy spectrum and intensity). To accomplished this, the MS-Windows programme EnergySet [1] was developed during 2002. A screen-shot of the programme user-interface is shown in

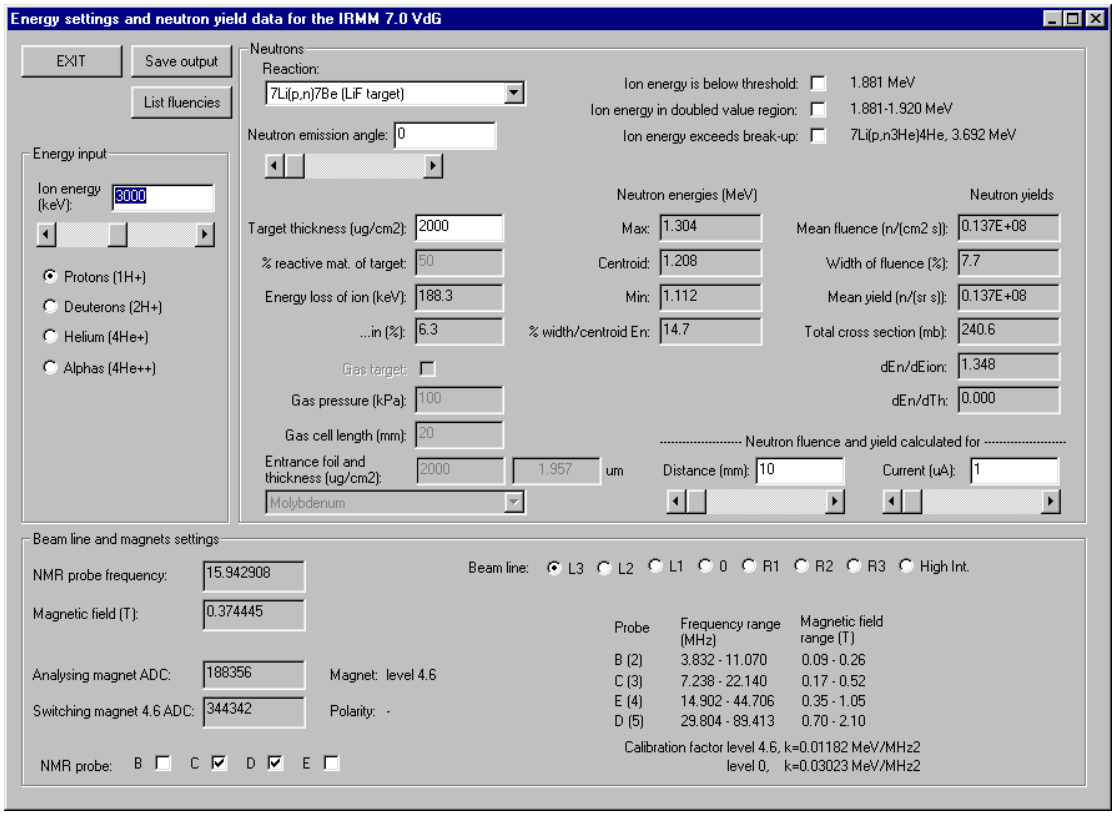

Fig. 4: Screen-shot of the MS-Windows programme EnergySet [1] developed during 2002.

Fig. 4.

[1] G. Lövestam, EnergySet - a programme to calculate accelerator settings and neutron yield data for the IRMM VdG laboratory, IRMM internal report GER/NP/2/2002/06/20

High-power cooling device for solid-state neutron-production targets

S. Oberstedt[1)], *V. Fritsch*[1)], *F.-J. Hambsch*[1)], *F. Tovesson*[1,2)]

[1] EC-JRC IRMM, B-2440 Geel, [2] Örebro University, SE-70182 Örebro

In the past solid-state neutron production targets, usually TiT, TiD or LiF deposited on a Ag-backing, have been cooled by means of a low-temperature high-pressure air-gun. There, the thermal power deposited by the proton(p)- or deuteron(d)-beam is dissipated by the cold air streaming along the outer part of the target backing. The advantage of this technique is, that the energy profile of the quasi mono-energetic neutron beam remains unchanged. However, the maximum power, which can be dissipated with this technique is limited to P $\approx$ 50 W. In paricular, when reaction cross-sections are only of the order of a few 100 mb or less, a considerable increase of the neutron fluence is indispensable in order to keep the irradiation time reasonable, thus, demanding much higher beam-currents.

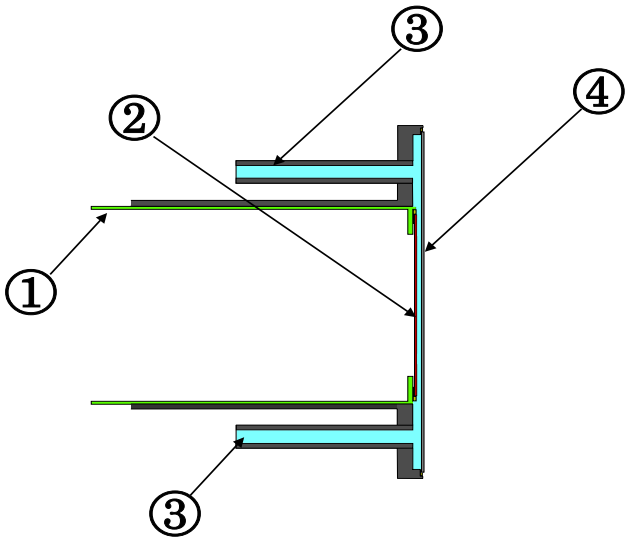

Fig. 1: Sketch of a target-can mounted to the proton/deuteron beam-line: (1) Al target-can, (2) TiT/TiD-target deposited on a Ag-backing (3) water supply, inlet (top) and outlet (bottom), (4) 1mm water layer. Protons/deuterons are coming from the left.

In the particular case, where an ionisation chamber (IC) is used for charged-particle detection, e. g. for the investigation of neutron-induced fission-fragment characteristics or reaction cross-sections, the air-stream is reflected from the target-can to the IC leading to an unfavourable degradation of the signal-to-noise ratio due to microphonic effects induced on the electrodes inside the chamber and, as a consequence, spoiling the good pulse-height resolution of this type of detector device. Mechanically, the limiting part is the glue, which is used to attach the solid-state target/backing to the

can. Overheating results either in a sputtering of the glue material into the accelerator beam-tube or in an eventual crack in the glue area. Both eventually lead to a break-down of the vacuum in the accelerator beam-tube and to a subsequent shutdown of the experiment. The same degradation will be observed, if a rubber seal is overheated, when the target is attached to the can with a fixation-skrew.

A much better solution is to cool the target-can by continuously flowing, de-mineralised water. The water is guided across the whole area of the target backing through a cap made of aluminium and mounted onto the target can as shown in Fig. 1. The thickness of the water-layer is 1 mm in order to minimise a deterioration of the energy-profile of the neutron-beam. A cryogenic device is added to the curcuit to keep the water in the reservoir well below room-temperature. However, from first tests it appeared, that the temperature at the water-inlet should not be below 10^{o}C, since a large temperature gradient may again cause cracking of the glue material.
In Fig. 2 the temperature profile is shown from a long-term irradiation of a TiT-target with protons at E_p = 4.68 MeV. On the right y-scale the corresponding beam current is given. The dissipated average power on the target was P = 280 W. From the measured temperatures it appears, that this does not indicate the upper limit for the cooling device, yet.

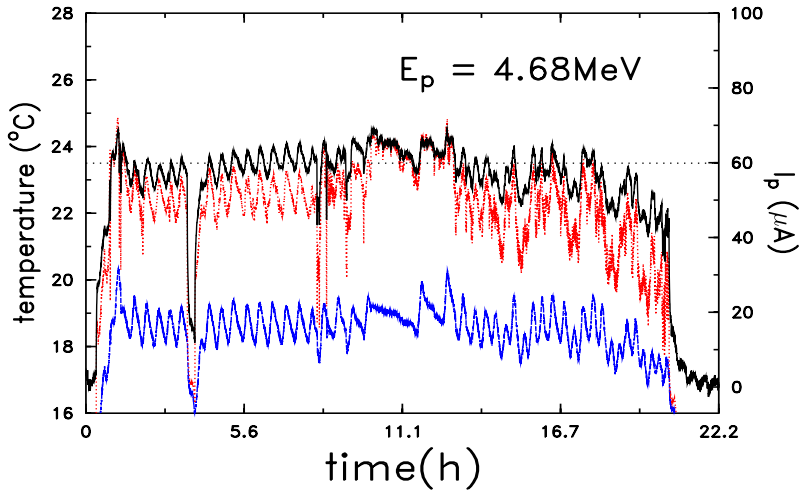

Fig. 2: Temperature record from an irradiation of a TiT target with protons at E_p = 4.68 MeV for about 20 h. The graphs give the temperature (left scale) for the water-layer (solid line), the water-outlet and the water-reservoir (broken lines). The modulation is due to the cooling-cycle of the cryogenic device. The right scale gives the corresponding beam current I_p. The horizontal line indicates the level, where a power of 280 W is dissipated on the target.

The new water-based cooling device for solid-state neutron-production targets allows an increase of neutron fluence by at least a factor of five compared to air-coold neutron sources. However, future investigations will have to concentrate on a possible degradation of the T- and/or D-deposit on the target, due to e. g. inhanced outgassing, when going to even higher beam-currents. Additionally, a possible broadening of the

neutron-energy profile due to scattering of the neutrons in the water-layer will have to be investigated quantitatively.

Improved cooling for D_2-gas neutron-production targets

S. Oberstedt[1)], *V. Fritsch*[1)], *F.-J. Hambsch*[1)], *F. Tovesson*[1,2)]

[1] EC-JRC IRMM, B-2440 Geel, [2] Örebro University, SE-70182 Örebro

At the EC-JRC IRMM VdG-driven neutron source quasi mono-energetic fast neutrons with energies between 5 to 10 MeV are generated from incident mono-energetic deuteron beams with energies between 2 to 7 MeV via the reaction ^{2}H(d, n)^{3}He. This is a convenient neutron-energy range for a number of nuclear scientific and/or technology applications as well as for significant contemporary interest for cross-section studies relevant to both basic and applied concern.
There are two distinct ways to make deuterium (D_2) targets. The first approach utilises a metal lattice, e. g. titanium, with absorbed deuterium gas, with a TiD density of typically 2 mg/cm^2. These particular metal-deuteride targets are relatively stable, when not in use, and commercially available. Additionally, dissipation of the deposited beam power is relatively simple to achieve [1]. However, the surface of the metal may oxidate giving rise to a non-negligable contribution of low-energetic neutrons from the secondary rection ^{16}O(d, n)^{17}F, which starts at a threshold energy for deuterons E_{thres} = 1.83 MeV [2]. Therefore, the second approach using a gas cell with pressurised molecular deuterium, where the collimated deuterium beam is entering through a window, is recommended for high resolution experiments. Here it is important, that the window is strong enough to contain the gas and, at the same time, thin enough in order to avoid degradation of the deuteron-beam energy profile. With a gaseous target a higher neutron intensity per unit beam-current as well as a narrower neutron energy distribution may be achieved. The difficulty here is to apply sufficient cooling to the entrance window of the gas-cell and the beam-stop.

Our design of the target/target-cooling device is based on ref. [3] but adapted to our particular needs. The following criteria had to be considered: (a) use of low-activation materials, (b) minimal degradation of the incident deuteron beam, (c) minimal perturbation of the primary neutron beam, (d) low/no neutron background due to secondary reactions in the target-cell material and, last but not least, (e) survival in a relatively high-current deuteron beam, i. e. $I_d \approx$ 15-25 μA, for at least 24 h and preferably 100 h.

In Fig. 1 a sketch through the D_2-gas target is shown. From the left the deuteron-beam is passing a tantalum collimator (1) with an open diameter of 6 mm before entering the gas cell through a 5 μm thick molybdenum window (2) and stopped in 1 mm thick tantalum (3). The gas-cell (5), made from brass material, has a length of 40 mm and is operated at a deuterium-gas pressure p = 2×10^5 Pa. From this a 15 times higher neutron intensity per unit beam-current may be expected.
The cooling water in- and outlets (4) are arranged such, that firstly, the bulk material of the gas-cell serves as cooling reservoir to the entrance window, and secondly, to avoid

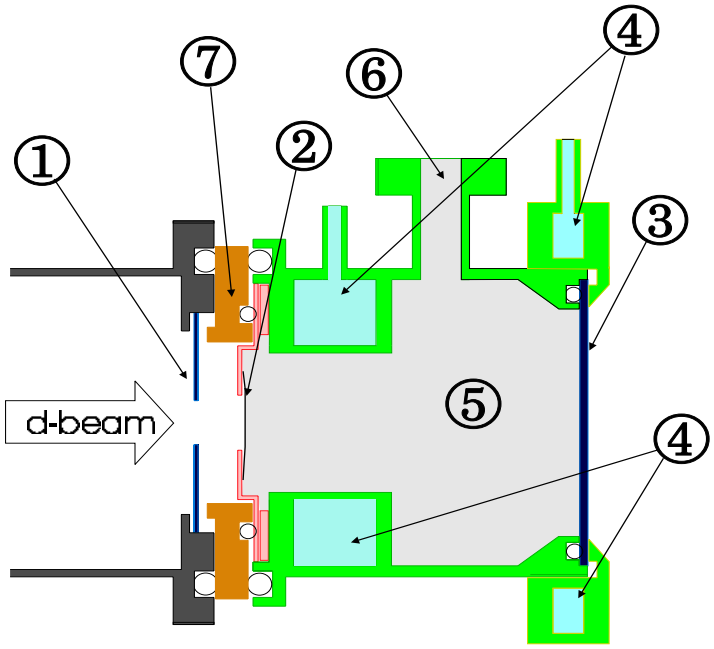

Fig. 1: Sketch of the D_2-gas target mounted to the deuteron beam-line: (1) tantalum collimator, diameter: 6 mm (2) 5 μm thick molybdenum entrance-window (3) 1 mm thick tantalum beam-stop (4) water reservoir inlet(top) and outlet(bottom) (5) D_2-gas volume (6) gas inlet (7) teflon seal for electric decoupling gas-cell from the accelerator beam-tube.

overheating of the rubber O-seal between the gas-cell and the beam-stop.

In Fig. 2 the temperature profile on the central part of the D_2-gas target beam-stop as a function of irradiation time during a first test irradiation of the D_2-gas target is shown. The direct response to the stepwise increased deuteron-beam current is visible. The plateau clearly shows equilibrium is achieved when the beam current is held on a constant value. In Fig. 3 the temperature profile close to the rubber O-seal was measured as a function of irradiation time at a deuteron-beam current of I_d = 15 μA. Equilibrium temperature did not exceed T = 40 ^{o}.

With the improved water-cooling for the D_2-gas neutron-production target a deuteron-beam power P = 75 W has been dissipated on the beam-stop during a first test irradiation. The measured temperature close to the rubber O-seal could be kept around T = 40^{o}C. From the observed temperature profile in the gas-target assembly there is no reason, why it should not be used with an even higher deuteron-beam power. Since the target/cooling geometry leads to a greater mean distance between neutron production and reaction target the net gain in neutron intensity is about 3 times compared to the use of a standard solid-state target.
However, in the future the deterioration of the mechanical stability of the molybdenum entrance-window under long-term high-current charged-particle bombardment (typically 15 - 25 μA during 4 d), leading to e. g. inhanced leakage rate due to creation of pin-holes, will have to be investigated.

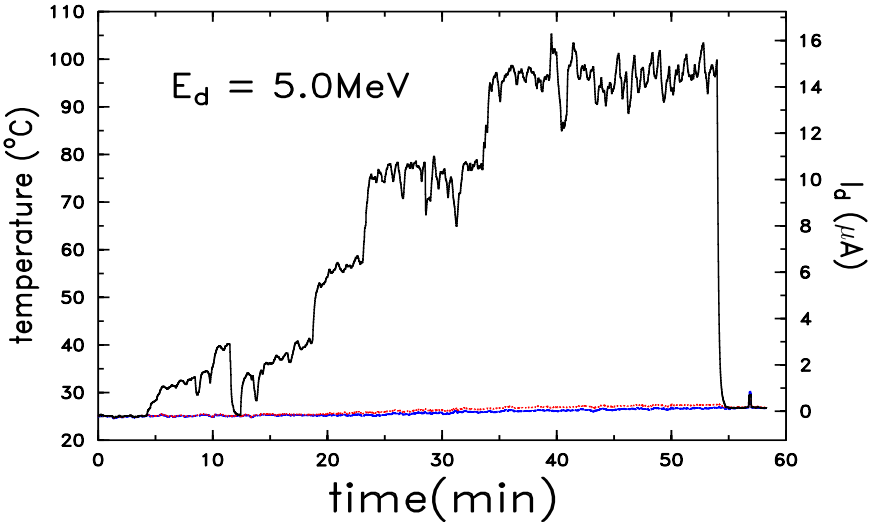

Fig. 2: Temperature profile (in C^o) on the central part of the D_2-gas target beam-stop as a function of irradiation time. The right scale gives the corresponding deuteron-beam current in μA.

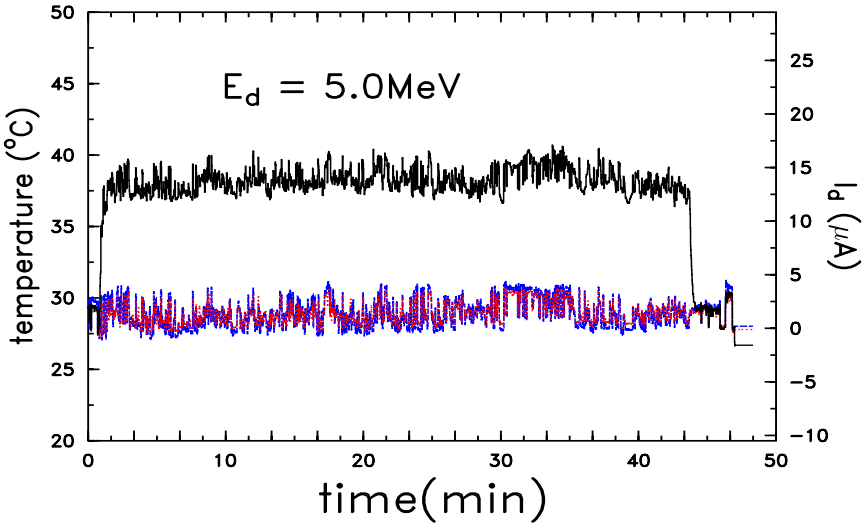

Fig. 3: Temperature profile (in C^o) close to the rubber O-seal of the D_2-gas target beam-stop as a function of irradiation time. The right scale gives the corresponding deuteron-beam current in μA.

[1] S. Oberstedt, V. Fritsch, F.-J. Hambsch, F. Tovesson, *High power cooling device for solid-state neutron-production targets*, see this Scientific Report

[2] J. R. Tesmer, *Accelerator Eneergy Calibration and Stability*, Handbook of Modern Ion Beam Materials Analysis, Material research Society, ISBN 1-55899-254-5 (1995) 687

[3] D. Feautrier and D. L. Smith, *Development and Testing of a Deuterium Gas Target Assembly for Neutron Production via the ^{2}H(d, n)^{3}He reaction at a Low-Energy Accelerator Facility*, Nuclear data and measurements series, ANL/NDM-122 (1992)

The Geel electron linear accelerator GELINA

W. Mondelaers, K. Cairns, M. Conti, C. Diaz Vizoso, C. Ganassin, W. Mota, G. Pettinicchi, J.-P. Sclavon, R. Van Bijlen

EC-JRC IRMM, B-2440 Geel

The Geel Electron Linear Accelerator facility GELINA is a pulsed white-spectrum neutron source in combination with a time-of-flight (TOF) facility used to determine the energy of the neutrons in the energy range covering 11 decades (1 meV - 20 MeV). Among the pulsed white spectrum neutron sources available in the world, GELINA is the one with the best time resolution. The excellent neutron energy resolution is made possible by a combination of four specially designed and distinct units: a high-power pulsed linear electron accelerator, a post-accelerating beam compression magnet system, a mercury-cooled uranium target, and very long flight paths.
The GELINA neutron source is based on a linear electron accelerator producing electron beams with a typical beam operation mode characterised by 100 MeV average energy, 10 ns pulse length, 800 Hz repetition rate, 12 A peak and 100 μA average current. Using a unique post-acceleration pulse compression system, the electron pulse width can be reduced to approximately 1 ns (FWHM) while preserving the current, resulting in a peak current of 120 A. The accelerated electrons produce Bremsstrahlung in an uranium target which in turn, by photonuclear reactions, produces neutrons. Within a 1 ns pulse a peak neutron production of 4.3×10^{10} neutrons is achieved (average flux of 3.4×10^{13} neutrons/s).

The neutron energy distribution emitted by the target ranges from subthermal to about 20 MeV, with a peak at 1-2 MeV. In order to have a significant number of neutrons in the energy range below 100 keV, a hydrogen-rich moderator is added. The partially moderated neutrons have an approximate 1/E energy dependence plus a Maxwellian peak at thermal energy. By using collimators and shadow bars moderated or unmoderated neutron beams are selected for the twelve neutron flight paths. Further tailoring of the spectral shape is done with movable filters. The up to 400 m long flight paths, which point radially to the uranium target, lead to experimental locations at distances of 10, 30, 50, 60, 100, 200, 300 and 400 m. These experimental stations are equipped with a wide variety of sophisticated detectors, and data acquisition and analysis systems. GELINA is a multi-user facility serving up to 10 different experiments simultaneously.

There are at present in the world four accelerator facilities addressing the same neutron data research community. GELINA and ORELA (located in Oak Ridge, TN, USA) are based on an electron accelerator with a photonuclear neutron target, while n_TOF (at CERN, Geneva, Switzerland) and WNR (at the Los Alamos National Laboratory, Los Alamos, NM, USA) are proton machines with a neutron spallation target. The recently built n-TOF facility at CERN produces extremely high neutron fluxes but at very low repetition rates (up to four pulses per 14.2 s). It has one TOF-path. The very

high peak flux makes this facility ideal for measurements on radioactive targets but total cross-section measurements in transmission geometry are not possible. Therefore, the characteristics of the CERN facility complement ideally the capabilities at GELINA and complementary measurements are at present part of a common collaboration.

Accelerator operation

During 2002, the linear electron accelerator was used exclusively in the framework of the neutron measurements programme. The facility produced neutron beams for experiments during 2853 hours. The detailed operation statistics are shown in Fig. 1. GELINA was serving up to 10 experiments simultaneously (6.3 on average) and the total number of data-taking hours, integrated over all experiments, was 17988 hours. In 2002 a maximum of three night shifts per week could be accomplished. For 2003 two additional members joined the GELINA crew, so that from January 2003, we run at a scheme of four night shifts per week. The accelerator was operated mainly in two modes:

- 'short' pulse mode with electron beams on target of 100 A peak current, 1 ns pulselength, 800 Hz repetition rate (80 μA average current). This operating mode is used for measurements with very high-energy resolution and covered 79% of the available beam-time.
- 'long' pulse mode with electron beams on target of 12 A peak current, 10 ns pulselength, 100 Hz repetition rate (12 muA average current). During 21% of the available beam-time the facility was used in this mode, allowing for measurements at very low neutron energies.

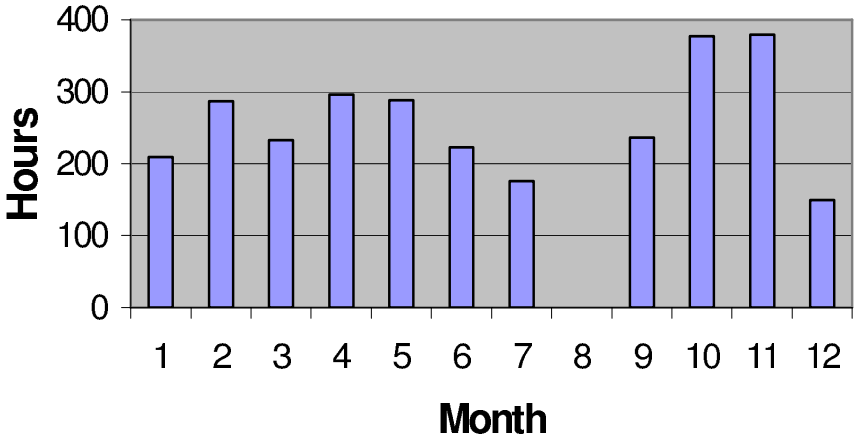

Fig. 1: Operation statistics for 2002 of GELINA.

Although the reliability of GELINA improved during 2002, we encountered several technical problems in the

- klystron modulators,
- injector,
- electron beam transport system.

Klystron Modulators
The three klystron modulators are presently the most critical components of the facility. Modulators convert AC line power into the train of high-voltage high-current pulses needed to drive the klystrons, which in turn generate the high-power radio frequency (RF) waves that accelerate the electron beams. The GELINA facility has several characteristics that are extremely demanding especially for its modulators. A particular challenge for the modulator operation is the combination of high pulse repetition frequencies with high peak klystron voltages and currents (230 kV, 210 A). The nominal pulse repetition frequency of 800 Hz is very high compared with the great majority of present pulse-line modulators, operating at much lower pulse rates (typically 50 Hz or lower).

The klystron modulator of accelerator section 1 was built in 1975, while the two modulators powering the klystrons 2 and 3 are even 12 years older. Consequently, these complex systems are known to be the major source of problems and associated loss of beam time. Simultaneous optimal operation of all three modulators is necessary to obtain the required neutron flux. Because there is no overall modulator redundancy, there is, for the majority of the modulator faults, no beam until the defective equipment is restored to its operational state.

Points of continuing concern, causing short machine interruptions, are circuit breaker trips, pulse cable mortality and obsolete interlocks. Among the failures that lasted more than two hours, we note mainly problems with reduced voltage-holding capacity of several critical high-voltage components and thyratron failures. The reduced voltage-holding capacity is due to ageing of the insulating materials. A severe arc occurred in one of the pulselines of modulator 3. The inverse fault voltage that was created destroyed almost all the PFN capacitors. It caused also damage to several minor peripheral components. During 2002 we had to replace four main thyratrons (CX1536): two suffered from a reduced voltage hold-off capacity and two showed excessive time jittering. As previously in modulators 2 and 3, we installed in 2002 also in modulator 1 a double-pulse trigger system for the main thyratron. Pre-pulsing of the lower grid to fully ionise the cathode space before the main trigger pulse is applied should be favourable for thyratron lifetime. This beneficial effect has not yet been verified in our modulators because of the limited number of thyratrons and life time data.

A consistent effort is necessary to improve where possible the reliability of the modulator systems. As described further we made during 2002 a thorough analysis to examine the critical GELINA modulator issues and to propose possible modifications that are needed to improve the present reliability, stability and reproducibility.

During 2001, a new type TH2155 replaced the klystrons TH2042, installed on sections 2 and 3, while section 1 still operates with the old klystrons. Although the new klystrons performed very well and no klystron has failed up to now, the new klystrons are a point of major concern. Because klystrons are long delivery items (typically one year) and in order to guarantee continuous GELINA operation, our policy is to have (at least) one spare klystron per RF socket. However, for administrative reasons, the procurement of spares for the new klystrons was postponed until the second half of 2002. The first of three spare klystrons will be delivered in Summer 2003, so that after a period of concern we will move than back to a safe situation.

Injector

The longest beam interruptions occurred due to an injector problem. In January 2002 we replaced an old exhausted injector cathode. During the consecutive five months machine operation was occasionally hampered by intermittent arcing in the gun region, causing 'ad random' destruction of several components in the hot deck pulser electronics. Also the new cathode suffered from the irregular voltage breakdowns, necessitating its replacement after only 1310 hours of operation. A careful analysis on a test bank of the dismounted electron gun assembly revealed a thermal microleak in the rear deck vacuum wall.

Electron beam transport system

Several electron beam transport system components are severely suffering from the harsh radiation conditions in the target hall. A radiation-hard large-bandwidth BERGOZ FCT fast current transformer was especially designed for the measurement of the 1 ns electron pulses hitting the electron-neutron conversion target. This beam diagnostic element plays a crucial role in the neutron cross-section data experiments, because it generates the trigger for the T0 start/stop signal of the neutron TOF (time-of-flight) measurements. As shown in Fig. 2, the current transformer is positioned in the small air gap between the electron exit window and the neutron target. As a result, it is very susceptible for changing characteristics due to radiation damage. Replacement of a damaged transformer is problematic because of the residual radioactivity in the target hall. BERGOZ developed for us a new version of the FCT transformer. The new transformer can now be mounted in vacuum, so that it can be moved away from the target, to a position allowing better radiation shielding. The new system will be installed during the scheduled summer stop in 2003.

Radiation damage problems were also encountered in a number of steering dipoles and in a quadrupole triplet. During the annual summer shutdown we replaced and realigned several electron beam line components. This action resulted in an improved electron beam transmission. We also removed an obsolete movable beam line that was located above the neutron target region. It was used in the past to direct the electron beams towards a photon beam production set-up in a building behind the target hall.

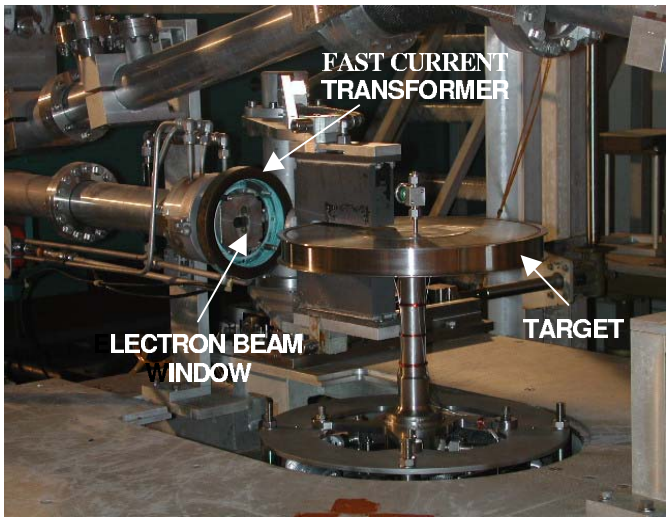

Fig. 2: Present fast current transformer and neutron target.

Accelerator modernisation

Electron beam transport system

In order to improve beam optics and ease optimisation of beam properties, the characteristics of the electron beam transport system have been fully reassessed. TRANSPORT (PBO-Lab) calculations are used to optimise the position and settings of the beam transport elements. A special difficulty for the optimisation process is the inherent large energy spread of the electron beams produced by GELINA, related to the transient beam loading effect associated with the very short accelerated electron pulses (10 ns) and high peak currents (several 10 A). The electrons within one pulse cover the energy range between 70 and 130 MeV. This energy spread forms the basis for the application of the post-acceleration relativistic electron pulse compression system. The beam optical optimisation process has to account for the variation with energy of the focal lengths of the focusing magnets and of the trajectory lengths in the compression magnet. The modified optics will be implemented during the summer break of 2003. Also new beam diagnostic elements will be incorporated in the system.

Control and interlock system

The conception of the present GELINA control and interlock system is more than 20 years old. The hard-wired control and interlock systems have been extended and modified during the many years of machine operation. The arrangement has become so complex that the initial logical structure of the system is completely lost. Many systems have become redundant or obsolete, or they are using components that are not supported anymore by industries. Also the existing 10 years old MACQ ELECTRONIQUE data acquisition and logging system, treating continuously more than 200 operational analog and logic variables, needs modernisation in the near future.

We are actually developing and constructing in a step-by-step procedure a new overall accelerator computer-based remote control and interlock scheme. Applications necessary to create this computer-based control are constructed using software components in the LabVIEW environment. The overall accelerator control scheme applies a modular structure with distributed nodes and network communication with the control room. For the decentralised nodes we are using FieldPoint modular I/O hardware with LabVIEW software support. 'Decentralised' in this context means that the FieldPoint systems are located as short as possible to the entity under control (injector, modulator, power supplies, ...). The FieldPoint system can monitor and control the entity as a stand-alone system, and also from the control room via a network connection. Extensive tests have shown that these Fieldpoint modules perform very well in the neigbourhood of the modulators. They show no interference effects. In 2002 the new scheme was introduced for the control of the power supplies for linac solenoids and beam transport dipoles and quaderupoles. It is developed by our own technicians and is implemented in a step-by-step procedure, without substantial interruption of machine operation. The system will be gradually extended during 2003 (complete control system) and 2004 (interlock system).

Modulators

During 2002 we made a thorough analysis of the critical GELINA modulator issues and failure rates in view of possible modifications that are needed to improve the present reliability, stability and reproducibility. Replacement of parts of the modulator system should also allow average power upgrading, in accordance with klystron power capacity. The goal is to increase the maximum pulse repetition frequency from 800 to 1000 Hz in the short pulse mode, and to increase the pulselengths of the long pulse mode at repetition frequencies below 100 Hz. However, the main priority is to increase the mean time between failures. To do so, the most significant problem to be tackled is the complete renewal of the 40 years old HV DC power supplies of modulators 2 and 3. Another priority will be the integration of new peripheral equipment for the main thyratrons (ranging of reservoir voltage for internal gas pressure stabilisation, pulse diagnostics) to improve thyratron lifetime and to allow a better assessment of thyraton end-of-life conditions. Along the same lines as discussed above we will also introduce a new control and interlock system for the modulators.

Study of properties of the GELINA neutron target

M. Flaska[1]*, D. Lathouwers*[2]*, W. Mondelaers*[1]*, A. Plompen*[1]*, A. Borella*[1]*, P. Schillebeeckx*[1]*, P. Rullhusen*[1]*, H. van Dam*[2]*, T. H. J. J. van der Hagen*[2]

[1] EC-JRC IRMM, B-2440 Geel, [2] IRI TU Delft, NL-1755 ZG Petten

The high-resolution time-of-flight facility GELINA [1] of the IRMM is one of the most powerful white spectrum neutron sources available in the world. It is especially designed to perform high-resolution neutron cross section measurements. It produces short bursts of neutrons mainly by (γ, n) and (γ, xn) reactions induced by bremsstrahlung of 70-140 MeV electrons impinging on uranium. The neutron source is a mercury cooled rotary target containing uranium sealed in a stainless steel disk 4 cm thick and with a diameter of 32.4 cm. In order to have a significant number of neutrons with energy below 100 keV, the fast neutrons produced in the target can subsequently be moderated to lower energies by using two 4 cm thick beryllium tanks filled with water placed above and below the target. Two flux distributions may be realised: one optimised for energies below 100 keV arising from the moderator and the other with fast neutrons arising directly from the uranium. Shadow bars placed between the source and the flight path shield the unwanted part of the neutron spectrum.

The neutron energy may be determined from the time difference between the neutron creation and its detection at a given distance from the source (TOF technique). These neutron time-of-flight measurements can be carried out simultaneously at 12 flight-paths with lengths ranging from 8 m to 400 m. Neutrons from the target with a particular energy have a distribution in time due to scattering in the target and moderator. This so-called resolution function [2] is influenced by the size and mass of the target and by the composition and shape of the moderator. Several other factors, like the neutron producing electron pulse, the detector and the acquisition electronics, give an additional contribution to the time spread. In order to optimise the accuracy of the measured neutron data, a large effort has been made to minimise all those effects.

The MCNP4C2 code [3] has been applied to study the neutron production characteristics. As a first step, steady-state and transient calculations of the existing target have been carried out. Because photonuclear reactions are the major phenomena of neutron production in our system we implemented new photonuclear libraries into the MC calculations to improve our results. In order to verify our approach we benchmarked our calculations with neutron spectrum measurements. In view of future target optimisations we also compared the physical properties of a simple cylindrical geometry with those of the present target.

In the photon energy range of interest neutron production in uranium is dominated by photonuclear processes in the Giant Dipole Resonance (GDR) range between 10 and 20 MeV [4]. The neutrons are produced mainly through photoneutron reactions (γ, n)

and (γ, 2n), and by photofission reactions (γ, f). The total photoneutron yield cross section is given by

$$\sigma(\gamma, xn) = \sigma(\gamma, n) + 2\sigma(\gamma, 2n) + ... + \bar{\nu}(\gamma, f) \quad (1)$$

which takes into account the multiplicity of neutrons emitted in each reaction event [5].

Two types of calculations were carried out. First, the steady-state properties of the GELINA target were investigated. Electrons with the energies of 70, 100, 140, and 70-140 MeV were used to bombard the target. Neutrons emitted from the target were sorted into equal lethargy intervals up to 20 MeV. In Fig. 1 the number of neutrons emitted from the target integrated over all angles as a function of energy, for different primary electron energies is compared. Integration of the curves immediately gives the normalized total neutron yield. Clearly the neutron yield (per initial electron) is directly proportional to the primary electron energy. Moreover, the average energy of the neutron spectra remains constant, irrespective of the energy of the source electron. This reflects the weak excitation energy dependence of the evaporated neutron spectra in the underlying photonuclear reactions.

The moderator significantly influences both the average energy of the neutron spectra and the neutron yield. If the moderator is present, the average neutron energy is decreased due to the elastic scattering of neutrons in the moderator. Although the neutron production yield increases due to backscattering of neutrons and subsequent fission in uranium, the neutron escape probability is lower by 3 % due to much higher neutron absorption. It came out from the analysis of the results that neutron absorption in the uranium was increased by 60 %, in case the moderator was present. Only a small part of the backscattered neutrons cause fission (below 1 %), the rest of them are simply captured in the target material. Neutron-induced fission in U-238 contributes 4.5 % to the neutron production, whereas the contribution of delayed neutrons to fission is negligible.

The next part of this work was aimed at the transient behaviour of the produced neutrons. A 1 ns electron pulse with different energies was applied in order to obtain the neutron time response of the target. For that reason, a sphere with radius of 25 cm was 'built' around the target and its surface served to tally all escaping neutrons. Thus time distributions correspond to neutrons escaped from the target and tallied at 25 cm from the target centre. Results presented in Fig. 2 show explicitly the strong influence of the moderator on the neutron time spread. The vertical axis represents the number of neutrons integrated over all angles and energies, per unit of time. It is apparent from the graphs that multiple scattering on light materials causes a significant increase of the times at which the neutrons emerge. Here t = 0 ns corresponds to the time of impact of the first electron on the uranium. It should be realised that the present calculated time distributions are integrated over all neutron energies, whereas in a next step we aim at resolving this distribution into the contributions arising from monoenergetic neutrons.

In order to check the validity of our simulations, we compared a neutron spectrum

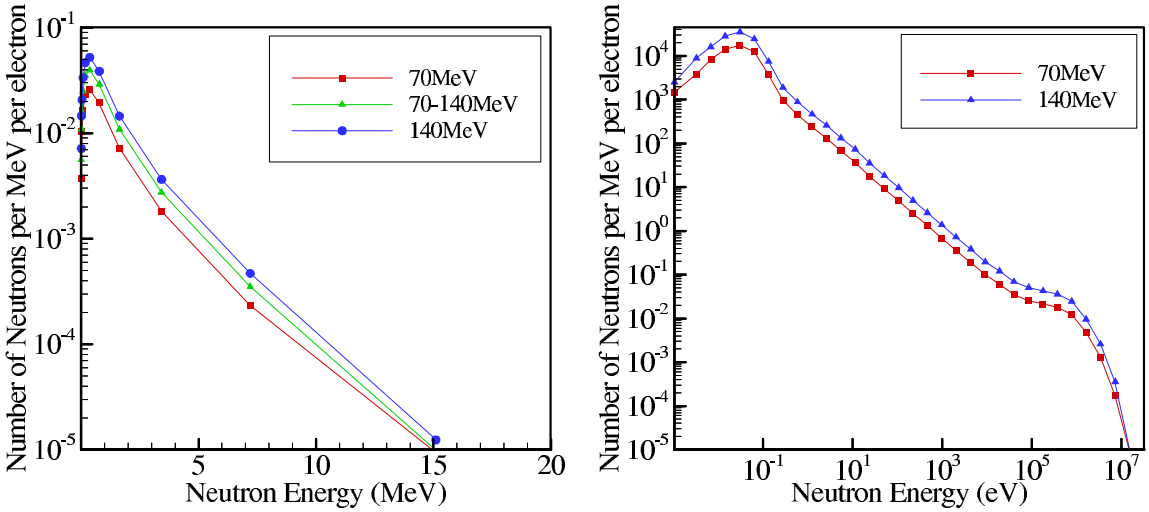

Fig. 1: Neutron energy distribution of GELINA target (a) without moderator and (b) with moderator

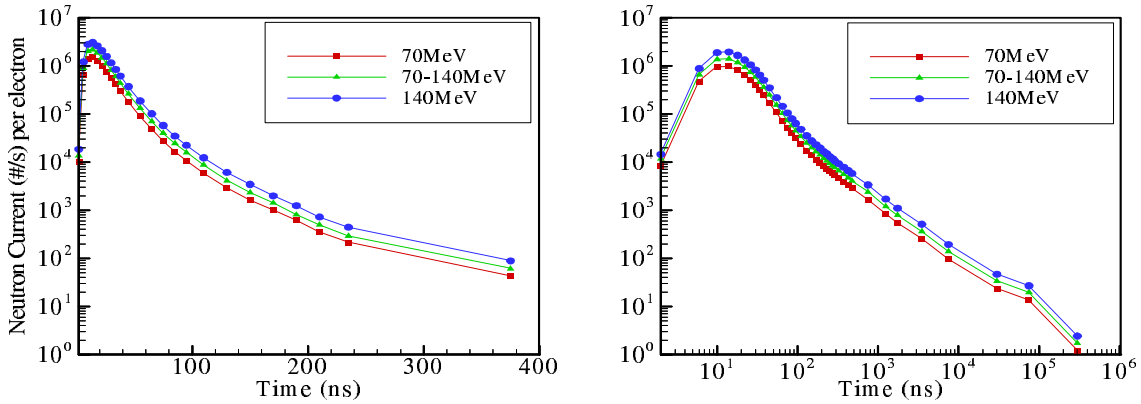

Fig. 2: Neutron time distribution of GELINA target (a) without moderator and (b) with moderator

measurement with our calculations. An experimental setup has been used on a neutron flight path at an angle of 81° with respect to the electron beam direction. The flight path length was 60 m. The neutron flux spectrum was measured with an ionization chamber with 6 boron layers having a total thickness of 210 μg/cm^2. The diameter of the neutron beam was 75 mm. The effective layer of the boron chamber had a diameter of 84 mm. The TOF technique was used to determine the neutron energy.

In the range below 100 keV the agreement between calculation and measurement is very good in relative terms. Absolute intercomparison was not possible because several experimental characteristics (detector area and efficiency, electron intensity, collimators, scattering in air,...) were not accurately known. The relative values of the neutron flux are reproduced within 10%. The slope of the energy spectrum is also very well described over 6 decades indicating that the moderation process is modelled with

a high accuracy. As expected, the spectrum is under-moderated, as can be deduced from the slope of the curve in the intermediate energy region (Fig. 3).

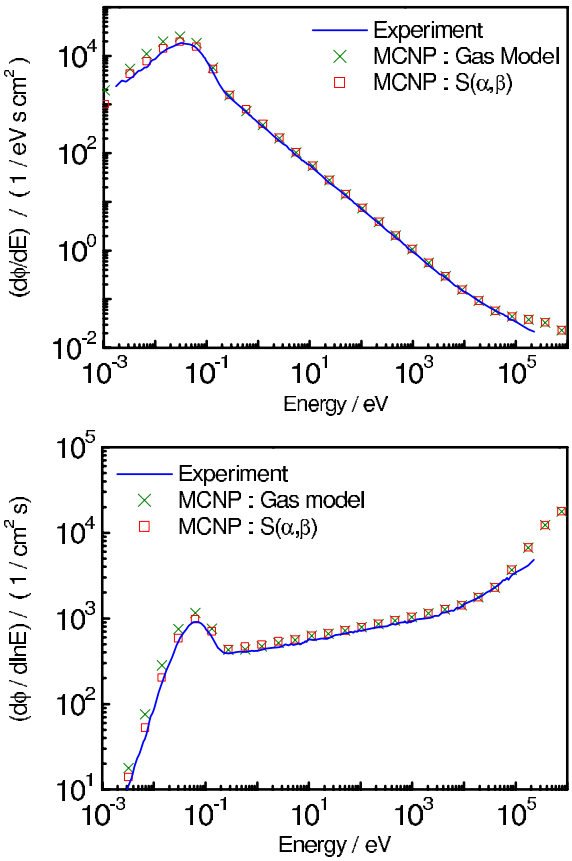

Fig. 3: Neutron flux in flight path 81° - 60 m (a) per unit of energy and (b) per unit of lethargy

In the thermal energy range the influence of two different MCNP4C2 treatments is shown. In case of a free gas model, the thermal treatment is based on the free gas approximation, which accounts for a thermal motion of atoms. If the S(α, β) model is used, the effects of chemical binding are taken into account below energies of about 4 eV. It is obvious that the MC calculation are in better agreement with measurement if the S(α, β) model is used. The discrepancy above 100 keV can be explained by the fact that the experimental setup was optimised for measurements with moderated neutrons. This was accomplished by a 10 cm lead shadow bar shielding the flight path from the uranium target. As the MC calculation included the whole neutron spectrum this shadow bar was not taken into account.

In order to evaluate the possible future improvements, a simple geometry with reduced mass has been investigated. Only steady-state calculations without moderator were performed. A cylinder of U-Mo with 10-wt % of Mo was chosen in such a way, that its height corresponded to 20 X_0, while the radius was 1.5 R_M. According to [6], about

90 % of the total energy is deposited in the cylinder having the radius of R_M. Some additional calculations were done which confirmed this prediction with an accuracy of a few %. The pencil electron beam bombarded the uranium at the point where the axis and base of the cylinder cross. It can be seen from the analysis of the results, that the neutron escape has been increased by 2 % due to the lower mass of uranium compared with the present target, which relates to the lower absorption. The contribution of fission to total neutron yield has been decreased to 3 % for the same reason. The average energy of neutrons escaping the target increased due to the lower number of scattering events.

For the first time the GELINA white neutron source has been modelled with the coupled electron-photon-neutron MCNP4C2 code. It was necessary to supplement MCNP4C2 with new photonuclear data libraries for 6 isotopes used in the target configuration. The steady-state energy spectra and time-dependent flux distributions were calculated with and without moderator. Neutron spectra measurements at a GELINA flight path were used to assess our MC approach. Calculations and measurements agree well in shape up to a neutron energy of 100 keV. An initial discrepancy in the thermal region revealed the importance of the application of the S(α, β) treatment. Our results show that the MCNP4C2 code together with the new photonuclear data libraries are ideally suited for the neutronics part of the new target design study. This project is aimed at the development of a reduced-mass neutron target and moderator system with better resolution function characteristics.

[1] A. Bensussan, J.M. Salome, "Gelina: a modern accelerator for high-resolution neutron time of flight experiments," Nucl. Inst. Meth. 155 (1978) 11-23.

[2] C. Coceva, M. Frisoni, M. Magnani, A. Mengoni, "On the figure of merit in neutron time-of-flight measurements," Nucl. Inst. Meth. 489, (2002) 346-356.

[3] J. F. Briesmeister, ed., "MCNP - A General Monte Carlo N-Particle Transport Code, Version 4C," LA-13709-M, LANL, Los Alamos, USA, April 2000.

[4] A. Veyssiere, H. Beil, R. Bergere, P. Carlos, A. Lepretre, "A study of the photofission and photoneutron processes in the giant dipole resonance of ^{232}Th, ^{238}U and ^{237}Np," Nucl. Phys. A199 (1973) 45

[5] IAEA-TECDOC-1178, Handbook on photonuclear data for applications: Cross sections and spectra, Vienna, Austria, October 2000

[6] R.M. Barnett et al., "Review of particle properties," Phys. Rev. D54 (1996)

Annex

List of publications

DEMATTE, L., HAMBSCH, F., BAX, H.J.U.
Discrimination of Pile up in a Fission Fragment Detection Experiment
Nuclear Instruments and Methods in Physics Research A, Vol. 480 (2002) 706

KORNILOV, N., KHRIACHKOV, V., DUNAEV, M., KAGALENKO, A., SEMENOVA, N., DEMENKOV, V., PLOMPEN, A.
Neutron Spectroscopy with Fast Waveform Digitizer
Nuclear Instruments and Methods A, Vol. 497 (2002) 467

HAMBSCH, F., OBERSTEDT, S., VLADUCA, G., TUDORA, A.
Prompt Fission Neutron Multiplicity and Spectra Evaluation in the Frame of the Multi-Modal Fission Model for ^{237}Np(n, f) and ^{238}U(n, f)
Nuclear Physics A, Vol. 709 (2002) 85

GAELENS, M., LOISELET, M., WAGEMANS, C., WAGEMANS, J., GOEMINNE, G.
Realization of Nuclear Targets by Ion Implantation. The ^{17}O Case
Nuclear Instruments and Methods in Physics Research A, Vol. 480 (2002) 233

GOEMINNE, G., WAGEMANS, C., WAGEMANS, J., KOESTER, U., GELTENBORT, P., DENECKE, B. W., JOHANSSON, L., POMME, S.
Preparation and Characterisation of an ^{39}Ar Sample and Study of the ^{39}Ar(n$_{th}$, α)^{36}S Reaction
Nuclear Instruments and Methods in Physics Research A, Vol. 489 (2002) 577

MASLOV, V., HAMBSCH, F.
Symmetric Uranium Neutron-Induced Fission
Nuclear Physics A, Vol. 705 (2002) 352

REIMER, P., HULT, M., PLOMPEN, A., JOHNSTON, P. N., AVRIGEANU, V., QAIM, S.
Measurement of the nat-Mo(n, x)^{94}Nb Cross Section Using Ultra-Low Level γ-Ray Spectrometry at HADES
Nuclear Physics A, Vol. 705 (2002) 265

WAGEMANS, J., WAGEMANS, C., GOEMINNE, G., SEROT, O., LOISELET, M., GAELENS, M.
The ^{17}O(n, α)^{14}C Reaction from Subthermal up to Approximately 350 keV Neutron Energy

Physical Review C, Vol. 65 (2002) 034614, 1

WAGEMANS, C., WAGEMANS, J., SEROT, O.
The ^{234}U(n$_{th}$, f) Cross Section Revised
Nuclear Science and Engineering, Vol. 141 (2002) 171

TOVESSON, F., HAMBSCH, F., OBERSTEDT, A., FOGELBERG, B., RAMSTROEM, E., OBERSTEDT, S.
Neutron-Induced Fission Cross-Section of ^{233}Pa between 1.0 and 3.0 MeV
Physics Review Letters, Vol. 88, No. 6 (2002) 062502, 1

AVRIGEANU, V., GLODARIU, T., PLOMPEN, A., WEIGMANN, H.
On Consistent Description of Nuclear Level Density
Journal of Nuclear Science and Technology, Suppl. 2 (2002) 746

PLOMPEN, A., REIMER, P., AVRIGEANU, V., QAIM, S.
Vanadium Cross-Section Measurements by the Activation Technique and Evaluations from Threshold to 20 MeV
Journal of Nuclear Science and Technology, Suppl. 2 (2002) 283

AVRIGEANU, M., AVRIGEANU, V., PLOMPEN, A.
Preequilibrium-Emission Surface Effects in Activation Reactions
Journal of Nuclear Science and Technology, Suppl. 2 (2002) 803

TOVESSON, F., HAMBSCH, F., OBERSTEDT, S., BAX, H. J. U.
Fission Fragment Properties and the Problem of the Pulse Height Defect
Journal of Nuclear Science and Technology, Suppl. 2 (2002) 673

TOVESSON, F., HAMBSCH, F., OBERSTEDT, S., OBERSTEDT, A., FOGELBERG, B., RAMSTROEM, R., BAX, H. J. U.
The ^{233}Pa Fission Cross-Section
Journal of Nuclear Science and Technology, Suppl. 2 (2002) 210

KALININ, V., DUSHIN, V., HAMBSCH, F., YAKOVLEV, V., KRAEV, I., LAPTEV, A., PETROV, B., PETROV, G., PLEVA, Y., SHCHERBAKOV, O., SOKOLOV, V., VOROBYEV, A.*
Measurements of Prompt Neutron Multiplicity Distributions in Correlation with Mass-Energy Distribution of Fission Fragments in Spontaneous Fission of ^{252}Cf, ^{244}Cm and ^{248}Cm
Journal of Nuclear Science and Technology, Suppl. 2 (2002) 250

HAMBSCH, F., BAX, H. J. U.
The ^{10}B Standard Branching Ratio
Journal of Nuclear Science and Technology, Suppl. 2 (2002) 1402

DUIJVESTIJN, M., KONING, A., HAMBSCH, F.

Nucleon-Induced Fission at Intermediate Energies
Journal of Nuclear Science and Technology, Suppl. 2 (2002) 754

LOBO, A., CORVI, F., IANEVA, N., MUTTI, P.
Measurement of the ^{232}Th Neutron Capture Cross-Section in the Region 5-200 keV
Journal of Nuclear Science and Technology, Suppl. 2 (2002) 429

MUTTI, P., BEER, H., BRUSEGAN, A., CORVI, F., GALLEANO, R.
Reinvestigation of ^{85}Kr Branching in the Light of New ^{82,84,86}Kr Neutron Capture Cross-Section Measurements
Journal of Nuclear Science and Technology, Suppl. 2 (2002) 569

PLOMPEN, A., SMITH, D., REIMER, P., QAIM, S., AVRIGEANU, V., SUDAR, S., CSERPAK, F.
Neutron Activation Cross-Section Measurements at Geel
Journal of Nuclear Science and Technology, Suppl. 2 (2002) 192

AVRIGEANU, V., GLODARIU, T., PLOMPEN, A., WEIGMANN, H.
On Consistent Description of Nuclear Level Density
Journal of Nuclear Science and Technology, Suppl. 2 (2002) 746

HAMBSCH, F., DEMATTE, L., BAX, H.J.U.
Fission of ^{239}Pu with Resonance Neutrons
Journal of Nuclear Science and Technology, Suppl. 2 (2002) 307

BRUSEGAN, A., GUNSING, F., NOGUERE, C.
The Resolution Function in Neutron Time-of-Flight Experiments
Journal of Nuclear Science and Technology, Suppl. 2 (2002) 685

CORVI, F., BRUSEGAN, A., HERAULT, N., GRESSIER, V., GUNSING, F., LEPRETRE, A., MACAVERO, E., MOUNIER, C., NOGUERE, G., RAPSAET, C.
CEA-IRMM Co-operation on Neutron Data Measurements for Waste Transmutation
Journal of Nuclear Science and Technology, Suppl. 2 (2002) 1067

VOROBYEV, A., DUSHIN, V., HAMBSCH, F., YAKOVLEV, V., KALININ, V., KRAEV, I., LAPTEV, A., PETROV, B., PETROV, G., PLEVA, Y., SHCHERBAKOV, O., SOKOLOV, V.
Methodological Description of a Study of Correlations between Neutron Multiplicity, Mass and Kinetic Energy of Fission Fragments
Journal of Nuclear Science and Technology, Suppl. 2 (2002) 630

WAGEMANS, C., WAGEMANS, J., GOEMINNE, G., LOISELET, M., GAELENS, M.
Preparation of Highly Enriched ^{17}O Samples for Neutron Induced Reaction Studies
Nuclear Instruments and Methods, Vol. 480 (2002) 229

List of conferences

POSTMA, H., BLAAUW, M., SCHILLEBEECKX, P.J., LOBO, G., HALBERTSMA, R., NIJBOER, A.
Non-Destructive Elemental Analysis of Copper-Alloy Artefacts with Epithermal Neutron-Resonance Capture
14^{th} Radiochemical Conference, TU Prague, 14-19 April 2002, Marinske Lzne (CZ)

POSTMA, H., BLAAUW, M., PEREGO, R., SCHILLEBEECKX, P. J., LOBO, G., NIJBOER, A.
The Elemental Composition of Bronze Artefacts Determined by Neutron-Resonance Capture-Analysis Using a Pulsed Beam of Epithermal Neutrons
33^{rd} International Symposium on Archeometry, ROB, 22-26 April 2002, Amsterdam (NL)

BLAAUW, M., POSTMA, H., MUTTI, P.
Quantitative Neutron Capture Resonance Analysis Verified with Instrumental Neutron Activation Analysis
Symposium on Radiation Measurements and Applications, 26-28 May 2002, Ann Arbor, Mich. (USA)

POSTMA, H., BLAAUW, M., CORVI, F.
Fully Non-Destructive Elemental Analyses of Copper-Alloy Artefacts with Neutron Resonance Capture between 1 eV and 10 keV
14^{th} Radiochemical Conference, 14-19 April 2002, Marinske Lzne (CZ)

LÖVESTAM, G.
The Van-de-Graaff accelerator facility at the EC-JRC Institute for Reference Materials and Measurements in Geel
SNEAP2002 symposium, October, 7-10, 2002, Lafayette, Louisiana, USA

TOVESSON, F., HAMBSCH, F., OBERSTEDT, S., FOGELBERG, B., OBERSTEDT, A., RAMSTROEM, E.
^{233}Pa(n, f) Cross-Section Data for Accelerator Driven Systems and Transmutation of Waste
Seminar Lecture at the Royal Institute of Technology, Reactor Physics Department, Stockholm, 18 October, 2002

HAMBSCH, F., TOVESSON, F., OBERSTEDT, S., FRITSCH, V., OBERSTEDT, A., FOGELBERG, B., RAMSTROEM, E.
First Direct Measurements of the ^{233}Pa Fission Cross Section up to 8.5 MeV
Proceedings of the 3^{rd} International Conference on Fission and Properties of Neutron-

Rich Nuclei, Vanderbilt Univ., 3-9 November 2002, Sanibel Island, Fla. (USA), World Scientific Publs., J.H. Hamilton, A.V. Ramayya (Eds.)

HAMBSCH, F., OBERSTEDT, S., VLADUCA, G., TUDORA, A.
Neutron Multiplicity, Spectra and Fission Cross-Section Evaluations within the Multi-Modal Fission Model for ^{237}Np(n, f) and ^{235}U(n, f)
Proceedings of the 3rd International Conference on Fission and Properties of Neutron-Rich Nuclei, Vanderbilt Univ., 3-9 November 2002, Sanibel Island, Fla. (USA), World Scientific Publs., J.H. Hamilton, A.V. Ramayya (Eds.)

HAMBSCH, F., RUSKOV, I., DEMATTE, L.
^{239}Pu(n, f) at Resonance Energies and its Multi- Modal Interpretation
Proceedings of the 3rd Intern. Conference on Fission and Properties of Neutron-Rich Nuclei, Vanderbilt Univ., 3-9 November 2002, Sanibel Island, Fla. (USA), World Scientific Publs., J.H. Hamilton, A.V. Ramayya (Eds.)

OHSAWA, T., HAMBSCH, F.
An Interpretation of Energy Dependence of Delayed Neutron Yields in the Resonance Region
Proceedings of PHYSOR 2002: Intern. Conference on New Frontiers of Nuclear Technology: Reactor Physics, Safety and High-Performance Computing, Reactor Phys. Div. of Korean Nucl. Soc., 7-10 October 2002, Seoul (Korea)

BAUMANN, P., JERICHA, E., KELIC, A., KORNILOV, N., LUKIC, S., NOGUERE, G., PAVLIK, A., PLOMPEN, A., RUDOLF, G., SIEGLER, P.
The Use of Ge Detectors for (n, xn) Cross Section Measurements at Intense and Low-frequency Pulsed Neutron Beams
Intern. Conference on Actinide and Fission Product Partitioning and Transmutation, OECD/NEA and Ministry of Science and Technology, Korea, 14-16 October 2002, Jeju (Rep. Korea)

HAMBSCH, F., TOVESSON, F., OBERSTEDT, S., FRITSCH, V., OBERSTEDT, A., FOGELBERG, B., RAMSTROEM, E.
First Measurement of the ^{233}Pa Fission Cross Section
Proceedings of the 10th International Seminar on Interaction of Neutrons with Nuclei: "Neutron Spectroscopy, Nuclear Structure, Related Topics" (ISINN-10), JINR, FLNP, 22-25 May, 2002, Dubna (Russia), W.I. Furman (Ed.), FLNP Publs.

ZEINALOV, S., HAMBSCH, F., TOVESSON, F.
Digital Signal Processing Application to Charged Particle Spectroscopy with Double Ionization Chamber
Proceedings of the 10th International Seminar on Interaction of Neutrons with Nuclei (ISINN-10), JINR, 22-25 May 2002, Dubna (Russia), W.I. Furman (Ed.), FLNP Publs.

BRUSEGAN, A.

Neutron Transmission Measurements at the IRMM Pulse Neutron Facility GELINA
Proceedings of the XVI International School on Nuclear Physics, Neutron Physics and Nuclear Energy, 25-30 September 2002, Varna (BUL)

KALININ, V., DUSHIN, V.N., PETROV, B.F., JAKOVLEV, V., VOROBYEV, A., KRAEV, I., LAPTEV, A., PETROV, G., PLEVA, Y., SHCHERBAKOV, O., SOKOLOV, V., HAMBSCH, F.
On Fssion Fragment de-Excitation at Scission Point
Proceedings of the 5th Conference on Dynamical Aspects of Nuclear Fission, JINR, Slovak Acad. Sc., 23-27 October 2001, Casta-Papernicka (SLO)

GIORGINIS, G., KHRIATCHKOV, V.
Cross-Section Measurements for the Reaction ^{10}B(n, α)^{7}Li from 1 to 4 MeV
10^{th} Intern. Seminar on Interaction of Neutrons with Nuclei (ISNN-10), Frank Lab. Neutron Phys., JINR, 22-25 May 2002, Dubna (Russia)

JERICHA, E., BAUMANN, P., KELIC, A., LUKIC, S., RUDOLF, G., KORNILOV, N., NOGUERE, G., PLOMPEN, A., SIEGLER, P.
Methodological Tests of Prompt γ-Ray Spectroscopy (n, xn) Cross-Section Measurements at Various Facilities
11th Intern. Symposium on Capture Gamma-Ray Spectroscopy and Related Topics, Charles Univ. Prague, 2-6 September 2002, Pruhonice (CZ), F. Becvar et al. (Eds.)

LUKIC, S., BAUMANN, P., BORCEA, C., JERICHA, E., JOKIC, S., KELIC, A., KORNILOV, N., MEULDERS, J., OLAH, L., PAVLIK, A., PLOMPEN, A., RUDOLF, G.
The Use of Ge Detectors for (n, xn) Cross-Section Measurements at Intense and Low Frequency Pulsed Neutron Beams
Proceedings of the 7th Information Exchange Meeting on Actinide and Fission Product Partitioning and Transmutation, NSC, NDC, KAERI, KEPRI, 14-16 October 2002, Jeju (Rep. Korea), Won Seok Park and Byung Chan Na (Eds.)

SEMKOVA, V., PLOMPEN, A., SMITH, D., AVRIGEANU, V., SUDAR, S.
Measurements of Neutron-Induced Reaction Cross-Section on Different Isotopes of Ni, Zr and Pb from Threshold to 20 MeV with the Activation Technique
Intern. Workshop on Fast Neutron Physics, TU Dresden, FZ Rossendorf, 5-7 September 2002, Dresden (D), H. Freiesleben, E. Grosse, K. Seidel, F.-P. Weiss (Eds.)

OBERSTEDT, S.
Research on fast-neutron induced reactions for innovative nuclear applications
Intern. Workshop on Fast Neutron Physics, TU Dresden, FZ Rossendorf, 5-7 September 2002, Dresden (D), H. Freiesleben, E. Grosse, K. Seidel, F.-P. Weiss (Eds.)

SEROT, O., WAGEMANS, C., WAGEMANS, J., GELTENBORT, P.
Influence of the Excitation Energy on the Ternary Triton Emission Probability
Proceedings of the 3^{rd} International Conference on Fission and Properties of Neutron-

Rich Nuclei, Vanderbilt Univ., 3-9 November 2002, Sanibel Island, Fla. (USA), World Scientific Publs., J.H. Hamilton, A.V. Ramayya (Eds)

WAGEMANS, C., GOEMINNE, G., DE SMET, L., WAGEMANS, J.
High Resolution Measurement of the ^{36}Cl(n, p)^{36}S and ^{36}Cl(n, α)^{33}P Reactions
Proceedings of the International Conference on Nuclear Physics in Astrophysics, 30 September - 4 October 2002, Debrecen (HU)

VIESTI, G., LUNARDON, M., NEBBIA, G., BARBUI, M., CINAUSERO, M., FIORETTO, E., PRETE, G., D ERASMO, P., PALOMBA, M., ABBRESCIA, M., IASELLI, G., LODDO, F., PATICCHIO, V., RANIERI, T., TRENTADUE, R., COLLA, A., MUSSO, A., PICCOTTI, A., POGGIO, F., DELLACASA, G., LAZZIZZERA, I., LECCA, P., OBHODAS, J., SUDAC, D., NAD, K., VALKOVIC, V., BRUSEGAN, A., LOBO, G., HLAVAC, S., CATARSI, F., FRANCHI, G., CHIANELLA, M., GALIMBERTI, D., PAVESI, L., ZORAT, A., KOESTER, A., PLEIN, M., MERZ, A., SCHNEIDER, H., VALLON, G.
The DIAMINE Landmine Detection System
Proceedings of the XVII International Conference on the Application of Accelerators in Research and Industry (CAARI 2002), Univ. North Texas, 12-16 November 2002, Denton, Tx (USA), Univ. N. Tex. Publs.

DUSHIN, V.N., HAMBSCH, F., JAKOVLEV, V., KALININ, V., LAPTEV, A., PETROV, B. F., SHCHERBAKOV, O., VOROBYEV, A.
Investigation of Neutron Multiplicity Distribution in Separate Channels of Reactions Using Gadolinium Loaded Large Liquid Scintillation Counters
Proceedings of the 3rd International Conference on Fission and Properties of Neutorn-Rich Nuclei, Vanderbilt University, 3-9 November 2002, Sanibel Island, Fla. (USA), World Scientific Publs., J.H. Hamilton, A.V. Ramayya (Eds.)

KALININ, V., DUSHIN, V.N., HAMBSCH, F., JAKOVLEV, V., LAPTEV, A., PETROV, B. F., SHCHERBAKOV, O., VOROBYEV, A.
Fission Fragment Deformation and Dynamical Effects in Spontaneous Fission of ^{252}Cf, ^{244}Cm and ^{248}Cm
Proceedings of the 3rd International Conference on Fission and Properties of Neutron-Rich Nuclei, Vanderbilt University, 3-9 November 2002, Sanibel Island, Fla. (USA), World Scientific (Publs.), J.H. Hamilton, A.V. Ramayya (Eds.)

GUNSING, F., PLOMPEN, A., RULLHUSEN, P., BORCEA, C.
Neutron Capture Measurements at the CERN-nTOF Facility for ADS Applications
Proceedings of the 11th Intern. Symposium on Capture γ-Ray Spectroscopy and Related Topics, Charles Univ., TU Prague, Acad. Sciences Prague, 2-6 September 2002, Pruhonice, Prague (CZ)

LETOURNEAU, A., BERTHOUMIEUX, E., DERUELLE, O., FADIL, M., FIONI, G., GUNSING, F., MARIE, F., PERROT, L., RIDIKAS, D., BOERNER, H., FAUST, H., MUTTI, P., SIMPSON, G., SCHILLEBEECKX, P.J.

Thermal Neutron Capture Branching Ratio of ^{209}Bi Using a γ-Ray Technique
Proceedings of the 11^{th} Intern. Symposium on Capture γ-Ray Spectroscopy and Related Topics, Univ. Prague, 2-6 September 2002, Prague (CZ)

KORNILOV, N., KHRIACHKOV, V., DUNAEV, M., KAGALENKO, A., SEMENOVA, N., DEMENKOV, V., PLOMPEN, A.
Neutron Spectroscopy with a Fast Waveform Digitizer
Proceedings of the 10th Intern. Seminar on the Interactions of Neutrons with Nuclei (ISINN- 10), JINR, 22-25 May 2002, Dubna (Russia), V.N. Shvetsov (Ed.)

PLOMPEN, A., AVRIGEANU, V., BORCEA, C., OLAH, L., SEMKOVA, V.
Measurements of Neutron-Induced Reaction Cross-Sections for ^{58}Ni, ^{63}Cu and ^{59}Co from Threshold to 20 MeV
Proceedings of the Intern. Conference on New Frontiers of Nuclear Technology (PHYSOR 2002), ANS, 7-10 October 2002, Seoul (Korea)

OBERSTEDT, S., OBERSTEDT, A., HAMBSCH, F., ROCHMAN, D., TSEKHANOVICH, I., GOENNENWEIN, F., RAMAN, S.
Light Charged Particle Emission in Thermal Neutron-Induced Fission of ^{252}Cf*
Spring Meeting of the German Physical Society, DPG, 11-15 March 2002, Mnster (D)

OBERSTEDT, S., OBERSTEDT, A., HAMBSCH, F., TOVESSON, F., FOGELBERG, B., RAMSTROEM, E.
^{233}Pa(n, f) Cross-Section for Acceleratore-Driven Systems
Spring Meeting of the German Physical Society, DPG, 11-15 March 2002, Mnster (D)

BLAAUW, M., POSTMA, H., MUTTI, P.
Demonstration of Neutron Resonance Capture Applied to a Cultural Heritage Study of an Antique Benin Bronze.
Proceedings of the 3^{rd} Intern. Symposium on Nuclear and Related Techniques (NURT 2001), 22-26 October 2001, Havanna (Cuba), Univ. Havanna

Internal and EUR reports

LÖVESTAM, G.
EnergySet - a programme to calculate accelerator settings and neutron yield data for the IRMM VdG laboratory
IRMM internal report GER/NP/2/2002/06/20

OBERSTEDT, S. and RULLHUSEN, P.
Scientific Report 2001
ISBN 92-894-4152-6 - EUR 20412/EN (2002)

Special publications

REIMER, P.
Fast Neutron Induced Reactions Leading to Activation Products. Selected Cases Relevant to Development of Low Activation Materials, Transmutation and Hazard Assessment of Nuclear Wastes
PhD Thesis - S.P./G.02.33

Author Index

Organisational chart NP Unit
status 1 February 2003

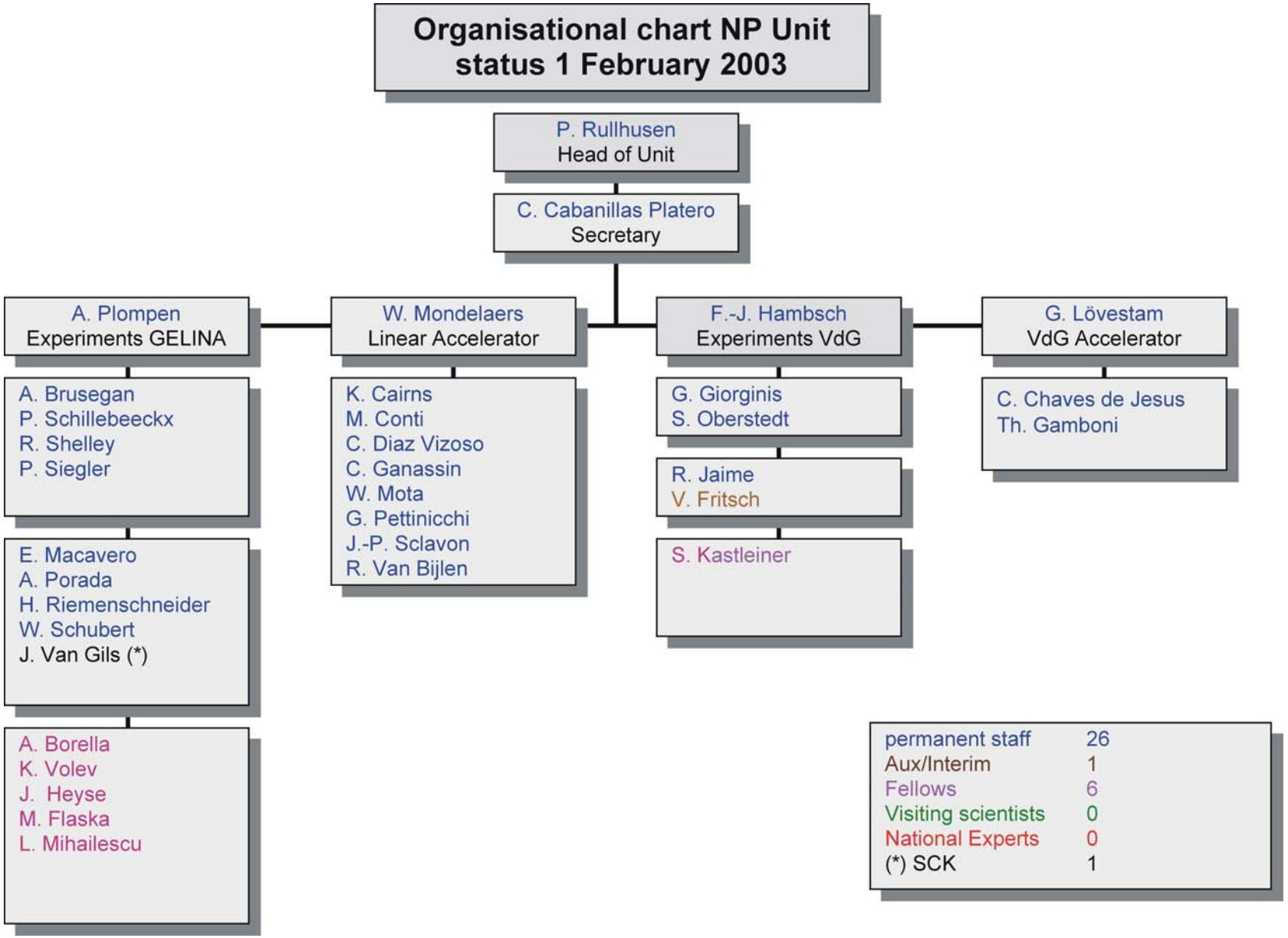

15

LA-NA-20684-EN-C

The mission of the JRC is to provide customer-driven scientific and technical support for the conception, development, implementation and monitoring of European Union policies. As a service of the European Commission, the JRC functions as a reference centre of science and technology for the Community. Close to the policy-making process, it serves the common interest of the Member States, while being independent of commercial or national interests.

Neutron Physics Unit
Institute for Reference Materials and Measurements,
Retieseweg, B-2440 Geel,
Phone +32 14 571 411, Fax +32 14 571 862, E-mail: carmen.cabanillas@irmm.jrc.be

http://www.irmm.jrc.be

ISBN 92-894-5514-4